

THESIS

MYCOBACTERIUM TUBERCULOSIS – MEDIATED MODULATION OF HOST MACROPHAGE  
METABOLISM IN THE GRANULOMA MICROENVIRONMENT

Submitted by

Dilara Kiran

Department of Microbiology, Immunology, and Pathology

In partial fulfillment of the requirements

For the Degree of Master of Science in Microbiology

Colorado State University

Fort Collins, Colorado

Summer 2020

Master's Committee:

Advisor: Randall Basaraba

Brendan Podell  
Andres Obregon-Henao  
Christine Olver  
Adam Chicco

Copyright by Dilara Kiran 2020

All Rights Reserved

## ABSTRACT

### MYCOBACTERIUM TUBERCULOSIS – MEDIATED MODULATION OF HOST MACROPHAGE METABOLISM IN THE GRANULOMA MICROENVIRONMENT

*Mycobacterium tuberculosis* (Mtb) is the leading cause of death by an infectious agent, and tuberculosis (TB) disease continues to be a prominent global health concern. Infection with Mtb incites granulomatous inflammation, chronic antigen stimulation, and the development of granuloma lesions. These lesions compress tissue architecture in a way that reduces blood supply and creates central regions of hypoxia. Complex lesion pathology, multi-drug resistance of Mtb, co-morbidities with other endemic diseases, the lack of an effective vaccine, and slow drug development pipelines have hindered progress in the field. Researchers have worked to combat these difficulties through their exploration of host-directed therapeutic strategies, which aim to better equip the host immune system to respond to Mtb infection, with a focus on immunometabolism as a target pathway.

The metabolism of host macrophages plays a role in modulating disease pathogenesis, with a metabolic switch from oxidative phosphorylation to glycolysis characterizing Mtb infected macrophages. This metabolic switch is primarily regulated at the transcriptional level by hypoxia inducible factor-1 $\alpha$  (HIF-1 $\alpha$ ), which regulates the cellular response to hypoxic stressors encountered within the chronic granuloma lesion microenvironment. Downstream impacts of HIF-1 $\alpha$  activation include increased glycolysis, increased lactate production, and increased lactate transport. HIF-1 $\alpha$  becomes stable and undergoes its transcriptional activity in conditions of low oxygen, as a result of prolyl hydroxylase (PHD) inhibition. Additionally, hypoxia-independent

factors interfere with PHD leading to HIF-1 $\alpha$  stabilization, including iron chelation. Bacteria, such as Mtb, have developed iron chelating siderophores to sequester iron from host cells, and knocking-out these iron chelators has been demonstrated to reduce stable HIF-1 $\alpha$  activation. As a result, we hypothesized that the Mtb siderophore, mycobactin, plays a role in driving stabilization of HIF-1 $\alpha$  during early infection, prior to the development of hypoxic lesion microenvironments. This would serve as a pathogen-driven mechanism that would support macrophage adaptation to hypoxia later during disease progression, and thus develop an Mtb survival niche.

Using purified iron chelators deferoxamine (DFO) and mycobactin J (MbtJ), we demonstrated that treated CD1 mouse bone marrow derived macrophages (BMDMs) increase HIF-1 $\alpha$  via Western Blot and potentially increase glycolytic metabolism as demonstrated by Seahorse Extracellular Flux Analysis. Additionally, the use of mycobactin synthase K (mbtK) knock-out, complement, or wild-type H37Rv strains of Mtb demonstrated the role that mycobactin plays in the metabolic response of macrophages *in vitro*, having a significant impact on oxidative metabolism. Hypoxia-independent mechanisms of HIF-1 $\alpha$  activation by mycobactin may be a critical pathway through which Mtb drives macrophages toward a phenotype conducive for bacterial survival.

Lactate produced as a result of increased glycolytic metabolism during infection may also play an important role as a metabolic intermediate and as a signaling molecule during Mtb infection. Metabolic symbioses exist in multiple systems between highly glycolytic, hypoxic cells and more oxidative, normoxic cells, wherein glycolytic cells uptake glucose, convert glucose to lactate via lactate dehydrogenase (LDHA) and export lactate in large amounts via monocarboxylate transporter 4 (MCT4). Normoxic cells import lactate via monocarboxylate transporter 1 (MCT1) and convert it back to pyruvate via lactate dehydrogenase B (LDHB) and utilize lactate-derived pyruvate to fuel mitochondrial respiration. This preserves glucose for hypoxic cells which rely heavily on glycolysis for metabolic survival. While this type of lactate shuttle has been

demonstrated to regulate the tumor microenvironment, it has yet to be explored within the context of the similar TB granuloma microenvironment.

As a result, we explored the role of a lactate shuttle within Mtb infection by detecting lactate in guinea pig plasma, detecting lactate shuttle components within guinea pig granuloma lesions, and by using the LDHA inhibitor sodium oxamate and the MCT1 inhibitor  $\alpha$ -Cyano-4-hydroxycinnamic acid ( $\alpha$ -CHC), both of which are commercially available. We showed that Mtb infection significantly increases lactate on both a systemic and cellular level. We successfully demonstrated that LDH and MCT inhibition augments metabolism in macrophages by blocking glycolysis and decreasing mitochondrial spare capacity. Through *in vitro* Mtb infection models, we were able to show that inhibitor treatment can reduce the amount of lactate accumulated. These studies demonstrated proof of concept for the role of a lactate shuttle in modulating macrophage metabolism during Mtb infection and maintaining infection dynamics within the granuloma microenvironment.

Overall, the research presented herein seeks to understand the ways in which Mtb infection drives host macrophages to alter their metabolic phenotype in a way that promotes Mtb survival and contributes to disease pathogenesis. A better understanding of the interactions which occur at the host-pathogen interface will provide important insight for the development of host-directed therapeutic strategies which will better equip host cells to combat Mtb infection.

## ACKNOWLEDGMENTS

To start, I want to thank my advisor, Dr. Randall Basaraba. He took the dual-degree program leap with me, never gave up on me, and continued to allow me to pursue my ideas and explore the TB field. Our mentor-mentee relationship was not always perfect, but I never doubted that he cared about me and his students. He always allowed me to be vulnerable, open, and honest throughout all aspects of my research journey, and I am extremely grateful that he put up with my highs and my lows. Additional thank yous go out to all members of the Basaraba Laboratory, past and present. I want to especially recognize Forrest Ackart, Jessie Haugen, and Alexandra Todd, who provided advice and expertise throughout all aspects of the research process, including experimental design, conducting experiments, data analysis and interpretation, as well as general emotional support. I could not have made it through without them. I also want to thank all external collaborators and funding agencies, particularly the NIH ORIP for funding my F30 award.

Next, I thank my committee members Dr. Brendan Podell, Dr. Andres Obregon-Henao, Dr. Christine Olver, and Dr. Adam Chicco. I want to thank them for always having an open-door policy when it came to bouncing off ideas, discussing my research road-blocks, and providing encouragement when it was greatly needed. They were always tough, but realistic, and pushed me to be the best that I could be. I know that I may not have met all their expectations, but I will always be grateful for their belief in my capabilities, my talent, and my success.

I want to thank those involved with administration of the DVM/PhD program, including Dr. Ed Hoover, Dr. Susan VandeWoude, Dr. Justin Lee, Dr. Dan Regan, and Dr. Melinda Frye. I thank them for seeing potential in me and for bringing me to Colorado. They fostered a community amongst the DVM/PhD students which provided a rich network of peer mentorship and support that I still believe is unmatched at any other similar program. Dual degree programs are unique,

and the experiences can only be completely understood by those who directly go through them. Even if the program was not the best fit for me in the end, I am grateful for the opportunities and learning that this program provided me. Without the barriers that I faced and the struggles I worked to combat; I would not be the same scientist I am today.

There are many others whom I consider mentors within MIP. Thank you to Heidi Runge and Collette Hageman for always being quick to answer my emails and for being a listening ear for both personal and programmatic concerns. I will be eternally grateful to Dr. Kelly Santangelo, for allowing me to say things out loud that I never admitted to myself, for asking me what I truly wanted, and for allowing me to admit that the degree program I started may no longer be the one that I want. I thank her for reminding me that my value and worth does not come from the letters behind my name. I am also grateful to Dr. Colleen Duncan, for reassuring me that there is a need for me in the policy space and allowing me to become involved in ongoing projects as I transition back into veterinary school.

Sometimes, we find mentors in the most unlikely places. I will never forget the day I received an email from my NIH F30 Fellowship Program Officer, Dr. Bruce Fuchs, which asked me to call him immediately. Ultimately, he had seen a social media post in which I described my decision to finally seek professional mental health counseling. I want to thank him for sending that email, for checking in when many others wouldn't, for sharing his personal experiences, and for providing guidance as I went through difficult decision-making processes about my degree program. Dr. Fuchs was always confident in my capabilities and the impact I will have on my profession in the future. I am grateful that he re-iterated things I knew deep down to be true, that my non-academic career goals are valid and important, that my contributions are needed, and that I will have all of the degrees, tools, and skills that will make me successful in the spheres I want to pursue.

No acknowledgement section would be complete without thanking my therapists, Dr. Laurie Fonken and Jessie Charbonneau. Dr. Fonken heard some of my earliest concerns and validated them. However, I wish I had gone to therapy more regularly and from the very beginning. My battles with anxiety and depression were too big for just me, and I spent too long living in negative, unhealthy head spaces, crippled by my own mind, convinced that I could find the solutions to my own demons. I thank Ms. Charbonneau for providing me with actionable solutions and coping mechanisms and allowing me to accept what I cannot change and grow from my experiences. I thank her for allowing me to re-discover what it feels like to wake up with joy instead of dread.

Not enough words can describe what the many organizations that I have been involved with throughout my time thus far have done for me. This includes SAVMA, ROLE, GWIS, Science in Action, MIP GSO, National Science Policy Network, ComSciCon RMW, in addition to the professional societies of which I am a member including AVMA, AAAS, and ASM. These organizations were my lifeblood during my graduate education and I do not regret for one second the time I spent cultivating those relationships. They have made me a stronger scientist and individual. I have been able to grow my network of mentors and friends through these groups in ways I never would have imagined. They have provided me with some of my most valuable graduate experiences to date. They allowed me to maintain my passion, vision, sanity, drive, and self-worth when I did not always feel those within the laboratory. I am indebted to all that I have encountered through those groups for making them what they were and impacting me in such a profound way.

A huge thank you goes out to all the friends I have made along the way and the ones I have carried with me from other chapters in my life, both inside and outside of academic spaces. They have always been there to commiserate, empathize, uplift, and allow me to vent. The graduate student friends I have made within the MIP PhD Program, the DVM Program, the combined



DVM/PhD program, and across campus constantly remind me of the value of peer support, and I am grateful that I had the opportunity to form lasting friendships throughout my research journey. There are too many names to list, but they know who they are.

Now, there are other acknowledgments that may be a bit unconventional, but I fully believe they deserve mention. To the coffee shops, especially Mugs in Old Town and the Wild Boar, that provided me with endless food and coffee, to the baristas who learned my name and orders, who checked in on me when they saw me studying, writing, reading for hours on end. I thank them for providing spaces of productivity and community. I thank the Poudre Valley Health & Wellness Orchestra for allowing me to continue to play my French horn, which has always been a critical part of my life and identity. I also thank the Fort Collins Board Games & Brews group through which I have made some of my closest friends and which allowed me to remember there is a world outside of the academic walls by sharing laughs, drinks, and fun. A big thank you goes out to the Fort Collins Dance Fitness community, through which I found a passion I never knew I had, and which allowed me to rejuvenate and invigorate my physical health and my mind. It is rare that I feel like I can truly let go, and those classes are one of those times. To my dog, Tanner, for being one of my first Colorado companions and for the unconditional love. I also want to recognize the Colorado sunshine, wilderness, and beauty – this is a state I have come to love and will greatly miss when/if I leave. All these things helped me discover and re-iterate the importance of my self-worth outside of being an academic. They helped me maintain my whole self, something I hold as a high priority. Scientists are human, too.

My relationship with my fiancé Bryce has grown as my experience throughout my graduate program has morphed. He endured the late nights, long days, tears, frustration, anger, and excitement. I thank him for always allowing me to express myself but challenging me to think critically and differently about my lived experiences. He has always encouraged me to focus on

ways that I can be a better person, on my own growth, and to not let my emotions get the best of me. He is a true best friend and partner in ways I could have never anticipated, but for which I am eternally grateful.

Lastly, and most importantly, the biggest thank you goes out to my parents, my brother Levent, and my sister Leyla. My family always instilled the value of the pursuit of knowledge and encouraged my interest in science. They have always loved and supported me unconditionally, never allowing anything to dim my spark. My father, especially, opened my eyes to the world of academic research and showed me what effective mentorship in academia looks like. My mother showed me the importance and impact of community engagement and organizational mission. My sister helped me normalize and process my mental health, and her strength is unmatched. My brother has always been a role model for my drive and ambition. I am forever grateful for the privileges I was afforded during my life that brought me to this point and the strong family ties that built me.

For anyone or anything that I have forgotten – I have been touched, shaped, molded, impacted by so many people, places, and things. It has all led me here. My scientific journey to date has not been without struggle, and it is not the path that I would have anticipated, both with respect to the highs and the lows. However, the more I learn, the more I realize that rarely is a path straightforward. This has been my journey to live. I am proud of where I've been and excited for what is to come.

Thank you, all, from the bottom of my heart.

## DEDICATION

*To all graduate students who have ever felt undervalued, who have ever felt as though they don't belong, or who have been made to feel guilty for having passions and career aspirations outside of the laboratory: I see you. I hear you. This is for you.*

## TABLE OF CONTENTS

ABSTRACT .....	ii
ACKNOWLEDGEMENTS .....	v
DEDICATION.....	x
Chapter 1: Mycobacterium tuberculosis-Mediated Modulation of Immune Cell Metabolism in the Granuloma Microenvironment: A Review .....	1
Global TB Burden and Barriers to Progress in the Field .....	1
Complexities of Granuloma Lesion Pathology .....	2
Rise of Host-Directed Therapeutic Strategies to Combat TB .....	3
Immunometabolism as an HDT Target .....	4
HIF-1 $\alpha$ as a Transcriptional Regulator .....	5
Hypoxia Independent Activation of HIF-1 $\alpha$ by Iron Chelation .....	7
The Importance of Lactate as a Metabolite.....	9
<i>Production and Accumulation of Lactate</i> .....	9
<i>The Role of Lactate Shuttles</i> .....	11
<i>Lactate Facilitating Crosstalk Between Diverse Cell Types</i> .....	13
<i>Lactate Shuttling &amp; Metabolism as a Therapeutic Target</i> .....	15
<i>The Immunomodulatory Effects of Lactate</i> .....	16
The Importance of Lactate as a Signaling Molecule.....	18
<i>Introduction to GPR81</i> .....	18
<i>Diverse Roles of GPR81 Signaling</i> .....	19
Mtb Driven Establishment of a Survival Niche via Metabolic Interactions.....	21
References .....	24
Chapter 2: Hypoxia Independent Activation of HIF-1 $\alpha$ by Mycobactin During Early Mycobacterium tuberculosis Infection Augments Macrophage Metabolism .....	52
Summary .....	52
Introduction .....	53
Materials & Methods.....	56
<i>Bone Marrow Derived Macrophage (BMDM) Cell Culture</i> .....	56
<i>Purification of Mycobactin J</i> .....	56
<i>Mycobactin Knock-out Mtb Strains</i> .....	57
<i>Extracellular Flux Analysis</i> .....	57
<i>Western Blot</i> .....	58
<i>Data Analysis</i> .....	59
Results .....	59
<i>Iron chelation increases HIF-1<math>\alpha</math> levels and potently increases glycolytic metabolism in uninfected macrophages</i> .....	59
<i>Mycobactin biosynthesis is critical for augmenting metabolic phenotype in mouse BMDMs infected with Mtb</i> .....	65
Discussion.....	70
References .....	77
Chapter 3: Investigating the Role of a Lactate Shuttle Within the Tuberculosis Granuloma Microenvironment .....	86
Summary .....	86
Introduction .....	87
Materials & Methods.....	91
<i>Bone Marrow Derived Macrophage (BMDM) Cell Culture</i> .....	91
<i>Extracellular Flux Analysis</i> .....	91

<i>In vitro</i> infection with H37Rv Mtb.....	92
Bacterial Burden/CFUs .....	92
Cell viability.....	92
Guinea pig infection with H37Rv Mtb .....	93
Detection of Lactate .....	93
Western Blot .....	93
Data Analysis.....	94
Results .....	94
<i>Plasma lactate is increased in infected guinea pigs and lactate shuttle components are present within lung lesions.....</i>	94
<i>LDH and MCT inhibition significantly impacts the metabolism of uninfected murine macrophages .....</i>	97
<i>Lactate accumulates in the supernatant of Mtb infected macrophages, and inhibiting the lactate shuttle can reduce lactate levels accumulated in vitro.....</i>	100
Discussion.....	104
References .....	111
Chapter 4: Concluding Remarks and Future Directions.....	120

## CHAPTER 1: MYCOBACTERIUM TUBERCULOSIS-MEDIATED MODULATION OF IMMUNE CELL METABOLISM IN THE GRANULOMA MICROENVIRONMENT: A REVIEW

### 1. Global TB Burden and Barriers to Progress in the Field

*Mycobacterium tuberculosis* (Mtb) is the leading cause of death by an infectious agent worldwide, with 10 million new cases and 1.2 million deaths due to tuberculosis (TB) disease in 2018 alone according to the most recent World Health Organization (WHO) Global Tuberculosis Report.<sup>1</sup> While the death rate has steadily declined over the past twenty years, slowly approaching goals set forth by the WHO, the incidence of new cases has remained relatively constant.

There are multiple critical barriers that contribute to high global TB incidence and which have slowed the progression toward a disease cure. The rise of multi-drug resistance (MDR) complicates treatment options. MDR-TB does not respond to the two first line treatments rifampicin and isoniazid and recent years have seen the development of extensively drug-resistant TB (XDR-TB) which is additionally refractory to fluoroquinolones and injectable therapeutics used as second line treatments.<sup>1</sup> Current recommended TB treatment involves six to nine months of a multi-drug cocktail, which can cause severe side effects such as liver toxicity and peripheral neuropathies.<sup>2</sup> Treatment duration is significantly extended with MDR or XDR cases. Treatments are also costly and require prolonged periods of compliance. While direct observational therapy strategies and enhanced financial support can improve treatment compliance, the poor health care infrastructure and low socioeconomic status in countries with highest endemicity of disease hinder the ability of those afflicted to complete treatments.<sup>3-5</sup> The slow developmental pipeline for the approval of new drugs by the Food and Drug Administration (FDA) has limited the ability for novel pharmaceuticals to become commercially available. Current research investigating new treatment regimens or repurposing antimicrobials also face challenges

in translating findings from bench-top to bedside, with significant hurdles to bring a treatment from preclinical to clinical application.<sup>2,6</sup>

An additional factor that complicates disease progression and treatment is the occurrence of co-morbidities of TB with both communicable and non-communicable diseases. Diseases such as HIV/AIDS and type 2 diabetes mellitus (T2DM), which also have high incidence in TB endemic regions, augment individual susceptibility to TB infection and worsen clinical outcomes of those with TB disease.<sup>7,8</sup> Specifically, T2DM accelerates the progression of TB disease, enhances the proinflammatory cytokine response, and results in more severe inflammation in the guinea pig model.<sup>9</sup> The interaction between multiple pathogenic disease processes severely impacts already high-risk populations and further exacerbates an already complex chronic disease progression. The Bacillus Calmette-Guérin (BCG) vaccine, while widely used to prevent disseminated TB in young children, is not effective against adult pulmonary TB.<sup>10</sup> Further, many individuals that are infected with TB will become latently infected, and may not show clinical signs for decades. It is still unclear what causes a latent Mtb infection to reactivate, and existing diagnostic capabilities to identify latent Mtb infections are limited.<sup>11,12</sup>

## **2. Complexities of Granuloma Lesion Pathology**

The nature of the granuloma lesion microenvironment also impacts TB research efforts. TB disease is characterized by pulmonary granulomatous inflammation.<sup>13,14</sup> The classic TB granuloma is comprised of a central core of macrophages, surrounded by a cuff of lymphocytes. As disease progresses, lesions undergo varying levels of necrosis, fibrosis, and mineralization. Mtb is not only present intracellularly within macrophages, but is present in extracellular populations as a result of extensive necrosis and release of bacteria from cells, and these populations have different responses to drug treatment.<sup>15-17</sup> Importantly, there is significant lesion heterogeneity between and within individuals, dependent upon both host and pathogen factors.<sup>18-</sup>

<sup>21</sup> This inherent lesion complexity and diversity contributes to the difficulty in translating research findings as not all animal models develop lesions in the same manner. For example, typical mouse models like C57BL/6 and BALB/c, do not develop central necrosis and hypoxia while guinea pig, non-human primate, and human lesions do.<sup>22</sup> As infected macrophages are walled-off within the granuloma structure, Mtb persists and Mtb antigens chronically stimulate the immune system. Debate still exists within the field regarding whether the granuloma lesion is a protective structure, containing bacterial dissemination and localizing infection, or if the lesion is harmful, masking the bacteria from immune infiltrates, limiting blood supply and therefore effective drug delivery, and limiting oxygen availability and resulting in the development of hypoxic, necrotic lesion cores.<sup>23-25</sup>

### **3. Rise of Host-Directed Therapeutic Strategies to Combat TB**

To combat difficulties in developing effective treatments and to address the debate of whether granuloma lesion development is protective or destructive, many in the field have shifted to the development of host-directed therapeutic (HDT) strategies. HDT involves developing treatments or repurposing previously approved compounds to target the host rather than the pathogen. In this way, HDT can shift host responses to be better equipped to combat infectious agents and can circumvent issues with antimicrobial resistance. The applicability of HDT to the treatment of TB has been extensively reviewed.<sup>26-31</sup> HDT for TB have included using corticosteroids for their anti-inflammatory properties, targeting angiogenesis to improve vascular perfusion to the granuloma lesion, and promoting tissue healing through matrix metalloproteinase activity.<sup>28</sup> Specifically, metformin, a biguanide and weak mitochondrial complex I inhibitor, has long been used as a primary treatment for patients with T2DM and has recently been explored as an HDT for TB. Metformin can restrict intracellular Mtb growth, induce mitochondrial reactive oxygen species production, reduce TB pathology and inflammatory cytokine expression, and decrease the risk of developing active TB in patients with T2DM.<sup>32-36</sup>



One additional area of interest has been augmenting immune cell metabolism. Cellular metabolism has been tightly linked to the development of chronic disease processes and different metabolic phenotypes correlate to different immune response phenotypes. The field of immunometabolism has seen a resurgence as more and more metabolites and metabolic processes are observed to regulate cellular response and signaling during both infectious and non-infectious disease processes.<sup>37-41</sup>

#### **4. Immunometabolism as an HDT Target**

A key finding at the interface of cell metabolism and disease progression was made by Otto Warburg in the 1950s.<sup>42-44</sup> Under normoxic conditions, cells typically rely on oxidative phosphorylation and the mitochondrial electron transport chain to generate energy in the form of ATP. This oxygen dependent metabolic process can be compromised when oxygen tension drops. As a result, cells shift to rely on glycolytic metabolic pathways, which do not require oxygen, to generate ATP. While less efficient, glycolysis allows cells to survive in conditions of hypoxia. This process generates lactate, which allows cells to regenerate NAD<sup>+</sup> to maintain glycolytic flux.<sup>45,46</sup> Warburg demonstrated that cancer cells are capable of a metabolic shift from oxidative phosphorylation to glycolysis, even in the presence of oxygen.<sup>42,43</sup> This effect deemed “aerobic glycolysis” or “The Warburg Effect” has now been described in multiple disease processes and is characteristic of immune cell activation phenotypes.<sup>47-50</sup> Contrary to Warburg’s original observations, it is now understood that mitochondrial metabolism does not shut down completely, but rather there is a relative increase in glycolytic metabolism.<sup>51-53</sup>

Specifically, in macrophages, immune cell phenotype is related to metabolic phenotype. Classically activated M1 macrophages are characterized by a highly glycolytic metabolic phenotype and are pro-inflammatory. They contribute to tissue damage and additional immune cell recruitment by the production of cytokines like IL-1 $\beta$ , IL-6, TNF- $\alpha$ , IFN- $\gamma$ .<sup>40,54,55</sup> In contrast, M2

macrophages have an anti-inflammatory role, contributing to tissue remodeling and tissue repair, and their metabolism is more oxidative in nature.<sup>40,54,55</sup> There is significant metabolic heterogeneity within macrophages associated with TB granulomas, including activated, inflammatory macrophages with an M1 phenotype, lipid laden foamy macrophages with increased fatty acid metabolism, epithelioid macrophages, multinucleated giant cells, and macrophages that exhibit an M2 phenotype and play a role in granuloma architecture remodeling.<sup>56</sup> The balance between M1 and M2 macrophage metabolic phenotypes can dictate chronic disease progression and maintenance of lesions. However, recent work indicates that macrophage subsets may not be as stable or concrete as once described, with cells responding to a combination of stimuli and sometimes expressing M1 and M2 signatures simultaneously.<sup>57,58</sup> Relevant to TB, alveolar macrophages were found to have a hybrid phenotype, expressing both M1 and M2 surface markers in healthy individuals, and this flexibility was posited to be helpful in maintaining a balance between protective immunity and tolerance within alveoli.<sup>59</sup>

## **5. HIF-1 $\alpha$ as a Transcriptional Regulator**

In part, the regulation of this metabolic shift occurs at the transcriptional level via hypoxia-inducible factor 1 (HIF-1). HIF-1 is a transcription factor that globally regulates the cellular response to hypoxic stress.<sup>60-62</sup> HIF-1 responsive genes are involved in angiogenesis, erythropoiesis, cell survival, and importantly, cellular metabolism.<sup>63</sup> The function of HIF-1 under normoxic and hypoxic conditions has been extensively studied. Under normoxic conditions, the HIF-1 $\alpha$  subunit is hydroxylated at proline residues by prolyl hydroxylases (PHDs).<sup>64-66</sup> This hydroxylation sequence tags HIF-1 $\alpha$  for ubiquitination via the von Hippel-Lindau factor and subsequent proteasomal degradation.<sup>64-66</sup> However, PHDs require oxygen as a cofactor for their activity. As a result, under conditions of hypoxia, HIF-1 $\alpha$  is not hydroxylated and is not degraded.<sup>64-66</sup> HIF-1 $\alpha$  can thus accumulate in the cytoplasm and translocate to the nucleus where it dimerizes with the HIF-1 $\beta$  subunit.<sup>64-66</sup> The active HIF-1 transcription factor then binds to hypoxia response elements in the

genome to transcribe genes which regulate glycolysis, as well as the production and transport of lactate (Figure 1.1).

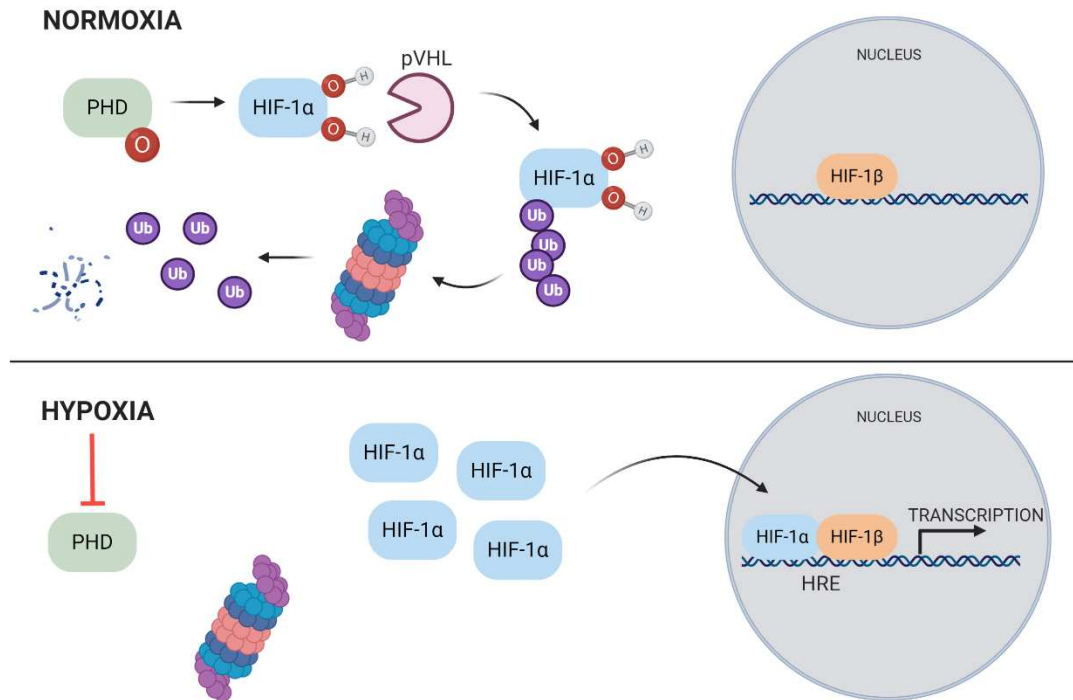


**Figure 1.1: HIF-1 $\alpha$  is stabilized under conditions of hypoxia.** Under normoxic conditions (top panel), prolyl hydroxylase (PHD) is functional due to the presence of oxygen. PHD can then hydroxylate proline residues on HIF-1 $\alpha$ , which tags it for ubiquitination via the von Hippel-Lindau factor (pVHL). This leads to subsequent proteasomal degradation. However, under conditions of hypoxia (bottom panel), low oxygen tension inhibits PHD activity. HIF-1 $\alpha$  is not tagged for degradation and accumulates within the cytoplasm. It can then translocate to the nucleus, dimerize with the HIF-1 $\beta$  subunit, and bind to hypoxia responsive elements (HRE) on the genome. This initiates the transcription of a myriad of genes involved with the host adaptation to hypoxia.

Multiple studies have demonstrated that HIF-1 $\alpha$  is expressed and active within TB lesions.<sup>67–73</sup> In zebrafish infection models using *Mycobacterium marinum*, HIF-1 $\alpha$  stabilization enhances IL-1 $\beta$  expression, and helps clear infections via activating neutrophils.<sup>74–76</sup> Deletion of HIF-1 $\alpha$  in myeloid cells accelerates granuloma necrosis and impairs host responses to *Mycobacterium avium* infection in mouse models.<sup>77</sup> Interestingly, in mice deficient of HIF-1 $\alpha$  only in the myeloid lineage of cells, deletion of HIF-1 $\alpha$  in chronic infection resulted in more extensive inflammation in

interstitial lung and caused earlier death, indicating HIF-1 $\alpha$  coordinates myeloid cell responses to Mtb.<sup>72</sup> Additionally, the metabolic shift to glycolysis has been observed in the context of *in vitro* macrophage Mtb infection at early time points.<sup>67,78–80</sup>

## 6. Hypoxia Independent Activation of HIF-1 $\alpha$ by Iron Chelation

The early time points at which glycolysis is upregulated during Mtb infection, however, are prior to the formation of chronic hypoxic lesion microenvironments. Interestingly, HIF-1 $\alpha$  can be activated under normoxic conditions by a variety of mechanisms. Cytokines<sup>81,82</sup>, chemicals<sup>83–85</sup>, metabolites<sup>86–88</sup>, and iron chelation<sup>89,90</sup> are all capable of stabilizing HIF-1 $\alpha$  by interfering with PHDs. Additional mechanisms are independent of hydroxylation, such as via protein kinase A (PKA) mediated phosphorylation of HIF-1 $\alpha$ .<sup>91,92</sup>

Specifically, the chelation of iron is relevant in the immune response to pathogens. Limiting iron availability is one of the first responses of the innate immune system.<sup>93–97</sup> Iron is a critical cofactor and metal for bacterial survival.<sup>98,99</sup> As a result, bacteria have evolved to produce iron chelating molecules of their own, called siderophores.<sup>100–103</sup> Mtb produces both a membrane bound siderophore, mycobactin, and a soluble siderophore, carboxymycobactin, which possess greater iron binding capacities than host iron-chelating molecules.<sup>104–109</sup> As a result, Mtb can efficiently scavenge iron away from its macrophage hosts. The chelation of iron away from labile host iron pools is capable of interfering with PHD activity, for PHDs require iron in addition to oxygen to perform their proline hydroxylating activity.<sup>110–112</sup> Bacterial iron chelators, such as deferoxamine (DFO) produced by *Streptomyces pilosus*, have been approved by the FDA for the treatment of iron overload disorders such as beta-thalassemia<sup>113–115</sup> Exogenous iron chelation treatment using DFO can upregulate macrophage glycolytic metabolism during Mtb infection and induce IL-1 $\beta$  production in a HIF-1 $\alpha$  dependent manner.<sup>116</sup> Importantly, intracellular Enterobacteriaceae species have been demonstrated to upregulate HIF-1 $\alpha$  via a hypoxia-independent mechanism,

via their siderophores.<sup>117</sup> Specifically, when the biosynthesis of siderophores produced by intracellular bacteria *Yersinia enterocolitica* and *Salmonella enterica* was knocked-out, stable HIF-1 $\alpha$  was significantly reduced.<sup>117</sup> This points to a pathogen driven mechanism of modulating cellular metabolism in a way that benefits their intercellular survival and primes the microenvironment to be able to withstand future hypoxic conditions.

The downstream metabolic impact of HIF-1 $\alpha$  is multifactorial. Pyruvate dehydrogenase kinase-1 is transcribed by HIF-1 $\alpha$ , and prevents the metabolism of pyruvate and its entry into the mitochondria and increases extracellular lactate at higher than normal concentrations when active.<sup>118</sup> HIF-1 $\alpha$  also controls expression of max interactor 1 and cytochrome c oxidase subunit 4, which further represses mitochondrial activity and decreases oxygen consumption during hypoxic conditions.<sup>119</sup> Not only does HIF-1 $\alpha$  directly upregulate the transcription of enzymes involved in the glycolytic metabolic pathway, but it upregulates the production of lactate dehydrogenase A (LDHA) and monocarboxylate transporter 4 (MCT4).<sup>120–124</sup> LDHA drives the production of lactate from pyruvate and MCT4 is responsible for lactate export from cells. Lactate itself, through its metabolism to pyruvate, can directly interfere with the proteasomal degradation of HIF-1 $\alpha$  and carbohydrate response elements are present in several glycolytic genes.<sup>125</sup> For a long time, lactate was believed to be a metabolic waste product. However, it has become increasingly clear that lactate serves a role in driving cellular metabolic changes that impact immune cell phenotypes, and that it can function as an extracellular signaling molecule to coordinate autocrine and paracrine responses to diverse microenvironments (Figure 1.2).

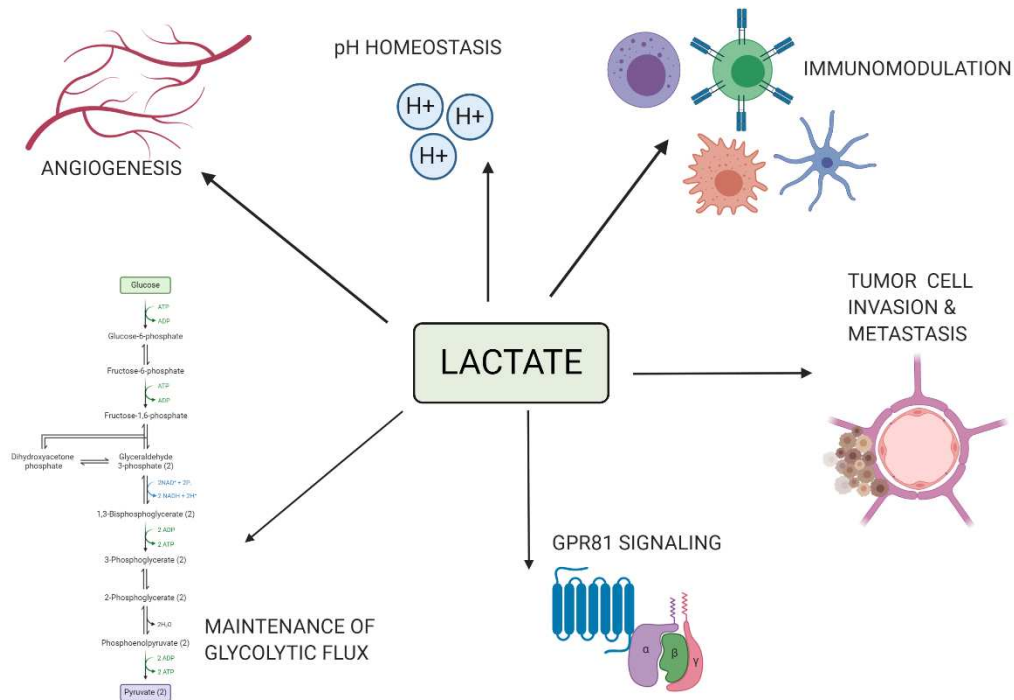


**Figure 1.2: Lactate has a diverse role as both a metabolite and signaling molecule.** Lactate has been demonstrated to impact many cellular processes, including angiogenesis, maintenance of pH homeostasis, modulation of immune cell function, invasion and metastasis of tumor cells, signaling through G protein coupled receptor 81 (GPR81), and maintaining glycolytic flux through the regeneration of NAD<sup>+</sup>. All these processes contribute to disease pathogenesis in several contexts.

## 7. The Importance of Lactate as a Metabolite

### 7.1. Production and Accumulation of Lactate

The promoter for lactate dehydrogenase A (LDHA), which catalyzes the conversion of pyruvate into lactate, has a binding site for HIF-1 $\alpha$ .<sup>122,123,126</sup> LDH isoforms are comprised of either all A subunits (pyruvate  $\rightarrow$  lactate), all B subunits (lactate  $\rightarrow$  pyruvate), or a combination of both. While LDH is present in all tissues, the ratio of LDHA to LDHB subunits is tissue specific.<sup>127</sup> Isoforms with only LDHA subunits have the highest efficiency to convert pyruvate to lactate and are correlated with increased HIF-1 $\alpha$  expression, increased VEGF, enhanced metastatic potential, enhanced tumor size, and poor prognosis in cancer<sup>128–130</sup>. However, some researchers do not believe the LDH enzyme distribution has an impact on the cell's ability to produce or use lactate,

but rather affects the rate of the equilibrium of the reaction.<sup>131</sup> LDH has a prognostic role in solid tumors, with high LDH associated with poor progression free survival and lower disease free survival.<sup>132</sup> LDH has also been detected in elevated levels in bronchoalveolar lavage (BAL) fluid of active pulmonary TB patients, and BAL LDH correlates with increased serum LDH.<sup>133</sup> Interestingly, sputum positive cases of TB show increased serum levels of LDH1, LDH2, and LDH3, which contain four, three, or two B subunits, respectively.<sup>134</sup> This indicates that LDH levels and isoform specificity may also be diagnostic or prognostic indicators for TB.

Much of what is known about the role of lactate comes from extensive reviews of the tumor microenvironment.<sup>135,136</sup> Lactate accumulates in the tumor microenvironment both in hypoxic solid tumors and during aerobic conditions due to the Warburg Effect, and malignant transformation is associated with increases in glycolytic flux.<sup>125</sup> Lactate enhances the release of macrophage pro-angiogenic factors, increases metastatic activity, enhances collagen deposition, and worsens cancer prognosis.<sup>137,138</sup> Lactate is also capable of diffusing from solid tumors and malignant cells to stimulate tumor associated fibroblasts, generating extracellular matrix rearrangement which allows for tumor cell migration and increases in tumor cell mobility.<sup>125</sup> Interestingly, oxidative cancer cells are sensitive to lactate signaling whereas glycolytic cancer cells are not and do not take up lactate and do not respond to exogenous lactate treatment.<sup>139</sup> While cancer fields have led the effort in understanding the role of lactate in modulating disease pathogenesis, much learned from this work can be applied in the realm of infectious disease. Early in Mtb infection, shifts to glycolytic metabolism are observed within macrophages leading to increased lactate production<sup>67,78-80,140</sup> and high lactate concentrations are observable within granuloma lesions, reaching levels comparable to tumors.<sup>141,142</sup>

## 7.2. *The Role of Lactate Shuttles*

Lactate was largely considered to be a metabolic waste product of glycolysis until the 1980s, when the shuttling of lactate between cells and tissues was first described.<sup>143–148</sup> One of the first described lactate shuttles was within muscle, with fast-twitch, glycolytic muscle fibers accumulating and releasing lactate and slow-twitch, oxidative muscle fibers importing and metabolizing lactate for energy.<sup>149–151</sup> Mitochondria have a role to play in shuttling lactate intracellularly, with LDH enzymes present in the mitochondrial intermembrane space and in the mitochondrial matrix, and monocarboxylate transporters (MCTs) present in the inner mitochondrial membrane to transfer lactate.<sup>149,152,153</sup> This is further evidenced by LDHB localizing to the mitochondria at greater densities than to other locations, and LDHA not localizing to the mitochondria.<sup>154</sup> Additionally, mitochondrial LDH is highly expressed and more active in cancerous prostate cells than normal ones, contributing to the anaplerosis of TCA cycle intermediates to help fuel cancer progression.<sup>155</sup> However, some have demonstrated that lactate must be first converted to pyruvate before it can enter the mitochondrial matrix and have challenged the hypothesis that lactate can be directly oxidized by mitochondria.<sup>156,157</sup> Lactate shuttles have also been described between astrocytes and neurons, and mitochondrial LDH has been shown to play a role in allowing astrocytes to use lactate in the production of ATP via oxidative phosphorylation.<sup>158,159</sup> Lactate has been demonstrated in multiple studies to be effectively metabolized by cancer cells and, in some instances, lactate is preferentially metabolized over other energy sources such as glucose<sup>160,161</sup>

Monocarboxylate transporters (MCTs) are responsible for shutting lactate across membranes. Multiple MCTs exist, and cellular expression of MCTs depends on the physiological role of the cell.<sup>162,163</sup> Highly glycolytic cells express MCT4, a low affinity transporter adapted to the export of lactate, while more oxidative cells predominantly express MCT1, which has a higher substrate affinity and is adapted for lactate import.<sup>164,165</sup> MCT1 has been demonstrated to be expressed in



macrophages and increased upon LPS, TNF- $\alpha$ , or NO treatment.<sup>166</sup> The expression of MCT1 and MCT4 is associated with the expression of the chaperone CD147, which has transmembrane and cytoplasmic domains that interact with MCTs and help organize their distribution and localization on the plasma membrane.<sup>165,167</sup> CD147 has pro-tumoral effects via its control of lactic acid transport, and knocking down CD147 reduces MCT1 and MCT4 expression and reduces the glycolytic rate by 50%.<sup>168</sup> The invasive capability of human lung cancer cells was correlated with the expression of MCT1 and MCT4 and proliferation was reduced when these MCTs were inhibited.<sup>169</sup> Importantly, MCT4 is hypoxia-inducible, exhibiting 3-5 fold mRNA increases during hypoxia and showing significantly higher tissue expression in hypoxic areas as shown by colocalization with pimonidazole staining.<sup>121,168</sup> CD147 expression has also been demonstrated to be regulated by HIF-1 $\alpha$ , promoting glycolysis and inhibiting tumor cell apoptosis.<sup>170,171</sup> In some cancers, MCT1, MCT4, and CD147 have been identified as prognostic biomarkers which predicts poor patient survival.<sup>172-174</sup>

The lactate shuttle hypothesis posits that a metabolic symbiosis between hypoxic and oxidative tumor cells exists, wherein hypoxic, glycolytic cells produce lactate at high levels, and this lactate is transported to oxidative tumor cells, which convert lactate back into pyruvate to fuel their metabolism, and conserve glucose for hypoxic cells.<sup>175</sup> (Figure 1.3). Metabolically distinct cell populations should have unique signatures showing different expression levels of relevant metabolic enzymes and transporters, with glycolytic cells having increases in MCT4, LDHA, HIF-1 $\alpha$ , while oxidative cells will have MCT1, LDHB, and will accumulate lactate.<sup>176</sup> Metabolic modulations which characterize the TB granuloma are similar to those described to occur within the tumor microenvironment. Therefore, these enzyme and transporter expression profiles which occur in different regions of the tumor microenvironment may directly apply to different regions of the granuloma microenvironment. However, an evaluation of the expression of these targets in the granuloma has not yet been described.

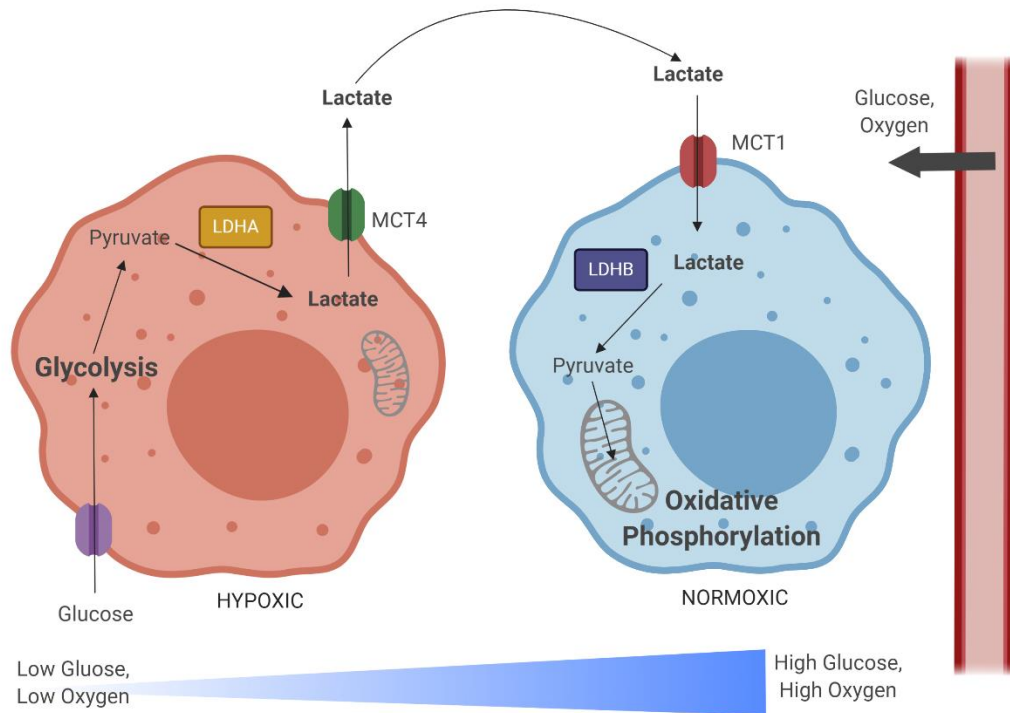


**Figure 1.3: The lactate shuttle hypothesis illustrates a metabolic relationship between hypoxic and normoxic tumor cells.** As glucose and oxygen diffuse out of tumor vascular supply, a gradient develops, with normoxic regions developing closer to the periphery and hypoxic regions developing within the lesion core. Hypoxic cells import glucose and rely on the glycolytic metabolic pathway to generate pyruvate. Pyruvate is converted to lactate by lactate dehydrogenase A (LDHA), and then exported in large quantities by monocarboxylate transporter 4 (MCT4). This lactate is imported by normoxic cells via monocarboxylate transporter 1 (MCT1). These normoxic cells preserve glucose that is otherwise needed for hypoxic cell metabolism and instead convert lactate back into pyruvate via lactate dehydrogenase B (LDHB). This lactate-derived pyruvate can then be used as fuel for the TCA cycle, oxidative phosphorylation, and mitochondrial respiration.

### 7.3. Lactate Facilitating Crosstalk Between Diverse Cell Types

Other cell types also interact to shuttle and utilize lactate. Lactate modulates endothelial cells, and MCT1 driven lactate uptake in endothelial cells leads to significant increases in IL-8 production through the NF $\kappa$ B-pathway.<sup>177</sup> Additionally, lactate released from cancer cells via MCT4 stimulates IL-8 production, tumor angiogenesis, and tissue perfusion, supporting a model where tumor cell lactate can stimulate angiogenesis in endothelial cells.<sup>177</sup> The impact of lactate on angiogenesis has been shown to be critical for the acceleration of healing in ischemic wounds,

preventing muscle atrophy, and stimulating the production and release of angiogenic factors such as IL-8, bFGF, VEGF and VEGFR.<sup>178,179</sup> Crosstalk between cancer cells and endothelial cells via lactate release and MCT transport of lactate has also been demonstrated in glioma models.<sup>180</sup>

In what has been deemed the “Reverse Warburg Effect,” cancer cells secrete hydrogen peroxide, which induces oxidative stress in cancer associated fibroblasts, causes them to undergo aerobic glycolysis in response, which produces large amounts of lactate that is then shuttled to tumor cells to fuel mitochondrial oxidative phosphorylation.<sup>181–184</sup> Further evidence of this is that MCT4, which exports lactate, is present in cancer associated fibroblasts and is upregulated by oxidative stress, and cancer cell MCT1 is upregulated when co-cultured with fibroblasts.<sup>181–184</sup> This metabolic synergy between cancer associated fibroblasts and cancer cells allows carcinomas that have been highly infiltrated by reactive stromal cells to shift stromal metabolism to produce large quantities of lactate and export it via MCT4, and allow tumor cells to exploit the lactate produced, via MCT1 influx, and use it to fuel metabolism under glucose limited environments.<sup>185,186</sup> Lactate stimulates MCT1 expression in stromal cells, but reduces it in tumor cells, further suggesting that lactate is exported by tumor cells and taken up by stromal cells.<sup>187</sup> Thus, the metabolic perturbations within the tumor microenvironment create spatial gradients based on differential sensitivity to lactate between cancer cells and stromal cells, such as tumor associated macrophages, and restricted perfusion contributes to these metabolic gradients, with cancer cells able to survive better in high lactate, hypoxic regions.<sup>188</sup> Spatial gradients exist within the context of the TB granuloma, with different immune transcript and proteomic profiles within necrotic, central regions as compared to the rim of the granuloma.<sup>189,190</sup> There is also an oxygen tension gradient and impaired perfusion, leading to hypoxia within the center of granuloma lesions. Based on similarities between the granuloma and tumor microenvironments, it is likely that spatial differences in lactate metabolism and diverse crosstalk between heterogeneous cell types exists within the context of the TB granuloma.

#### 7.4. *Lactate Shuttling & Metabolism as a Therapeutic Target*

Importantly, the lactate shuttle has been explored as a therapeutic target for diseases such as cancer, as lactate is a key regulator for carcinogenesis<sup>135,191–195</sup>. To exploit the need for glycolytic and oxidative tumor cells to shuttle lactate, researchers have explored MCT1 inhibition with  $\alpha$ -CHC and have demonstrated that MCT1 inhibition can slow tumor progression and growth.<sup>175</sup> Lactate, released in the hypoxic tumor cell compartment, fuels the oxidative metabolism of cells that are in more vascularized, oxidized regions. This spares glucose for use in the hypoxic cells which depend heavily on glycolysis. Inhibiting MCT1 thus induces a switch in oxidative cells from lactate fueled respiration to glycolysis; hypoxic cells die from glucose starvation, and cells that remain are more oxygenated and more susceptible to chemotherapies and radiation.<sup>175,196</sup> In malignant glioma, silencing MCTs decreases lactate efflux, and induces apoptosis and necrosis.<sup>197</sup> Activated T cells rely on glycolysis for energy, produce increased amounts of lactate, have higher MCT1 and MCT4 expression than resting cells, and as a result blocking lactate transport via MCT1 inhibits rapid phases of T cell division.<sup>198</sup> Targeting MCT1 in endothelial cells can block the activation of HIF-1 $\alpha$  by preventing lactate uptake and its conversion to pyruvate by LDHB, which subsequently competes with 2-oxoglutarate to inhibit PHDs needed to degrade HIF-1 $\alpha$ .<sup>199</sup> This also blocks the downstream activation of angiogenesis. Inhibiting MCT1 can impair glycolysis and upregulate mitochondrial metabolism, improving the cellular bioenergetic state.<sup>200</sup> Additionally, disrupting CD147, and therefore MCT1 and MCT4 expression, can sensitize lung cancer cells to biguanides like phenformin and metformin.<sup>201</sup> Sensitization to phenformin could also be achieved by genetic knock out of MCT1 and CD147.<sup>202</sup> MCT1 knockdown is more effective in hypoxia, resulting in larger decreases in lactate levels, cell biomass, cell invasion, and drastic reduction in breast cancer growth, and treatment with metformin could increase the response/efficacy of the MCT1 inhibition.<sup>203</sup> Inhibiting MCTs has yet to be explored in the context of Mtb infection.

Targeting LDHA has also been investigated.<sup>204</sup> LDHA inhibition was found to increase apoptosis of A549 cancer cells.<sup>205</sup> Inhibiting LDHA with compound FX11 decreased ATP levels, reduced mitochondrial membrane potential, increased oxidative stress linked to cell death, activated AMPK, and inhibited tumor xenograft progression in transformed human B cell lymphoma.<sup>206</sup> Recent work demonstrates that inhibiting LDH via FX11 reduces the bacterial burden in Mtb infected mouse lungs, reduces the number of necrotic lesions, and potentiates isoniazid treatment.<sup>207</sup> Simultaneously inhibiting LDHA via sodium oxamate and respiratory complex I via metformin depletes the cellular ATP pool, causing cancer cells to undergo metabolic catastrophe, leading to tumor cell growth arrest and cell death, leading to significant decreases in tumor size.<sup>208</sup> LDH inhibition via oxamate can also activate AKT/mTOR pathways to induce autophagy, and antagonize apoptotic cell death in cancers.<sup>209</sup> Mtb is able to oxidize lactate via a quinone-dependent L-lactate dehydrogenase and, interestingly, lactate oxidation appears to be required for intracellular Mtb growth.<sup>210</sup> Inhibiting macrophage production of lactate may therefore be a viable host-directed therapeutic strategy for combating Mtb infection.

### 7.5. *The Immunomodulatory Effects of Lactate*

Lactate also has distinct immunomodulatory effects.<sup>211</sup> Accumulated lactate in the tumor microenvironment, which can reach up to 40 mM concentrations, decelerates energy metabolism and induces suppressed phenotypes in infiltrating T cells by decreasing antigen-specific proliferation, and impairing T cell production of IL-1, IFN- $\gamma$ , perforin and granzyme B.<sup>212,213</sup> Lactate inhibits CD4<sup>+</sup> T cell chemotaxis, induces IL-17 production, and inhibits CD8<sup>+</sup> T cell cytolytic activity.<sup>214</sup> Macrophage LDHA is critical for macrophage dependent activation of antitumor CD8<sup>+</sup> T cells and boosts IL-17 mediated immunity.<sup>215</sup> IFN- $\gamma$  producing CD4 T cells are predominant responders in antimycobacterial immunity; however, their role in TB pathogenesis is complex and these cells can stimulate neutrophil and macrophage mediated disruption of granuloma tissue architecture.<sup>216</sup> Cytolytic CD8 T cell function plays a critical role in Mtb infection, especially for

long term control of infection.<sup>217</sup> Th-17 cells also play a diverse role in the pathogenesis of Mtb infection, particularly through their recruitment of neutrophils to the site of infection.<sup>218,219</sup>

Regulatory T cells (Tregs) are resistant to the suppressive effects of lactate on effector T cells, making these populations better able to survive in high lactate environments and assist in cancer immune evasion.<sup>220</sup> Tregs can antagonize the protective cellular immunity of Th1 and Th17 responses, which could result in loss of control of TB disease and the production of anti-inflammatory mediators early in infection could enhance mycobacterial growth by suppressing the immune response.<sup>221</sup> However, Tregs are also required to control inflammation, especially in prevention of autoimmune disorders. Interestingly, the regulation of the Th-17 versus Treg balance has been demonstrated to be a result of HIF-1 $\alpha$  regulation.<sup>222,223</sup> It is clear that a delicate balance of T cell regulation is key to the enhancement or resolution of TB pathology, and lactate accumulated within the granuloma may play a critical role in augmenting this balance.

NK cell production of granzyme B and perforin is also reduced in the presence of lactate, and NK cells treated with lactate express fewer activation receptors.<sup>224</sup> Additionally, LDHA deficient tumors have significantly higher NK cell activity and fewer myeloid derived suppressor cells present.<sup>224</sup> Tumor derived LDH can induce NK cell ligands on myeloid cells, which causes NK cells to downregulate associated receptors and impairs their anti-tumor activity.<sup>225</sup> The high levels of lactic acid that inhibit CD8 T cell and NK cell activity is mainly through the inhibition of the transcription factor NFAT.<sup>226</sup> NK cells are known to play a role in Mtb infection, via cytotoxic release of perforin and granzyme as well as through activation of macrophages and enhancing phagolysosomal fusion via IL-22 and IFN- $\gamma$  production.<sup>227</sup>

Tumor derived lactate also significantly inhibits monocyte TNF- $\alpha$  secretion, impairs monocyte glycolytic flux, stimulates macrophage VEGF and TGF $\beta$ , upregulates monocyte IL-23 production,

and inhibits the differentiation of monocytes to dendritic cells.<sup>228,229</sup> Migration of monocytes is inhibited, while the migration of cancer cells is enhanced in lactate enriched environments, further contributing to tumor immune escape.<sup>229</sup> Mtb is also capable of escaping the immune system through inhibiting phagolysosomal fusion, inhibiting apoptosis, reducing antigen presentation, and impairing dendritic cell maturation and migration.<sup>230–232</sup> In the presence of lactate, GM-CSF activated macrophages are not able to produce pro-inflammatory cytokines and lactate facilitates tumor associated macrophages to undergo M2 polarization, even diverting differentiation of monocytes from dendritic cells toward M2 macrophages.<sup>233–236</sup> This would reduce antigen presentation and induce tissue remodeling. Lactic acid can also interfere with TLR signaling and delay the chemokine and cytokine response to LPS stimulated inflammation<sup>237</sup> Deleting LDHA in specific tumors reverses immunosuppression in the tumor microenvironment, likely through reduced PD-L1 and VEGF.<sup>215</sup> The anti-inflammatory nature of lactate has also been demonstrated in models of intestinal inflammation, whereby treatment with lactate prevented TNBS induced colitis, reduced epithelial damage and edema, decreased the production of circulating IL-6, and prevented bacterial translocation to the liver.<sup>238</sup> Thus, lactate likely plays a critical role in regulating monocytes, macrophages, and dendritic cells critical for initial responses to Mtb infection and antigen presentation. Lactate's role in modulating immune cell energetics and cellular phenotype points to more than just a role as an intermediary in metabolism, but points to critical roles in cell-cell signaling.

## **8. The Importance of Lactate as A Signaling Molecule**

### *8.1. Introduction to GPR81*

Lactate is one of many metabolites which signals through G-protein coupled receptors.<sup>239–242</sup> Lactate was revealed to be an endogenous ligand for GPR81 through the discovery that GPR81 activation in adipose tissue suppressed lipolysis and mediated insulin-induced antilipolytic effects in an autocrine fashion.<sup>243–246</sup> GPR81 is expressed in brown fat, white fat, kidney, liver, skeletal

muscle, brain, and lung, among other tissues and expression profiles are similar across mouse and human tissue.<sup>244</sup> Receptor structural residues are also conserved across species from humans to zebrafish.<sup>247</sup> GPR81 is coupled to a Gi subunit, which inhibits adenylyl cyclase, decreasing intracellular cAMP and causing protein kinase A (PKA) to be less active.<sup>243,248</sup> Downstream signaling of GPR81 also activates the ERK1/2 pathway, PKC, PI3K, and Src kinases.<sup>249</sup> As previously mentioned, PKA has the ability to activate HIF-1 in a hypoxia-independent manner.<sup>91,92</sup> Interestingly, since elevated cAMP and PKA signaling inhibits IFN- $\gamma$  secretion by T cells during Mtb infection, activation of GPR81 may be a viable strategy to enhance Mtb directed immunity.<sup>250</sup> Thiazolidinediones such as rosiglitazone can induce the expression of GPR81 through PPAR $\gamma$ .<sup>248</sup> PPAR $\gamma$  has been demonstrated to have a role in Mtb infection, as knock-out of PPAR $\gamma$  in lung macrophages reduces Mtb growth and reduces granulomatous inflammation.<sup>251</sup> Mtb also limits host cell apoptosis through PPAR $\gamma$  induction.<sup>252</sup> Multiple agonists of GPR81 have been identified, some of which are commercially available, including 3-chloro-5-hydroxybenzoic acid and 3,5 dihydroxybenzoic acid (DHBA).<sup>253–257</sup> These agonists have been investigated as alternative dyslipidemic agents to niacin, which signals through GPR109A and causes an undesired flushing reaction due to prostaglandin activation of Langerhans cells, but have yet to be actively explored as therapeutics for infectious disease applications.<sup>253–255</sup>

## 8.2. Diverse Roles of GPR81 Signaling

GPR81 plays a role in signal transduction across multiple body systems. Inflammation in adipose tissue initiated by LPS, zymosan, or turpentine stimuli resulted in the decreased expression of GPR81.<sup>258</sup> GPR81 is also downregulated when adipocytes are exposed to macrophage derived inflammatory mediators via conditioned media.<sup>259</sup> Further, lactate suppresses the induction of the NLRP3 inflammasome and IL1 $\beta$  via GPR81 activation, regulates TLR activation via interactions with arrestin B2 downstream of GPR81, and protects against inflammatory injury in pancreatitis and hepatitis models through GPR81 signaling.<sup>260</sup> Mtb infection has been demonstrated to inhibit



NLRP3 inflammasome activation and IL-1 $\beta$  processing, and increased inflammasome activity has been associated with protection against active TB.<sup>261–263</sup> GPR81 has been demonstrated to be expressed by nonhematopoietic and immune cells such as macrophages and neutrophils, and these innate immune cells expressing GPR81 were critical in protecting mice from experimental colitis, and were involved in regulating the balance between IL-17 producing cells and Tregs.<sup>264</sup>

Within the CNS, GPR81 is concentrated along the plasma membranes of vascular endothelial cells, acting as a volume transmitter and serving as a feedback mechanism to counteract damage and save energy under hypoxic conditions.<sup>265–269</sup> GPR81 is highly enriched in leptomeningeal fibroblast like cells surrounding pial blood cells, and its activation stimulates cerebral VEGF and angiogenesis.<sup>270</sup> However, in some conditions, such as ischemic brain injury, inhibiting lactate signaling through GPR81 can reduce ischemia induced apoptosis and provide neuroprotection, potentially indicating a dual role of lactate at low versus high concentrations.<sup>271</sup> Importantly, within the context of the TB granuloma, vascularization and angiogenesis are important for enhancing oxygen delivery and drug delivery to central lesion lesions. Angiogenesis has also been implicated in allowing for increased dissemination of Mtb, as inhibiting angiogenesis via VEGF inactivation abolishes mycobacterial spread.<sup>272</sup> Thus, lactate's role in endothelial cell signaling through GPR81 may augment TB pathogenesis.

GPR81 has been shown to play a critical role in cancer, where silencing GPR81 in tumor cells reduced tumor growth, metastasis, cell proliferation, and mitochondrial activity.<sup>273,274</sup> GPR81 expression is significantly higher in cancer tissue compared to adjacent noncancerous tissues and GPR81 promotes cancer aggressiveness, malignant phenotype, cell migration, and promotes amphiregulin transcription, contributing to angiogenesis.<sup>275</sup> Tumor cell derived lactate can activate GPR81 on dendritic cells, and prevent the presentation of tumor specific antigens to other cells.<sup>276</sup> Further, GPR81 signaling facilitates higher rates of fatty acid synthesis by inhibiting lipolysis,

which allows for cancer cells to have increased viability and higher proliferation rates.<sup>277</sup> Mtb is known to rely on fatty acids and augment host lipid metabolism during infection<sup>278,279</sup> Signaling through GPR81 has been shown to induce the expression of PD-L1, which can lead to suppressed T cell function and immune evasion in the tumor microenvironment, and blocking lactate production can improve PD-1 targeted immune checkpoint therapies.<sup>280–282</sup> PD-1 has been demonstrated to interfere with effector T cell function during Mtb infection, and blocking PD-1 can bolster IFN- $\gamma$  responses.<sup>283</sup> However, mice deficient in PD-1 have been shown to be very susceptible to Mtb infection.<sup>284,285</sup> GPR81 activation stimulates the expression of ABC transporters which contribute to chemoresistance of cancer cells and GPR81 signaling enhances DNA repair mechanisms.<sup>286,287</sup> These transporters may play a role in cellular resistance to antimicrobial therapies for Mtb. Additionally, GPR81 agonism can induce a vasoconstriction response, diverting blood flow away from the kidney and inducing hypertension across multiple species.<sup>288</sup> Vasoconstrictive responses may impede blood flow to the TB granuloma, contributing to tissue hypoxia.

GPR81 plays a critical role in many processes that are important to the pathogenesis of TB. The anti-inflammatory responses stimulated by lactate activation of GPR81 may contribute to immune evasion by Mtb but may also be critical for controlling chronic inflammatory processes and limiting disease severity. The evaluation of the role of this receptor during Mtb infection has yet to be conducted, either via agonizing or antagonizing this receptor *in vitro* and *in vivo*, but GPR81 shows promise as a novel HDT target to modulate TB disease.

## **9. Mtb Driven Establishment of a Survival Niche via Metabolic Interactions**

All and all, this body of literature paints a complex picture. This research seeks to understand the ways in which Mtb can drive changes in host macrophage metabolic dynamics. Mechanistic knowledge of the metabolic interactions occurring at the host-pathogen interface will aid in the

development of host-directed therapeutic strategies that can augment cellular metabolism, thereby shifting immune cell phenotypes to those that are better equipped to combat TB disease. In the context of Mtb, shifting macrophage metabolism and augmenting the granuloma microenvironment will better equip the host to resolve lesions and slow disease progression, potentially limiting the establishment of latent infections. Specifically, we asked overarching questions regarding the mechanisms by which Mtb induces metabolic changes within the granuloma microenvironment, and how immune cell metabolism can be augmented to improve pathogen clearance and infection outcome. This included investigating the role of the mycobacterial iron chelator, mycobactin, on HIF-1 $\alpha$  activation and downstream metabolic impacts, and the role of lactate as both a metabolite and a signaling molecule during Mtb infection.

We hypothesized that Mtb driven upregulation of HIF-1 $\alpha$  through mycobactin-mediated iron chelation leads to a shift to glycolytic metabolism which is followed by production of large quantities of lactate. This lactate can then be shuttled to more oxidative regions of the granuloma microenvironment to preserve glucose for hypoxic cells. Lactate within the granuloma microenvironment can then serve as both an autocrine and paracrine anti-inflammatory, immunomodulatory signal via GPR81, augmenting the immune response to Mtb infection. Ultimately, pathogen driven mechanisms of metabolic alteration lead to the establishment of a survival niche for Mtb and enhance disease progression (Figure 1.4).

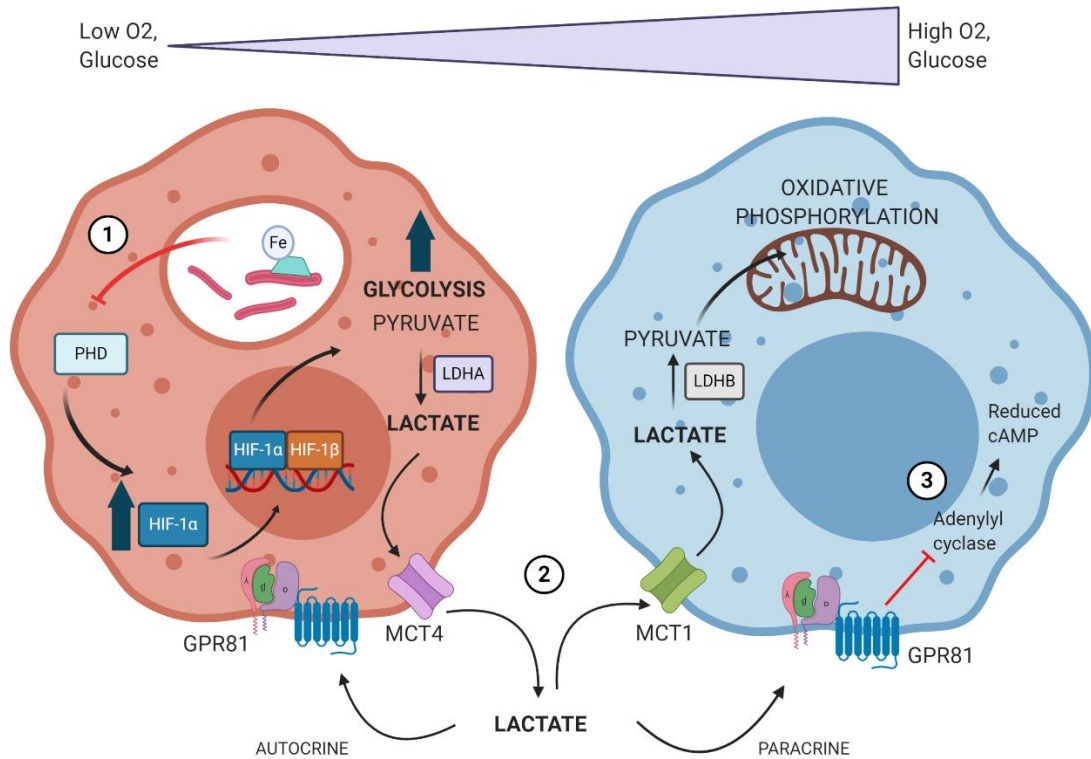


**Figure 1.4: Mtb infection drives changes in immune cell metabolism to establish its survival niche.** 1) The Mtb produced iron chelator, mycobactin, sequesters intracellular iron from host macrophages, which inhibits prolyl hydroxylase (PHD) activity. This leads to the accumulation and stabilization of HIF-1 $\alpha$ , subsequent translocation to the nucleus, and transcription of genes related to glycolysis, lactate metabolism, and lactate transport. 2) In addition to the Mtb mediated shifts in macrophage metabolism, the oxygen gradient present within the context of the TB granuloma, hypoxic cells within the granuloma lesion core rely heavily on glycolysis and produce large amounts of lactate. This lactate is produced via LDHA and exported via MCT4. Lactate is then shuttle to more normoxic cells closer to the lesion periphery, where it is imported via MCT1 and converted back into pyruvate by LDHB. Lactate is then used preferentially over glucose as a source for pyruvate and can drive oxidative phosphorylation and mitochondrial respiration. 3) Lactate accumulating within the granuloma microenvironment can signal in both an autocrine and paracrine fashion through GPR81. GPR81 signaling inhibits adenylyl cyclase, reducing intracellular levels of cAMP. This initiates downstream signaling impacts that are anti-inflammatory and immunomodulatory.

## REFERENCES

1. WHO | Global tuberculosis report 2019. *WHO*  
[http://www.who.int/tb/publications/global\\_report/en/](http://www.who.int/tb/publications/global_report/en/).
2. Tornheim, J. A. & Dooley, K. E. The Global Landscape of Tuberculosis Therapeutics. *Annual Review of Medicine* **70**, 105–120 (2019).
3. Story, A. *et al.* Smartphone-enabled video-observed versus directly observed treatment for tuberculosis: a multicentre, analyst-blinded, randomised, controlled superiority trial. *The Lancet* **393**, 1216–1224 (2019).
4. McLaren, Z. M., Milliken, A. A., Meyer, A. J. & Sharp, A. R. Does directly observed therapy improve tuberculosis treatment? More evidence is needed to guide tuberculosis policy. *BMC Infect Dis* **16**, 537 (2016).
5. Singh, P. *et al.* Breaking the Transmission of TB: A Roadmap to Bridge the Gaps in Controlling TB in Endemic Settings. in *Mycobacterium Tuberculosis: Molecular Infection Biology, Pathogenesis, Diagnostics and New Interventions* (eds. Hasnain, S. E., Ehtesham, N. Z. & Grover, S.) 451–461 (Springer, 2019). doi:10.1007/978-981-32-9413-4\_24.
6. Dooley, K. E., Hanna, D., Mave, V., Eisenach, K. & Savic, R. M. Advancing the development of new tuberculosis treatment regimens: The essential role of translational and clinical pharmacology and microbiology. *PLoS Med* **16**, (2019).
7. Bates, M., Marais, B. J. & Zumla, A. Tuberculosis Comorbidity with Communicable and Noncommunicable Diseases. *Cold Spring Harb Perspect Med* **5**, a017889 (2015).
8. Marais, B. J. *et al.* Tuberculosis comorbidity with communicable and non-communicable diseases: integrating health services and control efforts. *The Lancet Infectious Diseases* **13**, 436–448 (2013).

9. Podell, B. K. *et al.* Increased Severity of Tuberculosis in Guinea Pigs with Type 2 Diabetes: A Model of Diabetes-Tuberculosis Comorbidity. *The American Journal of Pathology* **184**, 1104–1118 (2014).
10. Tang, J., Yam, W.-C. & Chen, Z. Mycobacterium tuberculosis infection and vaccine development. *Tuberculosis* **98**, 30–41 (2016).
11. Alsdurf, H., Hill, P. C., Matteelli, A., Getahun, H. & Menzies, D. The cascade of care in diagnosis and treatment of latent tuberculosis infection: a systematic review and meta-analysis. *The Lancet Infectious Diseases* **16**, 1269–1278 (2016).
12. Cohen, A., Mathiasen, V. D., Schön, T. & Wejse, C. The global prevalence of latent tuberculosis: a systematic review and meta-analysis. *European Respiratory Journal* **54**, (2019).
13. Orme, I. M. & Basaraba, R. J. The formation of the granuloma in tuberculosis infection. *Seminars in Immunology* **26**, 601–609 (2014).
14. Orme, I. M. A new unifying theory of the pathogenesis of tuberculosis. *Tuberculosis* **94**, 8–14 (2014).
15. Ackart, D. F. *et al.* Reversal of Mycobacterium tuberculosis phenotypic drug resistance by 2-aminoimidazole-based small molecules. *Pathogens and Disease* **70**, 370–378 (2014).
16. Hartkoorn, R. C. *et al.* Differential drug susceptibility of intracellular and extracellular tuberculosis, and the impact of P-glycoprotein. *Tuberculosis* **87**, 248–255 (2007).
17. Karakousis, P. C. *et al.* Dormancy Phenotype Displayed by Extracellular Mycobacterium tuberculosis within Artificial Granulomas in Mice. *J Exp Med* **200**, 647–657 (2004).
18. Lenaerts, A., Barry, C. E. & Dartois, V. Heterogeneity in tuberculosis pathology, microenvironments and therapeutic responses. *Immunol Rev* **264**, 288–307 (2015).
19. Matty, M. A., Roca, F. J., Cronan, M. R. & Tobin, D. M. Adventures within the speckled band: heterogeneity, angiogenesis, and balanced inflammation in the tuberculous granuloma. *Immunol Rev* **264**, 276–287 (2015).

20. Lanoix, J.-P., Lenaerts, A. J. & Nuermberger, E. L. Heterogeneous disease progression and treatment response in a C3HeB/FeJ mouse model of tuberculosis. *Dis. Model. Mech.* **8**, 603–610 (2015).
21. Irwin, S. M. *et al.* Presence of multiple lesion types with vastly different microenvironments in C3HeB/FeJ mice following aerosol infection with *Mycobacterium tuberculosis*. *Dis. Model. Mech.* **8**, 591–602 (2015).
22. Via, L. E. *et al.* Tuberculous Granulomas Are Hypoxic in Guinea Pigs, Rabbits, and Nonhuman Primates. *Infect Immun* **76**, 2333–2340 (2008).
23. Orme, I. M., Robinson, R. T. & Cooper, A. M. The balance between protective and pathogenic immune responses in the TB-infected lung. *Nat Immunol* **16**, 57–63 (2015).
24. Bold, T. D. & Ernst, J. D. Who Benefits from Granulomas, Mycobacteria or Host? *Cell* **136**, 17–19 (2009).
25. Cooper, A. M. & Torrado, E. Protection versus pathology in tuberculosis: recent insights. *Current Opinion in Immunology* **24**, 431–437 (2012).
26. Wallis, R. S. *et al.* Tuberculosis—advances in development of new drugs, treatment regimens, host-directed therapies, and biomarkers. *The Lancet Infectious Diseases* **16**, e34–e46 (2016).
27. Wallis, R. S. & Hafner, R. Advancing host-directed therapy for tuberculosis. *Nat Rev Immunol* **15**, 255–263 (2015).
28. Kiran, D., Podell, B. K., Chambers, M. & Basaraba, R. J. Host-directed therapy targeting the *Mycobacterium tuberculosis* granuloma: a review. *Semin Immunopathol* **38**, 167–183 (2015).
29. Zumla, A. *et al.* Host-Directed Therapies for Tackling Multi-Drug Resistant Tuberculosis: Learning From the Pasteur-Bechamp Debates. *Clin Infect Dis.* **61**, 1432–1438 (2015).
30. Zumla, A., Rao, M., Doodoo, E. & Maeurer, M. Potential of immunomodulatory agents as adjunct host-directed therapies for multidrug-resistant tuberculosis. *BMC Med* **14**, (2016).

31. Hawn, T. R., Shah, J. A. & Kalman, D. New tricks for old dogs: countering antibiotic resistance in tuberculosis with host-directed therapeutics. *Immunol Rev* **264**, 344–362 (2015).
32. Yew, W. W., Chang, K. C., Chan, D. P. & Zhang, Y. Metformin as a host-directed therapeutic in tuberculosis: Is there a promise? *Tuberculosis* **115**, 76–80 (2019).
33. Rodriguez-Carlos, A. *et al.* Metformin promotes Mycobacterium tuberculosis killing and increases the production of human  $\beta$ -defensins in lung epithelial cells and macrophages. *Microbes and Infection* **22**, 111–118 (2020).
34. Oglesby, W., Kara, A. M., Granados, H. & Cervantes, J. L. Metformin in tuberculosis: beyond control of hyperglycemia. *Infection* **47**, 697–702 (2019).
35. Lachmandas, E. *et al.* Metformin Alters Human Host Responses to Mycobacterium tuberculosis in Healthy Subjects. *J Infect Dis* **220**, 139–150 (2019).
36. Lin, S.-Y. *et al.* Metformin is associated with a lower risk of active tuberculosis in patients with type 2 diabetes. *Respirology* **23**, 1063–1073 (2018).
37. Pålsson-McDermott, E. M. & O’Neill, L. A. J. Targeting immunometabolism as an anti-inflammatory strategy. *Cell Research* 1–15 (2020) doi:10.1038/s41422-020-0291-z.
38. Russell, D. G., Huang, L. & VanderVen, B. C. Immunometabolism at the interface between macrophages and pathogens. *Nat Rev Immunol* **19**, 291–304 (2019).
39. Singer, K., Cheng, W.-C., Kreutz, M., Ho, P.-C. & Siska, P. J. Immunometabolism in cancer at a glance. *Disease Models & Mechanisms* **11**, dmm034272 (2018).
40. Van den Bossche, J., O’Neill, L. A. & Menon, D. Macrophage Immunometabolism: Where Are We (Going)? *Trends in Immunology* **38**, 395–406 (2017).
41. Shi, L., Eugenin, E. A. & Subbian, S. Immunometabolism in Tuberculosis. *Front Immunol* **7**, (2016).
42. Warburg, O. On the Origin of Cancer Cells. *Science* **123**, 309–314 (1956).



43. Weinhouse, S., Warburg, O., Burk, D. & Schade, A. L. On Respiratory Impairment in Cancer Cells. *Science* **124**, 267–272 (1956).
44. Koppenol, W. H., Bounds, P. L. & Dang, C. V. Otto Warburg's contributions to current concepts of cancer metabolism. *Nat Rev Cancer* **11**, 325–337 (2011).
45. Hosios, A. M. & Heiden, M. G. V. The redox requirements of proliferating mammalian cells. *J. Biol. Chem.* **293**, 7490–7498 (2018).
46. Walker, M. A. & Tian, R. NAD(H) in mitochondrial energy transduction: implications for health and disease. *Current Opinion in Physiology* **3**, 101–109 (2018).
47. Potter, M., Newport, E. & Morten, K. J. The Warburg effect: 80 years on. *Biochem Soc Trans* **44**, 1499–1505 (2016).
48. Schwartz, L., T. Supuran, C. & O. Alfarouk, K. The Warburg Effect and the Hallmarks of Cancer. *Anti-Cancer Agents in Medicinal Chemistry- Anti-Cancer Agents* **17**, 164–170 (2017).
49. Chen, Z., Liu, M., Li, L. & Chen, L. Involvement of the Warburg effect in non-tumor diseases processes. *Journal of Cellular Physiology* **233**, 2839–2849 (2018).
50. Escoll, P. & Buchrieser, C. Metabolic reprogramming of host cells upon bacterial infection: Why shift to a Warburg-like metabolism? *The FEBS Journal* **285**, 2146–2160 (2018).
51. Danhier, P. *et al.* Cancer metabolism in space and time: Beyond the Warburg effect. *Biochimica et Biophysica Acta (BBA) - Bioenergetics* **1858**, 556–572 (2017).
52. Palsson-McDermott, E. M. & O'Neill, L. A. J. The Warburg effect then and now: From cancer to inflammatory diseases. *BioEssays* **35**, 965–973 (2013).
53. Lu, J., Tan, M. & Cai, Q. The Warburg effect in tumor progression: Mitochondrial oxidative metabolism as an anti-metastasis mechanism. *Cancer Letters* **356**, 156–164 (2015).
54. Wang, S. *et al.* Metabolic reprogramming of macrophages during infections and cancer. *Cancer Letters* **452**, 14–22 (2019).

55. Hobson-Gutierrez, S. A. & Carmona-Fontaine, C. The metabolic axis of macrophage and immune cell polarization. *Disease Models & Mechanisms* **11**, dmm034462 (2018).
56. Marakalala, M. J., Martinez, F. O., Plüddemann, A. & Gordon, S. Macrophage Heterogeneity in the Immunopathogenesis of Tuberculosis. *Front. Microbiol.* **9**, (2018).
57. Martinez, F. O. & Gordon, S. The M1 and M2 paradigm of macrophage activation: time for reassessment. *F1000Prime Rep* **6**, (2014).
58. Chávez-Galán, L., Olleros, M. L., Vesin, D. & Garcia, I. Much More than M1 and M2 Macrophages, There are also CD169+ and TCR+ Macrophages. *Front. Immunol.* **6**, (2015).
59. Mitsi, E. *et al.* Human alveolar macrophages predominately express combined classical M1 and M2 surface markers in steady state. *Respiratory Research* **19**, 66 (2018).
60. Wang, G. L. & Semenza, G. L. Purification and Characterization of Hypoxia-inducible Factor 1. *J. Biol. Chem.* **270**, 1230–1237 (1995).
61. Wang, G. L., Jiang, B. H., Rue, E. A. & Semenza, G. L. Hypoxia-inducible factor 1 is a basic-helix-loop-helix-PAS heterodimer regulated by cellular O<sub>2</sub> tension. *PNAS* **92**, 5510–5514 (1995).
62. Greijer, A. E. *et al.* Up-regulation of gene expression by hypoxia is mediated predominantly by hypoxia-inducible factor 1 (HIF-1). *The Journal of Pathology* **206**, 291–304 (2005).
63. Balamurugan, K. HIF-1 at the crossroads of hypoxia, inflammation, and cancer. *Int. J. Cancer* **138**, 1058–1066 (2016).
64. Jaakkola, P. *et al.* Targeting of HIF- $\alpha$  to the von Hippel-Lindau Ubiquitylation Complex by O<sub>2</sub>-Regulated Prolyl Hydroxylation. *Science* **292**, 468–472 (2001).
65. Kaluz, S., Kaluzová, M. & Stanbridge, E. J. Proteasomal Inhibition Attenuates Transcriptional Activity of Hypoxia-Inducible Factor 1 (HIF-1) via Specific Effect on the HIF-1 $\alpha$  C-Terminal Activation Domain. *Mol. Cell. Biol.* **26**, 5895–5907 (2006).
66. Ivan, M. *et al.* HIF $\alpha$  Targeted for VHL-Mediated Destruction by Proline Hydroxylation: Implications for O<sub>2</sub> Sensing. *Science* **292**, 464–468 (2001).

67. Shi, L. *et al.* Infection with *Mycobacterium tuberculosis* induces the Warburg effect in mouse lungs. *Scientific Reports* **5**, 18176 (2015).
68. Prosser, G. *et al.* The bacillary and macrophage response to hypoxia in tuberculosis and the consequences for T cell antigen recognition. *Microbes and Infection* **19**, 177–192 (2017).
69. Braverman, J., Sogi, K. M., Benjamin, D., Nomura, D. K. & Stanley, S. A. HIF-1 $\alpha$  Is an Essential Mediator of IFN- $\gamma$ -Dependent Immunity to *Mycobacterium tuberculosis*. *J Immunol* 1600266 (2016) doi:10.4049/jimmunol.1600266.
70. Werth, N. *et al.* Activation of Hypoxia Inducible Factor 1 Is a General Phenomenon in Infections with Human Pathogens. *PLoS One* **5**, (2010).
71. Baay-Guzman, G. J. *et al.* Dual role of hypoxia-inducible factor 1  $\alpha$  in experimental pulmonary tuberculosis: its implication as a new therapeutic target. *Future Microbiology* (2018) doi:10.2217/fmb-2017-0168.
72. Resende, M. *et al.* Myeloid HIF-1 $\alpha$  regulates pulmonary inflammation during experimental *Mycobacterium tuberculosis* infection. *Immunology* **159**, 121–129 (2020).
73. Knight, M. & Stanley, S. HIF-1 $\alpha$  as a central mediator of cellular resistance to intracellular pathogens. *Current Opinion in Immunology* **60**, 111–116 (2019).
74. Schild, Y., Mohamed, A., Wootton, E. J., Lewis, A. & Elks, P. M. Hif-1alpha stabilisation is protective against infection in a zebrafish model of comorbidity. *bioRxiv* 797480 (2019) doi:10.1101/797480.
75. Ogryzko, N. V. *et al.* Hif-1alpha induced expression of Il-1beta protects against mycobacterial infection in zebrafish. *bioRxiv* 306506 (2018) doi:10.1101/306506.
76. Elks, P. M. *et al.* Hypoxia Inducible Factor Signaling Modulates Susceptibility to Mycobacterial Infection via a Nitric Oxide Dependent Mechanism. *PLoS Pathog* **9**, (2013).
77. Cardoso, M. S., Silva, T. M., Resende, M., Appelberg, R. & Borges, M. Lack of the Transcription Factor Hypoxia-Inducible Factor 1 $\alpha$  (HIF-1 $\alpha$ ) in Macrophages Accelerates the

- Necrosis of Mycobacterium avium-Induced Granulomas. *Infect. Immun.* **83**, 3534–3544 (2015).
78. Shi, L., Jiang, Q., Bushkin, Y., Subbian, S. & Tyagi, S. Biphasic Dynamics of Macrophage Immunometabolism during Mycobacterium tuberculosis Infection. *mBio* **10**, e02550-18 (2019).
79. Gleeson, L. E. *et al.* Cutting Edge: Mycobacterium tuberculosis Induces Aerobic Glycolysis in Human Alveolar Macrophages That Is Required for Control of Intracellular Bacillary Replication. *J Immunol* **196**, 2444–2449 (2016).
80. Qualls, J. E. & Murray, P. J. Immunometabolism within the tuberculosis granuloma: amino acids, hypoxia, and cellular respiration. *Semin Immunopathol* **38**, 139–152 (2015).
81. Jung, Y.-J., Isaacs, J. S., Lee, S., Trepel, J. & Neckers, L. IL-1 $\beta$  mediated up-regulation of HIF-1 $\alpha$  via an NF $\kappa$ B/COX-2 pathway identifies HIF-1 as a critical link between inflammation and oncogenesis. *FASEB J* (2003) doi:10.1096/fj.03-0329fje.
82. Feldhoff, L. M. *et al.* IL-1 $\beta$  induced HIF-1 $\alpha$  inhibits the differentiation of human FOXP3 + T cells. *Scientific Reports* **7**, 465 (2017).
83. Al Okail, M. S. Cobalt chloride, a chemical inducer of hypoxia-inducible factor-1 $\alpha$  in U251 human glioblastoma cell line. *Journal of Saudi Chemical Society* **14**, 197–201 (2010).
84. Muñoz-Sánchez, J. & Cháñez-Cárdenas, M. E. The use of cobalt chloride as a chemical hypoxia model. *Journal of Applied Toxicology* **39**, 556–570 (2019).
85. Xia, M. *et al.* Identification of Chemical Compounds that Induce HIF-1 $\alpha$  Activity. *Toxicol Sci* **112**, 153–163 (2009).
86. Tannahill, G. M. *et al.* Succinate is an inflammatory signal that induces IL-1 $\beta$  through HIF-1 $\alpha$ . *Nature* **496**, 238–242 (2013).
87. Lukyanova, L. D., Kirova, Y. I. & Germanova, E. L. The Role of Succinate in Regulation of Immediate HIF-1 $\alpha$  Expression in Hypoxia. *Bull Exp Biol Med* **164**, 298–303 (2018).

88. Bailey, P. S. J. & Nathan, J. A. Metabolic Regulation of Hypoxia-Inducible Transcription Factors: The Role of Small Molecule Metabolites and Iron. *Biomedicines* **6**, (2018).
89. Hirota, K. An intimate crosstalk between iron homeostasis and oxygen metabolism regulated by the hypoxia-inducible factors (HIFs). *Free Radical Biology and Medicine* (2018) doi:10.1016/j.freeradbiomed.2018.07.018.
90. Woo, K. J., Lee, T.-J., Park, J.-W. & Kwon, T. K. Desferrioxamine, an iron chelator, enhances HIF-1 $\alpha$  accumulation via cyclooxygenase-2 signaling pathway. *Biochemical and Biophysical Research Communications* **343**, 8–14 (2006).
91. McNamee, E. N., Vohwinkel, C. & Eltzschig, H. K. Hydroxylation-independent HIF-1 $\alpha$  stabilization through PKA: A new paradigm for hypoxia signaling. *Sci. Signal.* **9**, fs11–fs11 (2016).
92. Bullen, J. W. *et al.* Protein kinase A–dependent phosphorylation stimulates the transcriptional activity of hypoxia-inducible factor 1. *Sci. Signal.* **9**, ra56–ra56 (2016).
93. Cassat, J. E. & Skaar, E. P. Iron in Infection and Immunity. *Cell Host & Microbe* **13**, 509–519 (2013).
94. Nairz, M., Theurl, I., Swirski, F. K. & Weiss, G. “Pumping iron”—how macrophages handle iron at the systemic, microenvironmental, and cellular levels. *Pflugers Arch - Eur J Physiol* **469**, 397–418 (2017).
95. Ali, M. K. *et al.* Role of iron in the pathogenesis of respiratory disease. *The International Journal of Biochemistry & Cell Biology* **88**, 181–195 (2017).
96. P. Skaar, E. & Raffatellu, M. Metals in infectious diseases and nutritional immunity. *Metallomics* **7**, 926–928 (2015).
97. Marchetti, M. *et al.* Iron Metabolism at the Interface between Host and Pathogen: From Nutritional Immunity to Antibacterial Development. *International Journal of Molecular Sciences* **21**, 2145 (2020).

98. Palmer, L. D. & Skaar, E. P. Transition Metals and Virulence in Bacteria. *Annual Review of Genetics* **50**, 67–91 (2016).
99. Chandrangu, P., Rensing, C. & Helmann, J. D. Metal homeostasis and resistance in bacteria. *Nature Reviews Microbiology* **15**, 338–350 (2017).
100. Ellermann, M. & Arthur, J. C. Siderophore-mediated iron acquisition and modulation of host-bacterial interactions. *Free Radical Biology and Medicine* **105**, 68–78 (2017).
101. Saha, M. *et al.* Microbial siderophores and their potential applications: a review. *Environ Sci Pollut Res* **23**, 3984–3999 (2015).
102. Li, K., Chen, W.-H. & Bruner, S. D. Microbial siderophore-based iron assimilation and therapeutic applications. *Biometals* **29**, 377–388 (2016).
103. Golonka, R., Yeoh, B. S. & Vijay-Kumar, M. The Iron Tug-of-War between Bacterial Siderophores and Innate Immunity. *JIN* **11**, 249–262 (2019).
104. Sritharan, M. Iron Homeostasis in Mycobacterium tuberculosis: Mechanistic Insights into Siderophore-Mediated Iron Uptake. *J. Bacteriol.* **198**, 2399–2409 (2016).
105. Snow, G. A. Isolation and structure of mycobactin T, a growth factor from Mycobacterium tuberculosis. *Biochemical Journal* **97**, 166–175 (1965).
106. Madigan, C. A. *et al.* Lipidomic Analysis Links Mycobactin Synthase K to Iron Uptake and Virulence in M. tuberculosis. *PLoS Pathog* **11**, e1004792 (2015).
107. McMahon, M. D., Rush, J. S. & Thomas, M. G. Analyses of MbtB, MbtE, and MbtF Suggest Revisions to the Mycobactin Biosynthesis Pathway in Mycobacterium tuberculosis. *J Bacteriol* **194**, 2809–2818 (2012).
108. Krithika, R. *et al.* A genetic locus required for iron acquisition in Mycobacterium tuberculosis. *Proc Natl Acad Sci U S A* **103**, 2069–2074 (2006).
109. Quadri, L. E. N., Sello, J., Keating, T. A., Weinreb, P. H. & Walsh, C. T. Identification of a Mycobacterium tuberculosis gene cluster encoding the biosynthetic enzymes for assembly of the virulence-conferring siderophore mycobactin. *Chemistry & Biology* **5**, 631–645 (1998).

110. Nandal, A. *et al.* Activation of the HIF Prolyl Hydroxylase by the Iron Chaperones PCBP1 and PCBP2. *Cell Metabolism* **14**, 647–657 (2011).
111. Cho, E. A. *et al.* Differential in vitro and cellular effects of iron chelators for hypoxia inducible factor hydroxylases. *J. Cell. Biochem.* **114**, 864–873 (2013).
112. Fong, G.-H. & Takeda, K. Role and regulation of prolyl hydroxylase domain proteins. *Cell Death & Differentiation* **15**, 635–641 (2008).
113. Holden, P. & Nair, L. S. Deferoxamine: An Angiogenic and Antioxidant Molecule for Tissue Regeneration. *Tissue Engineering Part B: Reviews* **25**, 461–470 (2019).
114. Mobarra, N. *et al.* A Review on Iron Chelators in Treatment of Iron Overload Syndromes. *Int J Hematol Oncol Stem Cell Res* **10**, 239–247 (2016).
115. Wilson, B. R., Bogdan, A. R., Miyazawa, M., Hashimoto, K. & Tsuji, Y. Siderophores in Iron Metabolism: From Mechanism to Therapy Potential. *Trends in Molecular Medicine* **22**, 1077–1090 (2016).
116. Phelan, J. J. *et al.* Desferrioxamine Supports Metabolic Function in Primary Human Macrophages Infected With Mycobacterium tuberculosis. *Front. Immunol.* **11**, (2020).
117. Hartmann, H. *et al.* Hypoxia-Independent Activation of HIF-1 by Enterobacteriaceae and Their Siderophores. *Gastroenterology* **134**, 756-767.e6 (2008).
118. Wigfield, S. M. *et al.* PDK-1 regulates lactate production in hypoxia and is associated with poor prognosis in head and neck squamous cancer. *Br J Cancer* **98**, 1975–1984 (2008).
119. Zhao, L., Mao, Y., Zhao, Y., Cao, Y. & Chen, X. Role of multifaceted regulators in cancer glucose metabolism and their clinical significance. *Oncotarget* **7**, 31572–31585 (2016).
120. Ullah, M. S., Davies, A. J. & Halestrap, A. P. The Plasma Membrane Lactate Transporter MCT4, but Not MCT1, Is Up-regulated by Hypoxia through a HIF-1 $\alpha$ -dependent Mechanism. *J. Biol. Chem.* **281**, 9030–9037 (2006).

121. Rademakers, S. E., Lok, J., van der Kogel, A. J., Bussink, J. & Kaanders, J. H. Metabolic markers in relation to hypoxia; staining patterns and colocalization of pimonidazole, HIF-1 $\alpha$ , CAIX, LDH-5, GLUT-1, MCT1 and MCT4. *BMC Cancer* **11**, 167 (2011).
122. Firth, J. D., Ebert, B. L. & Ratcliffe, P. J. Hypoxic Regulation of Lactate Dehydrogenase A INTERACTION BETWEEN HYPOXIA-INDUCIBLE FACTOR 1 AND cAMP RESPONSE ELEMENTS. *J. Biol. Chem.* **270**, 21021–21027 (1995).
123. Semenza, G. L. *et al.* Hypoxia Response Elements in the Aldolase A, Enolase 1, and Lactate Dehydrogenase A Gene Promoters Contain Essential Binding Sites for Hypoxia-inducible Factor 1. *J. Biol. Chem.* **271**, 32529–32537 (1996).
124. Semenza, G. L., Roth, P. H., Fang, H. M. & Wang, G. L. Transcriptional regulation of genes encoding glycolytic enzymes by hypoxia-inducible factor 1. *J. Biol. Chem.* **269**, 23757–23763 (1994).
125. Walenta, S. & Mueller-Klieser, W. F. Lactate: mirror and motor of tumor malignancy. *Seminars in Radiation Oncology* **14**, 267–274 (2004).
126. Cui, X. *et al.* HIF1/2 $\alpha$  mediates hypoxia-induced LDHA expression in human pancreatic cancer cells. *Oncotarget* **8**, 24840–24852 (2017).
127. Adeva, M., González-Lucán, M., Seco, M. & Donapetry, C. Enzymes involved in l-lactate metabolism in humans. *Mitochondrion* **13**, 615–629 (2013).
128. Koukourakis, M. I. *et al.* Lactate dehydrogenase-5 (LDH-5) overexpression in non-small-cell lung cancer tissues is linked to tumour hypoxia, angiogenic factor production and poor prognosis. *Br J Cancer* **89**, 877–885 (2003).
129. Koukourakis, M. I., Giatromanolaki, A., Simopoulos, C., Polychronidis, A. & Sivridis, E. Lactate dehydrogenase 5 (LDH5) relates to up-regulated hypoxia inducible factor pathway and metastasis in colorectal cancer. *Clin Exp Metastasis* **22**, 25–30 (2005).
130. Kolev, Y., Uetake, H., Takagi, Y. & Sugihara, K. Lactate Dehydrogenase-5 (LDH-5) Expression in Human Gastric Cancer: Association with Hypoxia-Inducible Factor (HIF-1 $\alpha$ )



- Pathway, Angiogenic Factors Production and Poor Prognosis. *Ann Surg Oncol* **15**, 2336–2344 (2008).
131. Bak, L. K. & Schousboe, A. Misconceptions regarding basic thermodynamics and enzyme kinetics have led to erroneous conclusions regarding the metabolic importance of lactate dehydrogenase isoenzyme expression. *Journal of Neuroscience Research* **95**, 2098–2102 (2017).
132. Petrelli, F. *et al.* Prognostic role of lactate dehydrogenase in solid tumors: A systematic review and meta-analysis of 76 studies. *Acta Oncologica* **54**, 961–970 (2015).
133. Emad, A. & Rezaian, G. R. Lactate dehydrogenase in bronchoalveolar lavage fluid of patients with active pulmonary tuberculosis. *Respiration* **66**, 41–45 (1999).
134. Sharma, P. R., Jain, S., Bamezai, R. N. K. & Tiwari, P. K. Utility of serum LDH isoforms in the assessment of mycobacterium tuberculosis induced pathology in TB patients of Sahariya tribe. *Indian J Clin Biochem* **25**, 57–63 (2010).
135. San-Millán, I. & Brooks, G. A. Reexamining cancer metabolism: lactate production for carcinogenesis could be the purpose and explanation of the Warburg Effect. *Carcinogenesis* **38**, 119–133 (2017).
136. Pereira-Nunes, A., Afonso, J., Granja, S. & Baltazar, F. Lactate and Lactate Transporters as Key Players in the Maintenance of the Warburg Effect. in *Tumor Microenvironment: The Main Driver of Metabolic Adaptation* (ed. Serpa, J.) 51–74 (Springer International Publishing, 2020). doi:10.1007/978-3-030-34025-4\_3.
137. Crowther, M., Brown, N. J., Bishop, E. T. & Lewis, C. E. Microenvironmental influence on macrophage regulation of angiogenesis in wounds and malignant tumors. *Journal of Leukocyte Biology* **70**, 478–490 (2001).
138. Trabold, O. *et al.* Lactate and oxygen constitute a fundamental regulatory mechanism in wound healing. *Wound Repair and Regeneration* **11**, 504–509 (2003).

139. Pérez-Escuredo, J. *et al.* Lactate promotes glutamine uptake and metabolism in oxidative cancer cells. *Cell Cycle* **15**, 72–83 (2015).
140. Osada-Oka, M. *et al.* Metabolic adaptation to glycolysis is a basic defense mechanism of macrophages for *Mycobacterium tuberculosis* infection. *Int Immunol* (2019)  
doi:10.1093/intimm/dxz048.
141. Somashekar, B. S. *et al.* Metabolomic Signatures in Guinea Pigs Infected with Epidemic-Associated W-Beijing Strains of *Mycobacterium tuberculosis*. *J. Proteome Res.* **11**, 4873–4884 (2012).
142. Somashekar, B. S. *et al.* Metabolic Profiling of Lung Granuloma in *Mycobacterium tuberculosis* Infected Guinea Pigs: Ex vivo 1H Magic Angle Spinning NMR Studies. *J. Proteome Res.* **10**, 4186–4195 (2011).
143. Gladden, L. B. Lactate metabolism: a new paradigm for the third millennium. *The Journal of Physiology* **558**, 5–30 (2004).
144. Brooks, G. A. Cell–cell and intracellular lactate shuttles. *The Journal of Physiology* **587**, 5591–5600 (2009).
145. Sun, S., Li, H., Chen, J. & Qian, Q. Lactic Acid: No Longer an Inert and End-Product of Glycolysis. *Physiology* **32**, 453–463 (2017).
146. Brooks, G. A. The Science and Translation of Lactate Shuttle Theory. *Cell Metabolism* **27**, 757–785 (2018).
147. Ferguson, B. S. *et al.* Lactate metabolism: historical context, prior misinterpretations, and current understanding. *Eur J Appl Physiol* **118**, 691–728 (2018).
148. Brooks, G. A. The tortuous path of lactate shuttle discovery: From cinders and boards to the lab and ICU. *Journal of Sport and Health Science* (2020)  
doi:10.1016/j.jshs.2020.02.006.

149. Brooks, G. A., Dubouchaud, H., Brown, M., Sicurello, J. P. & Butz, C. E. Role of mitochondrial lactate dehydrogenase and lactate oxidation in the intracellular lactate shuttle. *Proc Natl Acad Sci U S A* **96**, 1129–1134 (1999).
150. Brooks, G. A. The lactate shuttle during exercise and recovery. *Medicine & Science in Sports & Exercise* **18**, 360–368 (1986).
151. Brooks, G. A. Lactate:Glycolytic End Product and Oxidative Substrate During Sustained Exercise in Mammals — The “Lactate Shuttle”. in *Circulation, Respiration, and Metabolism* (ed. Gilles, R.) 208–218 (Springer, 1985). doi:10.1007/978-3-642-70610-3\_15.
152. De Bari, L., Atlante, A., Valenti, D. & Passarella, S. Partial reconstruction of in vitro gluconeogenesis arising from mitochondrial l-lactate uptake/metabolism and oxaloacetate export via novel L-lactate translocators. *Biochem J* **380**, 231–242 (2004).
153. Passarella, S. *et al.* Mitochondria and l-lactate metabolism. *FEBS Letters* **582**, 3569–3576 (2008).
154. Chen, Y.-J. *et al.* Lactate metabolism is associated with mammalian mitochondria. *Nature Chemical Biology* **12**, nchembio.2172 (2016).
155. De Bari, L., Chieppa, G., Marra, E. & Passarella, S. L-lactate metabolism can occur in normal and cancer prostate cells via the novel mitochondrial L-lactate dehydrogenase. *International Journal of Oncology* **37**, 1607–1620 (2010).
156. Jacobs, R. A., Meinild, A.-K., Nordsborg, N. B. & Lundby, C. Lactate oxidation in human skeletal muscle mitochondria. *American Journal of Physiology - Endocrinology and Metabolism* **304**, E686–E694 (2013).
157. Passarella, S., Paventi, G. & Pizzuto, R. The mitochondrial L-lactate dehydrogenase affair. *Front Neurosci* **8**, (2014).
158. Lemire, J., Mailloux, R. J. & Appanna, V. D. Mitochondrial Lactate Dehydrogenase Is Involved in Oxidative-Energy Metabolism in Human Astrocytoma Cells (CCF-STTG1). *PLoS ONE* **3**, (2008).

159. Magistretti, P. J. & Allaman, I. Lactate in the brain: from metabolic end-product to signalling molecule. *Nature Reviews Neuroscience* **19**, 235–249 (2018).
160. Kennedy, K. M. *et al.* Catabolism of Exogenous Lactate Reveals It as a Legitimate Metabolic Substrate in Breast Cancer. *PLoS One* **8**, (2013).
161. Faubert, B. *et al.* Lactate Metabolism in Human Lung Tumors. *Cell* **171**, 358-371.e9 (2017).
162. Halestrap, A. P. The monocarboxylate transporter family—Structure and functional characterization. *IUBMB Life* **64**, 1–9 (2012).
163. Felmler, M. A., Jones, R. S., Rodriguez-Cruz, V., Follman, K. E. & Morris, M. E. Monocarboxylate Transporters (SLC16): Function, Regulation, and Role in Health and Disease. *Pharmacol Rev* **72**, 466–485 (2020).
164. Dimmer, K. S., Friedrich, B., Lang, F., Deitmer, J. W. & Bröer, S. The low-affinity monocarboxylate transporter MCT4 is adapted to the export of lactate in highly glycolytic cells. *Biochem J* **350**, 219–227 (2000).
165. Kirk, P. *et al.* CD147 is tightly associated with lactate transporters MCT1 and MCT4 and facilitates their cell surface expression. *The EMBO Journal* **19**, 3896–3904 (2000).
166. Hahn, E. L., Halestrap, A. P. & Gamelli, R. L. Expression of the lactate transporter MCT1 in macrophages. *Shock* **13**, 253–260 (2000).
167. Walters, D. K., Arendt, B. K. & Jelinek, D. F. CD147 regulates the expression of MCT1 and lactate export in multiple myeloma cells. *Cell Cycle* **12**, 3175–3183 (2013).
168. Le Floch, R. *et al.* CD147 subunit of lactate/H<sup>+</sup> symporters MCT1 and hypoxia-inducible MCT4 is critical for energetics and growth of glycolytic tumors. *Proc Natl Acad Sci U S A* **108**, 16663–16668 (2011).
169. Izumi, H. *et al.* Monocarboxylate transporters 1 and 4 are involved in the invasion activity of human lung cancer cells. *Cancer Science* **102**, 1007–1013 (2011).

170. Ke, X. *et al.* Hypoxia upregulates CD147 through a combined effect of HIF-1 $\alpha$  and Sp1 to promote glycolysis and tumor progression in epithelial solid tumors. *Carcinogenesis* **33**, 1598–1607 (2012).
171. Ke, X., Chen, Y., Wang, P., Xing, J. & Chen, Z. Upregulation of CD147 protects hepatocellular carcinoma cell from apoptosis through glycolytic switch via HIF-1 and MCT-4 under hypoxia. *Hepatol Int* **8**, 405–414 (2014).
172. Latif, A. *et al.* Monocarboxylate Transporter 1 (MCT1) is an independent prognostic biomarker in endometrial cancer. *BMC Clin Pathol* **17**, (2017).
173. Luz, M. C. de B. *et al.* Evaluation of MCT1, MCT4 and CD147 Genes in Peripheral Blood Cells of Breast Cancer Patients and Their Potential Use as Diagnostic and Prognostic Markers. *Int J Mol Sci* **18**, (2017).
174. Ruan, Y. *et al.* High expression of monocarboxylate transporter 4 predicts poor prognosis in patients with lung adenocarcinoma. *Oncology Letters* **14**, 5727–5734 (2017).
175. Sonveaux, P. *et al.* Targeting lactate-fueled respiration selectively kills hypoxic tumor cells in mice. *J Clin Invest* **118**, 3930–3942 (2008).
176. Nakajima, E. C. & Van Houten, B. Metabolic symbiosis in cancer: Refocusing the Warburg lens. *Mol. Carcinog.* **52**, 329–337 (2013).
177. Végran, F., Boidot, R., Michiels, C., Sonveaux, P. & Feron, O. Lactate Influx through the Endothelial Cell Monocarboxylate Transporter MCT1 Supports an NF- $\kappa$ B/IL-8 Pathway that Drives Tumor Angiogenesis. *Cancer Res* **71**, 2550–2560 (2011).
178. Xiong, M., Elson, G., Legarda, D. & Leibovich, S. J. Production of Vascular Endothelial Growth Factor by Murine Macrophages: Regulation by Hypoxia, Lactate, and the Inducible Nitric Oxide Synthase Pathway. *The American Journal of Pathology* **153**, 587–598 (1998).
179. Porporato, P. E. *et al.* Lactate stimulates angiogenesis and accelerates the healing of superficial and ischemic wounds in mice. *Angiogenesis* **15**, 581–592 (2012).

180. Miranda-Gonçalves, V. *et al.* Monocarboxylate transporter 1 is a key player in glioma-endothelial cell crosstalk. *Mol Carcinog* **56**, 2630–2642 (2017).
181. Whitaker-Menezes, D. *et al.* Evidence for a stromal-epithelial “lactate shuttle” in human tumors. *Cell Cycle* **10**, 1772–1783 (2011).
182. Fu, Y. *et al.* The reverse Warburg effect is likely to be an Achilles’ heel of cancer that can be exploited for cancer therapy. *Oncotarget* **8**, 57813–57825 (2017).
183. Koukourakis, M. I. *et al.* Metabolic cooperation between co-cultured lung cancer cells and lung fibroblasts. *Laboratory Investigation* **97**, 1321–1331 (2017).
184. Wilde, L. *et al.* Metabolic coupling and the Reverse Warburg Effect in cancer: Implications for novel biomarker and anticancer agent development. *Seminars in Oncology* **44**, 198–203 (2017).
185. Fiaschi, T. *et al.* Reciprocal Metabolic Reprogramming through Lactate Shuttle Coordinately Influences Tumor-Stroma Interplay. *Cancer Res* **72**, 5130–5140 (2012).
186. Curry, J. M. *et al.* Cancer metabolism, stemness and tumor recurrence. *Cell Cycle* **12**, 1371–1384 (2013).
187. Rattigan, Y. I. *et al.* Lactate is a mediator of metabolic cooperation between stromal carcinoma associated fibroblasts and glycolytic tumor cells in the tumor microenvironment. *Experimental Cell Research* **318**, 326–335 (2012).
188. Carmona-Fontaine, C. *et al.* Emergence of spatial structure in the tumor microenvironment due to the Warburg effect. *Proc Natl Acad Sci U S A* **110**, 19402–19407 (2013).
189. Carow, B. *et al.* Spatial and temporal localization of immune transcripts defines hallmarks and diversity in the tuberculosis granuloma. *Nature Communications* **10**, 1823 (2019).
190. Marakalala, M. J. *et al.* Inflammatory signaling in human tuberculosis granulomas is spatially organized. *Nature Medicine* **22**, 531–538 (2016).

191. Danhier, P. *et al.* Optimization of Tumor Radiotherapy With Modulators of Cell Metabolism: Toward Clinical Applications. *Seminars in Radiation Oncology* **23**, 262–272 (2013).
192. Doherty, J. R. & Cleveland, J. L. Targeting lactate metabolism for cancer therapeutics. *J Clin Invest* **123**, 3685–3692 (2013).
193. Jones, R. & Morris, M. Monocarboxylate Transporters: Therapeutic Targets and Prognostic Factors in Disease. *Clin. Pharmacol. Ther.* **100**, 454–463 (2016).
194. Marchiq, I. & Pouyssegur, J. Hypoxia, cancer metabolism and the therapeutic benefit of targeting lactate/H<sup>+</sup> symporters. *J Mol Med* **94**, 155–171 (2016).
195. Pivovarova, A. I. & MacGregor, G. G. Glucose-dependent growth arrest of leukemia cells by MCT1 inhibition: Feeding Warburg's sweet tooth and blocking acid export as an anticancer strategy. *Biomedicine & Pharmacotherapy* **98**, 173–179 (2018).
196. Mendoza-Juez, B., Martínez-González, A., Calvo, G. F. & Pérez-García, V. M. A Mathematical Model for the Glucose-Lactate Metabolism of in Vitro Cancer Cells. *Bull Math Biol* **74**, 1125–1142 (2012).
197. Mathupala, S. P., Parajuli, P. & Sloan, A. E. Silencing of Monocarboxylate Transporters via Small Interfering Ribonucleic Acid Inhibits Glycolysis and Induces Cell Death in Malignant Glioma: An in Vitro Study. *Neurosurgery* **55**, 1410–1419 (2004).
198. Murray, C. M. *et al.* Monocarboxylate transporter MCT1 is a target for immunosuppression. *Nature Chemical Biology* **1**, 371 (2005).
199. Sonveaux, P. *et al.* Targeting the Lactate Transporter MCT1 in Endothelial Cells Inhibits Lactate-Induced HIF-1 Activation and Tumor Angiogenesis. *PLoS One* **7**, (2012).
200. Beloueche-Babari, M. *et al.* MCT1 Inhibitor AZD3965 Increases Mitochondrial Metabolism, Facilitating Combination Therapy and Noninvasive Magnetic Resonance Spectroscopy. *Cancer Res* **77**, 5913–5924 (2017).

201. Granja, S. *et al.* Disruption of BASIGIN decreases lactic acid export and sensitizes non-small cell lung cancer to biguanides independently of the LKB1 status. *Oncotarget* **6**, 6708–6721 (2014).
202. Marchiq, I., Floch, R. L., Roux, D., Simon, M.-P. & Pouyssegur, J. Genetic Disruption of Lactate/H<sup>+</sup> Symporters (MCTs) and Their Subunit CD147/BASIGIN Sensitizes Glycolytic Tumor Cells to Phenformin. *Cancer Res* **75**, 171–180 (2015).
203. Morais-Santos, F. *et al.* Targeting lactate transport suppresses in vivo breast tumour growth. *Oncotarget* **6**, 19177–19189 (2015).
204. Miao, P., Sheng, S., Sun, X., Liu, J. & Huang, G. Lactate dehydrogenase a in cancer: A promising target for diagnosis and therapy. *IUBMB Life* **65**, 904–910 (2013).
205. Xie, H. *et al.* LDH-A inhibition, a therapeutic strategy for treatment of hereditary leiomyomatosis and renal cell cancer. *Mol Cancer Ther* **8**, 626–635 (2009).
206. Le, A. *et al.* Inhibition of lactate dehydrogenase A induces oxidative stress and inhibits tumor progression. *Proc Natl Acad Sci U S A* **107**, 2037–2042 (2010).
207. Krishnamoorthy, G. *et al.* FX11 limits *Mycobacterium tuberculosis* growth and potentiates bactericidal activity of isoniazid through host-directed activity. *Dis. Model. Mech.* dmm.041954 (2020) doi:10.1242/dmm.041954.
208. Chaube, B. *et al.* Targeting metabolic flexibility by simultaneously inhibiting respiratory complex I and lactate generation retards melanoma progression. *Oncotarget* **6**, 37281–37299 (2015).
209. Zhao, Z., Han, F., Yang, S., Wu, J. & Zhan, W. Oxamate-mediated inhibition of lactate dehydrogenase induces protective autophagy in gastric cancer cells: Involvement of the Akt–mTOR signaling pathway. *Cancer Letters* **358**, 17–26 (2015).
210. Billig, S. *et al.* Lactate oxidation facilitates growth of *Mycobacterium tuberculosis* in human macrophages. *Scientific Reports* **7**, 6484 (2017).



211. Morrot, A. *et al.* Metabolic Symbiosis and Immunomodulation: How Tumor Cell-Derived Lactate May Disturb Innate and Adaptive Immune Responses. *Front Oncol* **8**, (2018).
212. Fischer, K. *et al.* Inhibitory effect of tumor cell-derived lactic acid on human T cells. *Blood* **109**, 3812–3819 (2007).
213. Choi, S. Y. C., Collins, C. C., Gout, P. W. & Wang, Y. Cancer-generated lactic acid: a regulatory, immunosuppressive metabolite? *J. Pathol.* **230**, 350–355 (2013).
214. Haas, R. *et al.* Lactate Regulates Metabolic and Pro-inflammatory Circuits in Control of T Cell Migration and Effector Functions. *PLoS Biol* **13**, (2015).
215. Seth, P. *et al.* Deletion of Lactate Dehydrogenase-A in Myeloid Cells Triggers Antitumor Immunity. *Cancer Res* **77**, 3632–3643 (2017).
216. Kumar, P. IFN $\gamma$ -producing CD4 $^+$  T lymphocytes: the double-edged swords in tuberculosis. *Clinical and Translational Medicine* **6**, 21 (2017).
217. Lin, P. L. & Flynn, J. L. CD8 T cells and Mycobacterium tuberculosis infection. *Semin Immunopathol* **37**, 239–249 (2015).
218. Shen, H. & Chen, Z. W. The crucial roles of Th17-related cytokines/signal pathways in M. tuberculosis infection. *Cellular & Molecular Immunology* **15**, 216–225 (2018).
219. Lyadova, I. V. & Panteleev, A. V. Th1 and Th17 Cells in Tuberculosis: Protection, Pathology, and Biomarkers. *Mediators of Inflammation* vol. 2015 e854507 <https://www.hindawi.com/journals/mi/2015/854507/> (2015).
220. Angelin, A. *et al.* Foxp3 Reprograms T Cell Metabolism to Function in Low-Glucose, High-Lactate Environments. *Cell Metabolism* **25**, 1282-1293.e7 (2017).
221. Brightenti, S. & Ordway, D. J. Regulation of Immunity to Tuberculosis. in *Tuberculosis and the Tubercle Bacillus* 73–93 (John Wiley & Sons, Ltd, 2017).  
doi:10.1128/9781555819569.ch3.
222. Dang, E. V. *et al.* Control of TH17/Treg Balance by Hypoxia-inducible Factor 1. *Cell* **146**, 772–784 (2011).

223. Shi, L. Z. *et al.* HIF1 $\alpha$ -dependent glycolytic pathway orchestrates a metabolic checkpoint for the differentiation of TH17 and Treg cells. *Journal of Experimental Medicine* **208**, 1367–1376 (2011).
224. Husain, Z., Huang, Y., Seth, P. & Sukhatme, V. P. Tumor-Derived Lactate Modifies Antitumor Immune Response: Effect on Myeloid-Derived Suppressor Cells and NK Cells. *The Journal of Immunology* **191**, 1486–1495 (2013).
225. Crane, C. A. *et al.* Immune evasion mediated by tumor-derived lactate dehydrogenase induction of NKG2D ligands on myeloid cells in glioblastoma patients. *Proc Natl Acad Sci U S A* **111**, 12823–12828 (2014).
226. Brand, A. *et al.* LDHA-Associated Lactic Acid Production Blunts Tumor Immunosurveillance by T and NK Cells. *Cell Metabolism* **24**, 657–671 (2016).
227. Liu, C. H., Liu, H. & Ge, B. Innate immunity in tuberculosis: host defense vs pathogen evasion. *Cellular & Molecular Immunology* **14**, 963–975 (2017).
228. Dietl, K. *et al.* Lactic Acid and Acidification Inhibit TNF Secretion and Glycolysis of Human Monocytes. *The Journal of Immunology* **184**, 1200–1209 (2010).
229. Goetze, K., Walenta, S., Ksiazkiewicz, M., Kunz-Schughart, L. A. & Mueller-Klieser, W. Lactate enhances motility of tumor cells and inhibits monocyte migration and cytokine release. *International Journal of Oncology* **39**, 453–463 (2011).
230. Zhai, W., Wu, F., Zhang, Y., Fu, Y. & Liu, Z. The Immune Escape Mechanisms of Mycobacterium Tuberculosis. *International Journal of Molecular Sciences* **20**, 340 (2019).
231. Grace, P. S. & Ernst, J. D. Suboptimal Antigen Presentation Contributes to Virulence of Mycobacterium tuberculosis In Vivo. *The Journal of Immunology* **196**, 357–364 (2016).
232. Ernst, J. D. Mechanisms of M. tuberculosis Immune Evasion as Challenges to TB Vaccine Design. *Cell Host & Microbe* **24**, 34–42 (2018).
233. Su, S., Wu, W., He, C., Liu, Q. & Song, E. Breaking the vicious cycle between breast cancer cells and tumor-associated macrophages. *Oncoimmunology* **3**, (2014).

234. Zhao, Y. *et al.* Bladder cancer cells re-educate TAMs through lactate shuttling in the microfluidic cancer microenvironment. *Oncotarget* **6**, 39196–39210 (2015).
235. Selleri, S. *et al.* Human mesenchymal stromal cell-secreted lactate induces M2-macrophage differentiation by metabolic reprogramming. *Oncotarget* **7**, 30193–30210 (2016).
236. Ohashi, T. *et al.* M2-like macrophage polarization in high lactic acid-producing head and neck cancer. *Cancer Sci* **108**, 1128–1134 (2017).
237. Peter, K., Rehli, M., Singer, K., Renner-Sattler, K. & Kreutz, M. Lactic acid delays the inflammatory response of human monocytes. *Biochemical and Biophysical Research Communications* **457**, 412–418 (2015).
238. Iraporda, C. *et al.* Local Treatment with Lactate Prevents Intestinal Inflammation in the TNBS-Induced Colitis Model. *Front Immunol* **7**, (2016).
239. Offermanns, S. Free Fatty Acid (FFA) and Hydroxy Carboxylic Acid (HCA) Receptors. *Annual Review of Pharmacology and Toxicology* **54**, 407–434 (2014).
240. Offermanns, S. Hydroxy-Carboxylic Acid Receptor Actions in Metabolism. *Trends in Endocrinology & Metabolism* **28**, 227–236 (2017).
241. Husted, A. S., Trauelsen, M., Rudenko, O., Hjorth, S. A. & Schwartz, T. W. GPCR-Mediated Signaling of Metabolites. *Cell Metabolism* **25**, 777–796 (2017).
242. Ristic, B., Bhutia, Y. D. & Ganapathy, V. Cell-surface G-protein-coupled receptors for tumor-associated metabolites: A direct link to mitochondrial dysfunction in cancer. *Biochimica et Biophysica Acta (BBA) - Reviews on Cancer* **1868**, 246–257 (2017).
243. Cai, T.-Q. *et al.* Role of GPR81 in lactate-mediated reduction of adipose lipolysis. *Biochemical and Biophysical Research Communications* **377**, 987–991 (2008).
244. Liu, C. *et al.* Lactate Inhibits Lipolysis in Fat Cells through Activation of an Orphan G-protein-coupled Receptor, GPR81. *J. Biol. Chem.* **284**, 2811–2822 (2009).

245. Ahmed, K. *et al.* An Autocrine Lactate Loop Mediates Insulin-Dependent Inhibition of Lipolysis through GPR81. *Cell Metabolism* **11**, 311–319 (2010).
246. Lee, D. K. *et al.* Discovery and mapping of ten novel G protein-coupled receptor genes. *Gene* **275**, 83–91 (2001).
247. Kuei, C. *et al.* Study of GPR81, the Lactate Receptor, from Distant Species Identifies Residues and Motifs Critical for GPR81 Functions. *Mol Pharmacol* **80**, 848–858 (2011).
248. Jenninga, E. H. *et al.* Peroxisome Proliferator-activated Receptor  $\gamma$  Regulates Expression of the Anti-lipolytic G-protein-coupled Receptor 81 (GPR81/Gpr81). *J. Biol. Chem.* **284**, 26385–26393 (2009).
249. Li, G., Wang, H., Wang, L., Chen, R. & Liu, J. Distinct Pathways of ERK1/2 Activation by Hydroxy-Carboxylic Acid Receptor-1. *PLOS ONE* **9**, e93041 (2014).
250. Chung, Y. *et al.* Elevated cyclic AMP Acts through PKA type I to Inhibit Mycobacterium tuberculosis-induced IFN-gamma Secretion by T cells. *Faseb J.* **22**, (2008).
251. Guirado, E. *et al.* Deletion of PPAR $\gamma$  in lung macrophages provides an immunoprotective response against M. tuberculosis infection in mice. *Tuberculosis* **111**, 170–177 (2018).
252. Arnett, E. *et al.* PPAR $\gamma$  is critical for Mycobacterium tuberculosis induction of Mcl-1 and limitation of human macrophage apoptosis. *PLoS Pathog* **14**, (2018).
253. Dvorak, C. A. *et al.* Identification of Hydroxybenzoic Acids as Selective Lactate Receptor (GPR81) Agonists with Antilipolytic Effects. *ACS Med. Chem. Lett.* **3**, 637–639 (2012).
254. Liu, C. *et al.* 3,5-Dihydroxybenzoic Acid, a Specific Agonist for Hydroxycarboxylic Acid 1, Inhibits Lipolysis in Adipocytes. *J Pharmacol Exp Ther* **341**, 794–801 (2012).
255. Sakurai, T. *et al.* Identification of a novel GPR81-selective agonist that suppresses lipolysis in mice without cutaneous flushing. *European Journal of Pharmacology* **727**, 1–7 (2014).
256. Geyer, M. *et al.* Synthesis and Pharmacological Properties of Silicon-Containing GPR81 and GPR109A Agonists. *ChemMedChem* **10**, 2063–2070 (2015).

257. Davidsson, Ö. *et al.* Identification of novel GPR81 agonist lead series for target biology evaluation. *Bioorganic & Medicinal Chemistry Letters* 126953 (2020)  
doi:10.1016/j.bmcl.2020.126953.
258. Feingold, K. R., Moser, A., Shigenaga, J. K. & Grunfeld, C. Inflammation inhibits GPR81 expression in adipose tissue. *Inflamm. Res.* **60**, 991 (2011).
259. Rooney, K. & Trayhurn, P. Lactate and the GPR81 receptor in metabolic regulation: implications for adipose tissue function and fatty acid utilisation by muscle during exercise. *British Journal of Nutrition* **106**, 1310–1316 (2011).
260. Hoque, R., Farooq, A., Ghani, A., Gorelick, F. & Mehal, W. Z. Lactate Reduces Liver and Pancreatic Injury in Toll-Like Receptor– and Inflammasome-Mediated Inflammation via GPR81-Mediated Suppression of Innate Immunity. *Gastroenterology* **146**, 1763–1774 (2014).
261. Master, S. S. *et al.* Mycobacterium tuberculosis Prevents Inflammasome Activation. *Cell Host & Microbe* **3**, 224–232 (2008).
262. Briken, V., Ahlbrand, S. E. & Shah, S. Mycobacterium tuberculosis and the host cell inflammasome: a complex relationship. *Front. Cell. Infect. Microbiol.* **3**, (2013).
263. Souza de Lima, D., Ogusku, M. M., Sadahiro, A. & Pontillo, A. Inflammasome genetics contributes to the development and control of active pulmonary tuberculosis. *Infection, Genetics and Evolution* **41**, 240–244 (2016).
264. Ranganathan, P. *et al.* GPR81, a Cell-Surface Receptor for Lactate, Regulates Intestinal Homeostasis and Protects Mice from Experimental Colitis. *The Journal of Immunology* **200**, 1781–1789 (2018).
265. Bozzo, L., Puyal, J. & Chatton, J.-Y. Lactate Modulates the Activity of Primary Cortical Neurons through a Receptor-Mediated Pathway. *PLOS ONE* **8**, e71721 (2013).
266. Lauritzen, K. H. *et al.* Lactate Receptor Sites Link Neurotransmission, Neurovascular Coupling, and Brain Energy Metabolism. *Cereb Cortex* **24**, 2784–2795 (2014).

267. Morland, C. *et al.* The lactate receptor, G-protein-coupled receptor 81/hydroxycarboxylic acid receptor 1: Expression and action in brain. *Journal of Neuroscience Research* **93**, 1045–1055 (2015).
268. Mosienko, V., Teschemacher, A. G. & Kasparov, S. Is L-Lactate a Novel Signaling Molecule in the Brain? *J Cereb Blood Flow Metab* **35**, 1069–1075 (2015).
269. Abrantes, H. de C. *et al.* The Lactate Receptor HCAR1 Modulates Neuronal Network Activity through the Activation of G $\alpha$  and G $\beta\gamma$  Subunits. *J. Neurosci.* **39**, 4422–4433 (2019).
270. Morland, C. *et al.* Exercise induces cerebral VEGF and angiogenesis via the lactate receptor HCAR1. *Nature Communications* **8**, 15557 (2017).
271. Shen, Z. *et al.* Inhibition of G Protein-Coupled Receptor 81 (GPR81) Protects Against Ischemic Brain Injury. *CNS Neuroscience & Therapeutics* **21**, 271–279 (2015).
272. Polena, H. *et al.* Mycobacterium tuberculosis exploits the formation of new blood vessels for its dissemination. *Scientific Reports* **6**, 33162 (2016).
273. Roland, C. L. *et al.* Cell Surface Lactate Receptor GPR81 Is Crucial for Cancer Cell Survival. *Cancer Res* **74**, 5301–5310 (2014).
274. Brown, T. P. & Ganapathy, V. Lactate/GPR81 signaling and proton motive force in cancer: Role in angiogenesis, immune escape, nutrition, and Warburg phenomenon. *Pharmacology & Therapeutics* 107451 (2019) doi:10.1016/j.pharmthera.2019.107451.
275. Lee, Y. J. *et al.* G-protein-coupled receptor 81 promotes a malignant phenotype in breast cancer through angiogenic factor secretion. *Oncotarget* **7**, 70898–70911 (2016).
276. Brown, T. P. *et al.* The lactate receptor GPR81 promotes breast cancer growth via a paracrine mechanism involving antigen-presenting cells in the tumor microenvironment. *Oncogene* 1–13 (2020) doi:10.1038/s41388-020-1216-5.
277. Stäubert, C., Broom, O. J. & Nordström, A. Hydroxycarboxylic acid receptors are essential for breast cancer cells to control their lipid/fatty acid metabolism. *Oncotarget* **6**, 19706–19720 (2015).

278. Singh, V. *et al.* Mycobacterium tuberculosis-Driven Targeted Recalibration of Macrophage Lipid Homeostasis Promotes the Foamy Phenotype. *Cell Host & Microbe* **12**, 669–681 (2012).
279. Lee, W., VanderVen, B. C., Fahey, R. J. & Russell, D. G. Intracellular Mycobacterium tuberculosis Exploits Host-derived Fatty Acids to Limit Metabolic Stress. *J. Biol. Chem.* **288**, 6788–6800 (2013).
280. Feng, J. *et al.* Tumor cell-derived lactate induces TAZ-dependent upregulation of PD-L1 through GPR81 in human lung cancer cells. *Oncogene* **36**, 5829 (2017).
281. Daneshmandi, S., Wegiel, B. & Seth, P. Blockade of Lactate Dehydrogenase-A (LDH-A) Improves Efficacy of Anti-Programmed Cell Death-1 (PD-1) Therapy in Melanoma. *Cancers* **11**, 450 (2019).
282. Feichtinger, R. G. & Lang, R. Targeting L-Lactate Metabolism to Overcome Resistance to Immune Therapy of Melanoma and Other Tumor Entities. *Journal of Oncology* <https://www.hindawi.com/journals/jo/2019/2084195/abs/> (2019) doi:10.1155/2019/2084195.
283. Jurado, J. O. *et al.* Programmed Death (PD)-1:PD-Ligand 1/PD-Ligand 2 Pathway Inhibits T Cell Effector Functions during Human Tuberculosis. *The Journal of Immunology* **181**, 116–125 (2008).
284. Lázár-Molnár, E. *et al.* Programmed death-1 (PD-1)–deficient mice are extraordinarily sensitive to tuberculosis. *PNAS* **107**, 13402–13407 (2010).
285. Tousif, S. *et al.* T Cells from Programmed Death-1 Deficient Mice Respond Poorly to Mycobacterium tuberculosis Infection. *PLoS One* **6**, (2011).
286. Wagner, W., Kania, K. D., Blauz, A. & Ciszewski, W. M. THE LACTATE RECEPTOR (HCAR1/GPR81) CONTRIBUTES TO DOXORUBICIN CHEMORESISTANCE VIA ABCB1 TRANSPORTER UP-REGULATION IN HUMAN CERVICAL CANCER HeLa CELLS. 10 (2017).

287. Wagner, W., Kania, K. D. & Ciszewski, W. M. Stimulation of lactate receptor (HCAR1) affects cellular DNA repair capacity. *DNA Repair* **52**, 49–58 (2017).
288. Wallenius, K. *et al.* Involvement of the metabolic sensor GPR81 in cardiovascular control. *JCI Insight* **2**, (2017).



## CHAPTER 2: HYPOXIA INDEPENDENT ACTIVATION OF HIF-1 $\alpha$ BY MYCOBACTIN DURING EARLY MYCOBACTERIUM TUBERCULOSIS INFECTION AUGMENTS MACROPHAGE METABOLISM

### 1. Summary

Hypoxia inducible factor-1 $\alpha$  (HIF-1 $\alpha$ ) becomes active within host cells in response to hypoxia, regulating cellular metabolic shifts from oxidative phosphorylation to glycolysis. In the context of the tuberculosis (TB) granuloma microenvironment, hypoxia is a chronic lesion characteristic, and HIF-1 $\alpha$  expression has been observed within infected lungs. However, shifts to glycolytic metabolic phenotypes in macrophages have been observed very early during *in vitro* *Mycobacterium tuberculosis* (Mtb) infection, prior to when hypoxia would develop. Multiple hypoxia-independent mechanisms exist for HIF-1 $\alpha$  activation, including through iron chelation. Mtb possesses an iron-chelating siderophore, mycobactin, which effectively scavenges host iron. Based on this, we aimed to determine the effect of mycobactin on HIF-1 $\alpha$  activation and macrophage metabolic changes during early Mtb infection. Using iron chelators deferoxamine (DFO) and purified mycobactin J (MbtJ), we treated bone marrow derived macrophages (BMDMs) and analyzed cell lysates via Western Blot for HIF-1 $\alpha$ . Additionally, we used Seahorse Extracellular Flux Analyzer assays to determine the impact of iron chelation on macrophage metabolism, through both iron chelator treatments and by *in vitro* infection of CD1 mouse BMDMs with either mycobactin synthase K (mbtK) knock-out, complement, or wild-type H37Rv strains of Mtb. Iron chelation by MbtJ increased HIF-1 $\alpha$  levels in a dose-dependent manner and potently increased macrophage glycolytic metabolism. Infection with mbtK knock-out Mtb demonstrated the critical role that mycobactin plays in regulating the metabolic response of macrophages post-infection, decreasing oxidative metabolism and increasing glycolytic metabolism. Based on our results, hypoxia-independent mechanisms of HIF-1 $\alpha$  activation may play a role in establishing an

environment favorable for Mtb survival. Without a better understanding of the ways in which early Mtb infection influences host immune cell function, the global TB disease burden will remain high. The results herein provide mechanistic insight which may be utilized to design host directed therapeutic strategies which will better equip the host to combat Mtb infection.

## **2. Introduction**

*Mycobacterium tuberculosis* (Mtb) is the leading cause of death by an infectious disease, and the most recent World Health Organization Global Tuberculosis Report estimates that 10 million new cases and 1.2 million deaths due to tuberculosis (TB) occurred in 2018 alone.<sup>1</sup> Although the number of TB related deaths has declined over the past two decades, the number of new cases has remained stagnant. The rise of multi-drug resistance, lack of an efficacious adult pulmonary vaccine, co-morbidities of both communicable and non-communicable disease with TB, poor healthcare infrastructure in endemic regions, and a slow developmental pipeline for new therapeutics hinders progress toward reducing the number of cases each year.<sup>2-6</sup> As a result, recent research in the field has sought to investigate host-pathogen dynamics during infection in order to develop novel, host-directed therapeutic (HDT) strategies that will better equip the host to fight persistent Mtb infection.<sup>7-9</sup> Many HDT strategies seek to boost the host immune system, rather than target Mtb itself, thereby bypassing concerns for antimicrobial resistance, and allowing for drugs already approved to be repurposed in the context of TB disease.<sup>10,11</sup>

The complexity of the TB granuloma microenvironment adds to the difficulty in finding effective HDTs. TB granulomas have significant heterogeneity in lesion architecture within and between individuals and are characterized by chronic granulomatous inflammation incited by persistent Mtb antigens and an inability to clear Mtb bacilli.<sup>12-15</sup> Macrophages and lymphocytes progressively infiltrate the involved lesion area. Over time, lesions develop a necrotic central core, with varied

levels of fibrosis and calcification. Late stage lesions compress neighboring tissue structures, blocking blood and oxygen supply, which impairs drug delivery and disrupts cellular homeostasis.<sup>12-15</sup> As a result, in chronic stages of infection, the lesion microenvironment is significantly hypoxic.

To adapt to these hypoxic conditions in the granuloma core, the host has developed a transcriptionally regulated, global response. This is driven by the transcription factor hypoxia inducible factor-1 (HIF-1).<sup>16-18</sup> HIF-1 is responsible for regulating responses such as angiogenesis, erythropoiesis, cell survival, cell proliferation, and cellular metabolism with the intent to increase oxygen delivery to hypoxic regions.<sup>19</sup> Under normoxic conditions, HIF-1 $\alpha$  is hydroxylated on proline residues by prolyl hydroxylase (PHD) enzymes, tagging it for rapid degradation via von Hippau Lindau (VHL) factor and the ubiquitin-proteasome system.<sup>20-22</sup> However, under conditions of low oxygen tension, like those exhibited within the hypoxic core of the TB granuloma, PHD enzymes no longer have the critical oxygen cofactor needed for their enzymatic activity, and as a result HIF-1 $\alpha$  subunits are not targeted for degradation.<sup>20-22</sup> Instead, HIF-1 $\alpha$  accumulates in the cytoplasm, translocates to the nucleus, dimerizes with the constitutively expressed HIF-1 $\beta$  subunit, and initiates the transcription of regulated genes.<sup>20-22</sup>

The HIF-1 $\alpha$  directed metabolic response involves increased glucose transport, increased glycolysis through upregulation of enzyme production, increased lactate production, increased lactate export, and decreased conversion of pyruvate to acetyl-coA, impairing mitochondrial respiration.<sup>23-27</sup> This metabolic “switch” has been well described in cancer cells and in activated immune cells, even in the presence of oxygen, and has been coined the Warburg Effect.<sup>23-27</sup> In the case of Mtb infection, we and others have demonstrated that glycolysis is activated very early in the course of infection<sup>28-31</sup> and that HIF-1 $\alpha$  is detectable in primary lung lesions.<sup>28,32-37</sup> What has yet to be described is the mechanism of HIF-1 $\alpha$  activation. If glycolytic metabolism is

upregulated early in the course of Mtb infection, HIF-1 $\alpha$  would likely be upregulated prior to the formation of a hypoxic granuloma microenvironment. If this is the case, HIF-1 $\alpha$  must be activated in a hypoxia-independent fashion.

Cytokines<sup>38,39</sup>, chemicals<sup>40-42</sup>, metabolites<sup>43-45</sup>, and iron chelation<sup>46,47</sup> are all capable of stabilizing HIF-1 $\alpha$  in a hypoxia-independent manner. Specifically, PHDs require iron in addition to oxygen to carry out their function.<sup>48-50</sup> Iron is limited by hosts in the early innate immune responses to bacterial infections.<sup>51-55</sup> As a result, bacteria have evolved to produce iron chelating molecules, called siderophores, which possess iron binding capabilities that exceed that of host iron binding molecules such as transferrin.<sup>56-59</sup> This allows for bacterial scavenging of iron, which becomes important for intracellular infections like that of Mtb.

Importantly, research has demonstrated that knocking out the biosynthetic machinery used to produce siderophores in *Salmonella enterica* and *Yersinia enterocolitica* eliminates the activation of HIF-1 $\alpha$  during infection.<sup>60</sup> The mechanism of action was attributed to iron chelation mediated inhibition of PHD function. Certain iron chelators, such as deferoxamine (DFO), are already approved by the FDA for the treatment of iron overload disorders such as beta-thalassemia.<sup>61-63</sup> Mycobacterial species also possess iron chelating siderophores and complex iron acquisition machinery, and Mtb produces a membrane bound form called mycobactin.<sup>64-69</sup> Exogenous iron chelation treatment using DFO can upregulate macrophage glycolytic metabolism during Mtb infection in a HIF-1 $\alpha$  dependent manner.<sup>70</sup> This provides a potential mechanism for early observed changes to host immune cell metabolism during Mtb infection.

Based on this knowledge, we hypothesized that mycobactin mediates shifts in host macrophage metabolism by activating HIF-1 $\alpha$  early during Mtb infection. Our laboratory possesses a patent related to this hypothesis.<sup>71</sup> This serves as a pathogen-driven mechanism for adapting host cells

to low oxygen microenvironments encountered within the hypoxic core of the TB granuloma, preserving a bacterial intracellular survival niche. To test this hypothesis, we investigated the response of macrophages to purified mycobactin and used *in vitro* macrophage infection models with mycobactin biosynthesis knockouts. Through this work, we demonstrate a mechanistic link between mycobactin mediated iron chelation and HIF-1 $\alpha$  activation.

### **3. Materials & Methods**

#### *3.1. Bone Marrow Derived Macrophage (BMDM) Cell Culture*

Bone marrow was isolated from the femur of Strain 13 guinea pigs and CD1 mice and stock vials were maintained in liquid nitrogen. To differentiate guinea pig BMDMs, cells were maintained in complete RPMI (Sigma-Aldrich) (10% FBS (Atlas Biologicals), 1% antibiotic/antimycotic (Thermo Fischer)) with 20 ng/mL MCSF (Gemini) for seven days, changing media at day three. To differentiate CD1 mouse BMDMs, cells were maintained in media containing 30% L929 cell conditioned media, 20% FBS, and 1% antibiotic/antimycotic for seven days, changing media at day four. Post differentiation into BMDMs, cells were maintained in cRPMI + MCSF (guinea pig) or 5% L929 conditioned media, 10% FBS, 1% antibiotic/antimycotic (mouse). CD1 mouse cells were confirmed to express macrophage specific markers CD11b and F4/80 by flow cytometry.

#### *3.2. Purification of Mycobactin J*

Iron saturated mycobactin J was purchased from Allied Monitor (Fayette, MO) in crude form. Purification was conducted by Michio Kuruso (University of Tennessee Health Science Center, Memphis, TN) using the following protocol. The lyophilized Fe<sup>3+</sup>-mycobactin J complex was reconstituted in CHCl<sub>3</sub> and 4N HCl and the suspension was stirred for 30 minutes. The water

phase was separated and 4N HCL was added again. Another stir phase and removal of the water phase followed. This was repeated three additional times until a clear solution was obtained. The CHCl<sub>3</sub> phase was dried over Na<sub>2</sub>SO<sub>4</sub> and concentrated in a vacuum. Purification with SiO<sub>2</sub> (CHCl<sub>3</sub>:MeOH of 20:1) yielded iron free mycobactin J. Purity was determined by NMR spectroscopy. A crude preparation of 50 mgs of mycobactin J yielded 9.8 mg pure product post iron removal and purification. The iron binding capacity of iron free preparations were determined by the Ferrozine method with an iron binding capacity kit (Eagle Diagnostics, TX).

### 3.3. *Mycobactin Knock-Out Mtb Strains*

Parent H37RV, complemented, and knock-out of mycobactin synthase K (mbtK) strains of Mtb were obtained from Branch Moody (Brigham and Women's, Boston, MA). Stock cultures were prepared in BD Difco™ 7H9 broth media (VWR) supplemented with either 50 µg/mL hygromycin B (Thermo Fisher) (complement) or 2 µg/mL mycobactin J (Allied Monitor) (knock-out) or without supplementation (parent H37Rv). Stock titers were determined using BD Difco™ 7H11 agar (VWR) quad plates supplemented in the same way as the 7H9 media described above.

### 3.4. *Extracellular Flux Analysis*

CD1 mouse BMDMs were pre-treated with either deferoxamine (DFO) (Sigma-Aldrich) or purified mycobactin J (MbtJ) for four hours. 100,000 cells per well were transferred to a plate compatible with the XFe24 Seahorse Extracellular Flux Analyzer. A combined mitochondrial-glycolysis stress test was performed, with the following injections: oligomycin (Millipore) (port A, 1 µM), FCCP (Cayman Chemical) (port B, 1.5 µM), rotenone (Sigma-Aldrich)/antimycin A (Sigma-Aldrich) (port C, 0.5 µM each), and 2DG (Cayman Chemical) (port D, 50 mM). Parameters were calculated based on the raw instrument data. For *in vitro* infections with mbtK knock-out, complement, and

parent H37Rv strains of Mtb, cells were plated at 75,000 cells per well into a plate compatible with the XF96 Seahorse Extracellular Flux Analyzer. Mtb strains were added to wells at an MOI of 1:1, 5:1, or 10:1 and cells were incubated with bacteria for one hour prior to starting the extracellular flux assay. Measurements were taken consecutively over the course of eight hours, without any injections.

### 3.5. *Western Blot*

Guinea pig bone BMDMs and CD1 mouse BMDMs were pre-treated with deferoxamine or purified mycobactin J for six hours (guinea pig) or four hours (CD1 mouse). Protein was isolated from whole cell lysates using an immunoprecipitation buffer (1% Triton-X, 150 mM NaCl, 10 mM EDTA, 10 mM Tris, 0.5% NP-40, pH 7.4). A Pierce BCA assay (Thermo Fischer) was conducted to quantify protein in samples and to normalize protein loaded onto gels. 15 µg of protein were loaded per well into a 4-12% Bis-Tris SDS PAGE gel (NuPage, Invitrogen). The gel was run at constant voltage for one hour, and then transferred for two hours onto a 0.45-micron PVDF membrane (GVS) at a constant mAmp. The membrane was blocked with 5% BSA, 0.05% Tween 20 for one hour. Primary antibodies were incubated overnight in block buffer. TBS supplemented with Tween was used to wash blots for one hour prior to a two-hour incubation with secondary antibody. Blots were washed again for one hour prior to developing using a Pierce ECL chemiluminescence development kit (Thermo Fischer). Blots were imaged using an ImageQuant LAS 4000 and edited via Image J software. Antibodies were used against HIF-1α (Novus NB100-105), or beta-actin as control (Invitrogen AM4302).

### 3.6. *Data analysis*

Depending on the data set, a one-way or two-way ANOVA was used to determine differences between groups. P less than or equal to 0.05 was considered statistically significant. Tukey's IQR method was used to identify any outliers prior to calculations. Nonparametric tests were used if normality or homoscedasticity were not achieved. Multiple comparison testing was conducted using Tukey, Sidak's or Mann-Whitney multiple comparisons depending on the data analysis procedure. All statistical analysis was performed using GraphPad Prism version 8.3.

## 4. Results

### 4.1. *Iron chelation increases HIF-1 $\alpha$ levels and potently increases glycolytic metabolism in uninfected macrophages*

Bacterial iron chelators from Enterobacteriaceae have previously been shown to activate HIF-1 $\alpha$ ,<sup>60</sup> thus, we chose to investigate if mycobacterial chelators have a similar effect. CD1 mouse and guinea pig bone marrow BMDMs were treated with deferoxamine (DFO) or purified mycobactin J (MbtJ) and whole cell lysates analyzed for expression of HIF-1 $\alpha$  via Western Blot (Figure 2.1). DFO is an iron chelator that is FDA approved for the treatment of iron overload disorders<sup>61-63</sup> and served as a positive control for experiments. The MbtJ used was stripped of all iron to ensure maximum iron binding capacity. CD1 mouse BMDMs demonstrated concentration dependent increases in HIF-1 $\alpha$  protein levels up to 100  $\mu$ M (Figure 2.1A), and this effect was also observed in guinea pig BMDMs treated with DFO (Figure 2.1B). Significantly, MbtJ also demonstrated concentration dependent increases in HIF-1 $\alpha$  in guinea pig BMDMs (Figure 2.1B), and the impact of MbtJ on HIF-1 $\alpha$  levels was more pronounced than comparable concentrations of DFO. This is in line with previous literature which indicates that MbtJ has a higher iron binding constant than DFO.<sup>72,73</sup>



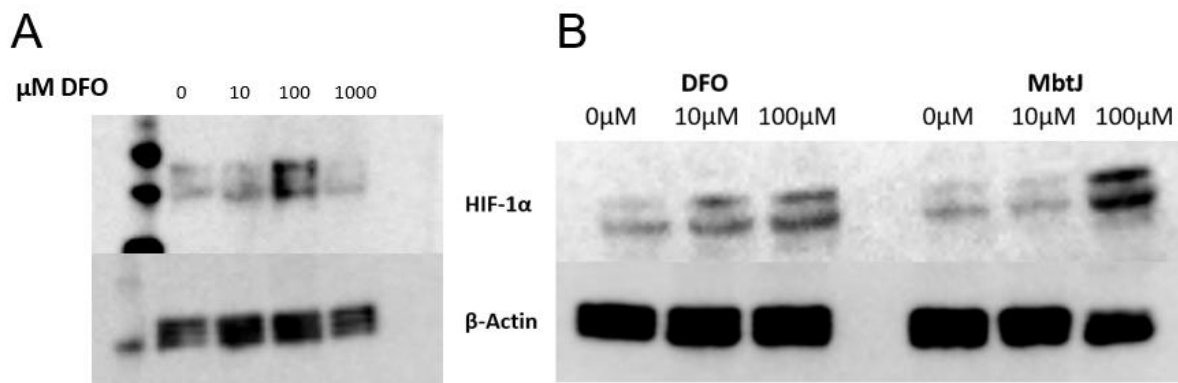


**Figure 2.1: Iron chelation stabilizes HIF-1 $\alpha$  in a dose dependent manner in bone marrow derived macrophages.** Bone marrow derived macrophages (BMDMs) of either A) CD1 mice or B) guinea pigs were treated with iron chelators deferoxamine (DFO) or mycobactin J (MbtJ) for four hours (A) or six hours (B). Western Blots on whole cell lysates demonstrated that HIF-1 $\alpha$  protein levels increased in a concentration-dependent manner. MbtJ increases HIF-1 $\alpha$  more than DFO at comparable concentrations in guinea pig BMDMs. Samples were normalized to protein concentration via BCA assay and representative images are shown.

For future metabolic experiments, we moved forward using CD1 mouse BMDMs due to an increased yield upon differentiation and ease of access to commercial reagents for mouse versus guinea pig models. As activation of HIF-1 $\alpha$  is known to upregulate glycolytic metabolism<sup>23–27</sup>, we next investigated the metabolic phenotype of uninfected CD1 mouse BMDMs treated with either DFO or MbtJ using a Seahorse Extracellular Flux Analyzer. CD1 mouse BMDMs were pre-treated with either DFO or MbtJ for four hours prior to performing extracellular flux analysis for both glycolytic and mitochondrial metabolic parameters (Figure 2.2).

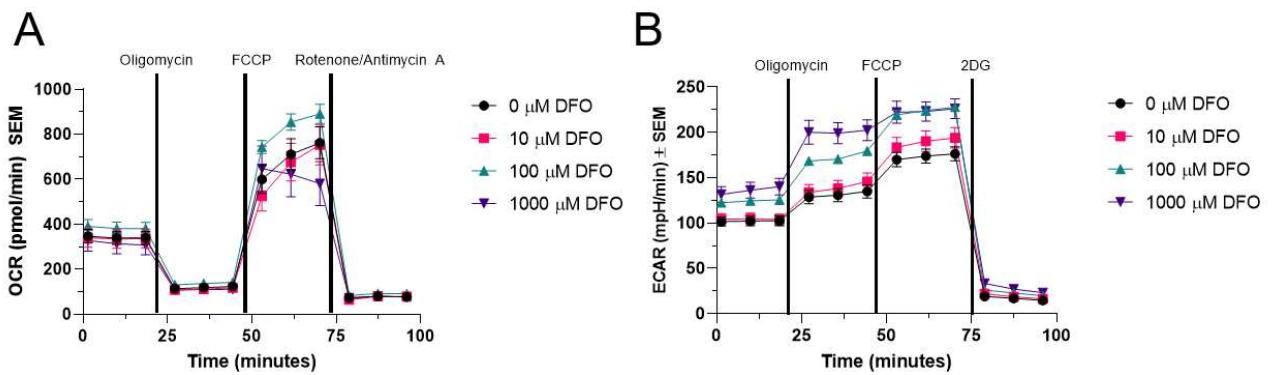


**Figure 2.2: Seahorse Extracellular Flux Analysis injection protocol for DFO and MbtJ experiments.** Representative line graphs are presented for oxygen consumption rate (OCR) (A) and extracellular acidification rate (ECAR) (B) to illustrate the order of injected inhibitors. Line graphs for DFO treatments are pictured; however, injection protocols were the same for MbtJ experiments.

DFO treatment significantly increased glycolytic metabolism of CD1 mouse BMDMs in a concentration dependent manner, as evidenced by an increase in basal extracellular acidification rate (ECAR) (Figure 2.3A) and a concurrent decrease in the oxygen consumption rate (OCR)/ECAR ratio (Figure 2.3B). The impact of DFO on glycolytic metabolism was further exemplified by increased glycolytic capacity (Figure 2.3C), maximum glycolysis (Figure 2.3D), and glycolytic reserve (Figure 2.3E). DFO had no significant impact on metabolic parameters related to oxidative metabolic function, including basal OCR (Figure 2.4A), ATP production (Figure 2.4B), mitochondrial spare capacity (Figure 2.4C), proton leak (Figure 2.4D), or maximum respiration (Figure 2.4E). This supported the hypothesis that iron chelation upregulates glycolytic metabolism in macrophages.

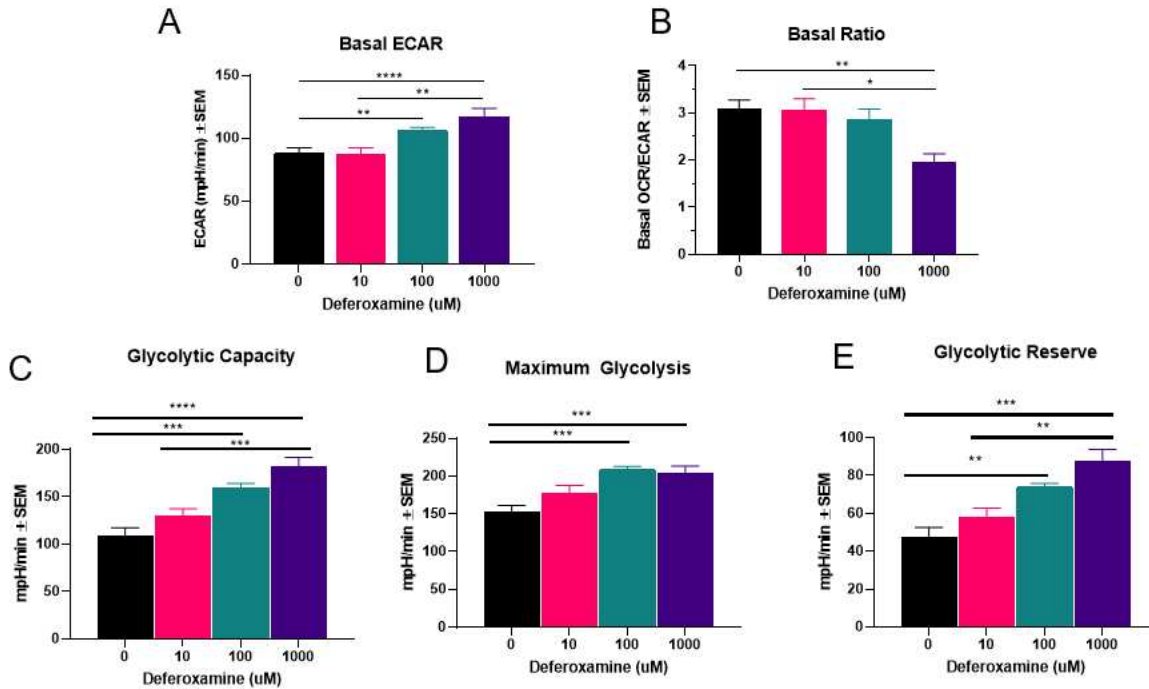


**Figure 2.3: Iron chelation by DFO increases glycolytic metabolism of CD1 mouse BMDMs in a concentration dependent manner.** CD1 mouse BMDMs were pre-treated with DFO for four hours and then assayed with a Seahorse Extracellular Flux Analyzer for glycolytic parameters. The basal extracellular acidification rate (ECAR) increased in a dose dependent manner (A). The basal ratio of oxygen consumption rate (OCR) to ECAR decreased in a dose dependent manner (B). Increased glycolytic metabolism is further indicated by concentration dependent increases in glycolytic capacity (C), maximum glycolysis (D), and glycolytic reserve (E). Overall, this supports the hypothesis that iron chelation increases glycolytic metabolism in macrophages. Data is presented as mean  $\pm$  SEM. Analysis was conducted via a one-way ANOVA, accounting for unequal variance and non-normal distributions when needed. 3 biological replicates,  $n = 10$  per group. \* =  $p < 0.05$ , \*\* =  $p < 0.01$ , \*\*\* =  $p < 0.001$ , \*\*\*\* =  $p < 0.0001$

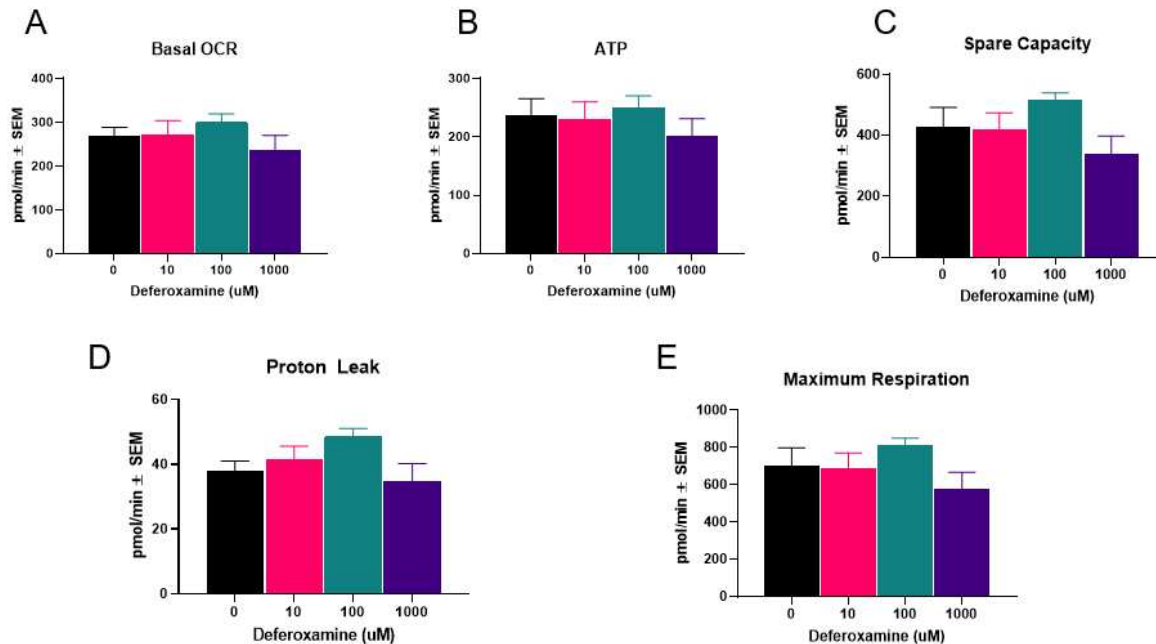


**Figure 2.4: Iron chelation by DFO does not significantly alter oxidative metabolic parameters.** CD1 mouse BMDMs were pre-treated with DFO for four hours and then assayed with a Seahorse Extracellular Flux Analyzer for oxidative metabolic parameters. The basal OCR (A), ATP (B), spare capacity (C), proton leak (D), and maximum respiration (E) were not impacted by increased concentration of DFO treatment. This indicates that iron chelation does not significantly impact the oxidative metabolic function of mouse BMDMs. Data is presented as mean  $\pm$  SEM. Analysis was conducted via a one-way ANOVA, accounting for unequal variance and non-normal distributions when needed. 3 biological replicates, n= 10 per group.

Similar effects were observed for MbtJ treatment. Concentration dependent increases in basal ECAR (Figure 2.5A) and concurrent decreases in OCR/ECAR ratio (Figure 2.5B) were observed post treatment, indicating a shift toward a glycolytic metabolic phenotype. This was further demonstrated through increases in glycolytic capacity (Figure 2.5C) and maximum glycolysis (Figure 2.5D). Interestingly, an opposing trend was observed with the glycolytic reserve parameter. MbtJ treatment decreased the glycolytic reserve of CD1 mouse BMDMs (Figure 2.5E), which contrasted with the impact of DFO on the same parameter (Figure 2.3E). MbtJ was also 100 times as potent as DFO with respect to glycolytic metabolic changes, as basal ECAR reached similar levels for DFO at 1000 μM that were achieved by MbtJ concentrations of 10 μM (Figure 2.3A, Figure 2.5A). While basal OCR (Figure 2.6A) and ATP production (Figure 2.6B) were not

significantly different between concentrations of MbtJ, there were some alterations in mitochondrial spare capacity (Figure 2.6C), proton leak (Figure 2.6D) and maximum respiration (Figure 2.6E). Those parameters increased at concentrations of 0.1  $\mu$ M and then plateaued to a non-significant level. The higher iron binding capacity of MbtJ may play a role in its ability to interfere directly with mitochondrial metabolism, as iron chelators have been demonstrated to directly alter mitochondrial electron transport chain activity and mitochondrial membrane potential.<sup>74–77</sup> In summary, these data demonstrate that mycobacterial iron chelators increase HIF-1 $\alpha$  and upregulate downstream glycolytic metabolism in a concentration dependent manner.

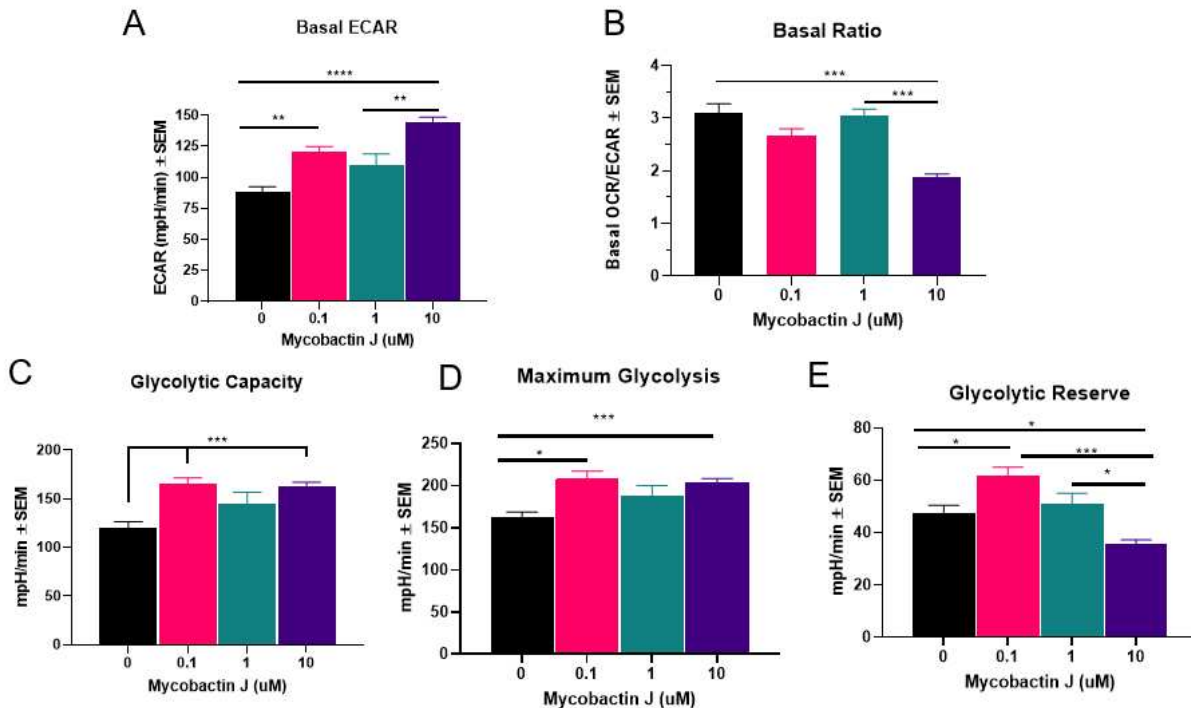


**Figure 2.5: Iron chelation by MbtJ increases glycolytic metabolism of CD1 mouse BMDMs in a concentration dependent manner.** CD1 mouse BMDMs were pre-treated with MbtJ for four hours and then assayed with a Seahorse Extracellular Flux Analyzer for glycolytic parameters. The basal extracellular acidification rate (ECAR) increased in a dose dependent manner (A). The basal ratio of oxygen consumption rate (OCR) to ECAR decreased in a dose dependent manner (B). Increased glycolytic metabolism is further indicated by concentration dependent increases in glycolytic capacity (C) and maximum glycolysis (D). However, MbtJ treatment at higher concentrations demonstrated a decrease in glycolytic reserve (E). Overall, this supports the hypothesis that iron chelation increases glycolytic metabolism in macrophages. Data is presented

as mean  $\pm$  SEM. Analysis was conducted via a one-way ANOVA, accounting for unequal variance and non-normal distributions when needed. 3 biological replicates, n= 7-10 per group. \* = p < 0.05, \*\* = p < 0.01, \*\*\* = p < 0.001, \*\*\*\* = p < 0.0001

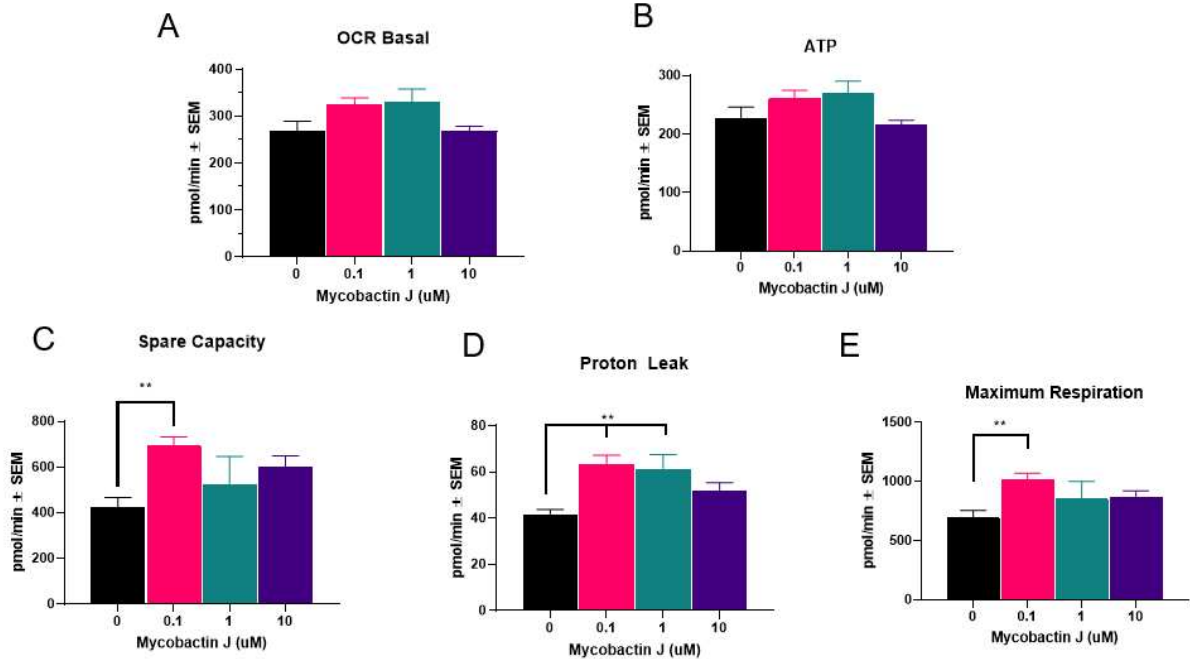


**Figure 2.6: Iron chelation by MbtJ minimally impacts oxidative metabolic parameters.** CD1 mouse BMDMs were pre-treated with MbtJ for four hours and then assayed with a Seahorse Extracellular Flux Analyzer for oxidative metabolic parameters. The basal OCR (A) and ATP production (B) levels were not significantly impacted by increasing MbtJ concentration. However, spare capacity (C), proton leak (D), and maximum respiration (E) all increased at the lowest MbtJ concentration, plateauing at higher concentrations. Data is presented as mean  $\pm$  SEM. Analysis was conducted via a one-way ANOVA, accounting for unequal variance and non-normal distributions when needed. 3 biological replicates, n= 7-10 per group. \*\* = p < 0.01

#### 4.2. *Mycobactin biosynthesis is critical for augmenting metabolic phenotype in mouse BMDMs infected with Mtb*

To further investigate the hypothesis that Mtb drives changes in macrophage metabolism via its iron chelating siderophore, mycobactin, we used an Mtb strain with a knock-out of mycobactin synthase K (mbtK). The mbtK gene encodes an acyl transferase which is critical for creating a functional mycobactin molecule.<sup>66</sup> CD1 mouse BMDMs were infected with either the mbtK knock-out (KO), complemented (Comp), or wild-type H37Rv Mtb (WT). Cells were incubated with

bacteria for one hour prior to assaying via a Seahorse Extracellular Flux Analyzer. Measurements were taken over the course of an eight-hour time period to determine changes in glycolytic and oxidative metabolic function over time, and then normalized to baseline measurement readings.

A significant reduction in oxidative metabolic function or OCR (%) was observed in WT Mtb infected CD1 mouse BMDMs as compared to those infected with the mbtK KO or complemented strains (Figure 2.7). Uninfected CD1 BMDMs maintained the highest rates of oxidative metabolism throughout the time course (Figure 2.7). The impact of different strains on oxidative cellular metabolism became more pronounced with increasing MOI and was most severe at an MOI of 10:1 (Figure 2.7C). The complemented strain exhibited oxidative metabolic changes that were more similar to the KO than the WT strain. These data indicate that CD1 mouse BMDMs infected with mycobactin producing Mtb are considerably less oxidative in their metabolic profile when compared to cells infected with a mbtK knock-out. Mycobactin is therefore critical to regulating macrophage metabolism during acute infection.

The impact of mycobactin on host macrophage metabolism was further evaluated with an analysis of glycolytic metabolic function or ECAR (%) (Figure 2.8). CD1 mouse BMDMs infected with a mbtK KO strain of Mtb exhibited minimal reductions in glycolytic metabolism over the experimental time course, when compared to cells infected with the complement or WT Mtb (Figure 2.8). The data trends remained similar across all MOIs but were not statistically significant (Figure 2.8). All cells regardless of infection status exhibited peak ECAR levels at 250 minutes post-assay start (Figure 2.8). The lack of more significant differences between ECAR values at higher MOIs may be a result of mouse BMDMs reaching peak activation status and their maximum glycolytic capacities at those higher MOIs. These data suggest that mycobactin biosynthesis may play a role in maintaining increased glycolytic metabolism during Mtb infection at acute time points.

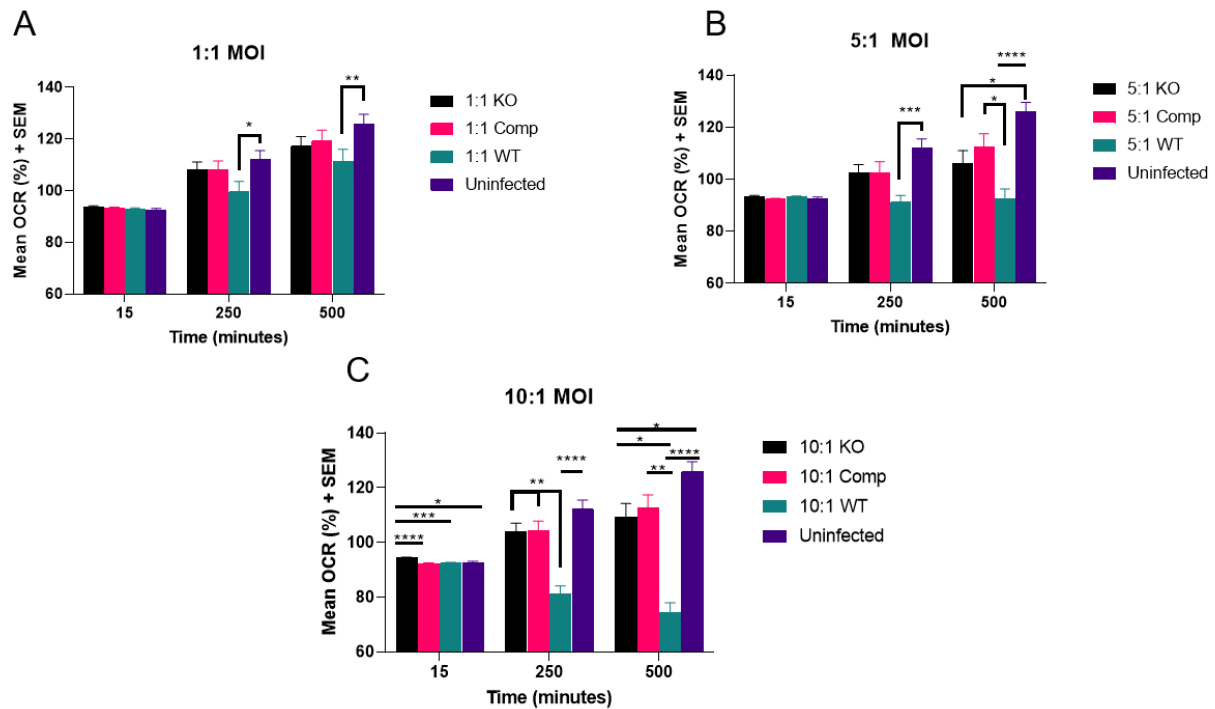


**Figure 2.7: CD1 mouse BMDMs infected with wild-type Mtb show significant reduction in oxidative metabolism when compared to those infected with a mycobactin knock-out.** CD1 mouse BMDMs infected with either wild-type Mtb H37Rv (WT), mycobactin K knock-out (KO), or complemented (Comp) were assayed on a Seahorse Extracellular Flux Analyzer for eight consecutive hours after a one-hour infection incubation. Measurements were baselined to the first reading and represented as a percent. Time points of 15, 250, and 500 minutes post-assay start are represented for an MOI of 1:1 (A), 5:1 (B), and 10:1 (C). WT Mtb infected cells show a decrease from baseline in percent oxidative consumption rate (OCR) over time, which becomes more severe with increasing MOI. BMDMs infected with mycobactin KO Mtb showcase increased oxidative metabolism compared to those infected with the WT, and this is maintained across increased MOI. Uninfected cells have the highest OCR. This indicates that mycobactin-producing strains of Mtb shift metabolism away from oxidative mechanisms. Data is presented as mean  $\pm$  SEM. Analysis was conducted via a one-way ANOVA, accounting for unequal variance and non-normal distributions when needed. 3 biological replicates,  $n \geq 12$ . . \* =  $p < 0.05$ , \*\* =  $p < 0.01$ , \*\*\* =  $p < 0.001$ , \*\*\*\* =  $p < 0.0001$



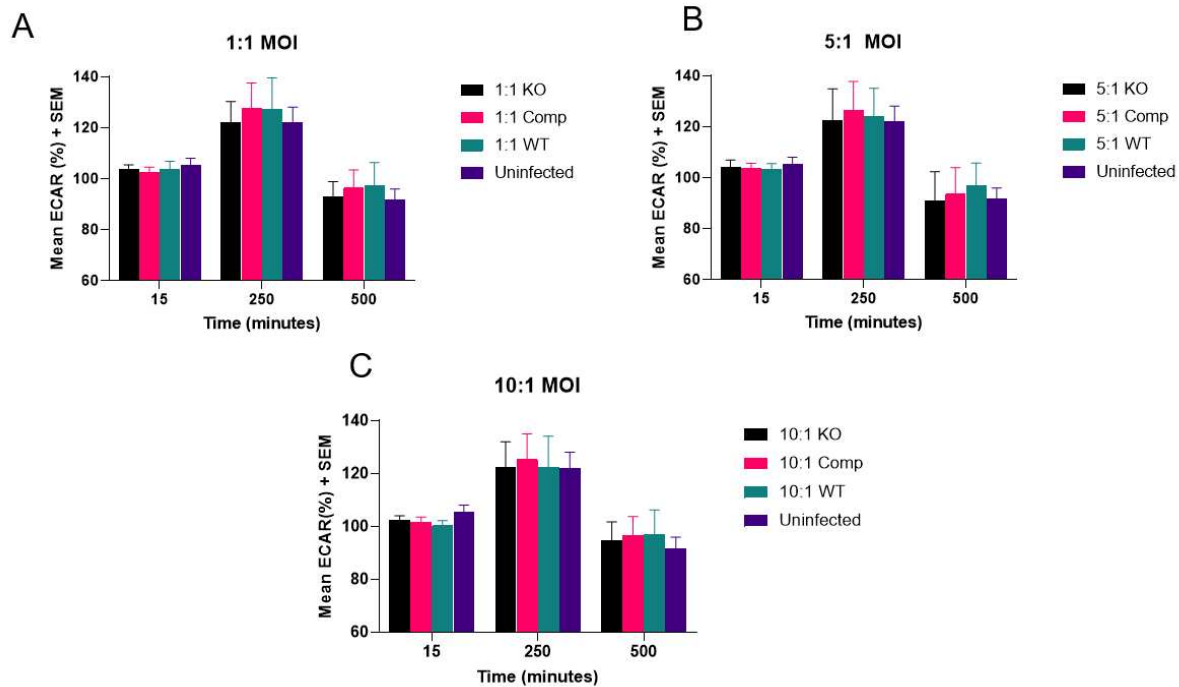


**Figure 2.8: CD1 mouse BMDMs infected with mycobactin knock-out Mtb exhibit a minimal reduction in glycolytic metabolism when compared to WT Mtb infected cells.** CD1 mouse BMDMs infected with either wild-type Mtb H37Rv (WT), mycobactin K knock-out (KO), or complemented (Comp) were assayed on a Seahorse Extracellular Flux Analyzer for eight consecutive hours after a one-hour infection incubation. Measurements were baselined to the first reading and represented as a percent. Time points of 15, 250, and 500 minutes post-assay start are represented for an MOI of 1:1 (A), 5:1 (B), and 10:1 (C). WT Mtb infected cells exhibit minimally increased levels of glycolytic metabolism, as represented by percent extracellular acidification rate (ECAR) over time. Mycobactin KO Mtb infected BMDMs have a minimal reduction in glycolytic metabolism compared to other groups. No statistical differences between groups are observed in any MOI. Data is presented as mean  $\pm$  SEM. Analysis was conducted via a one-way ANOVA, accounting for unequal variance and non-normal distributions when needed. 3 biological replicates,  $n \geq 12$ .

To further capture the metabolic phenotype of BMDMs infected with these varied strains of Mtb, we calculated the OCR/ECAR ratio of cells throughout the experimental time course (Figure 2.9). Uninfected cells had the highest OCR/ECAR ratio at the start of the extracellular flux assay, indicating that the hour exposure to Mtb prior to the assay start significantly increased glycolytic metabolism in these cells. The stratification of metabolic phenotype of CD1 mouse BMDMs infected with either mbtK KO, complement, or WT strains of Mtb was most pronounced at late time points of the assay, and became more pronounced with increasing MOI (Figure 2.9). We

demonstrated that the mean OCR/ECAR ratio is highest in CD1 mouse BMDMs infected with mbtK KO Mtb, lowest with WT Mtb, and an intermediate level with complemented Mtb, which was statistically significant at an MOI of 5:1 (Figure 2.9B). A lower OCR/ECAR ratio is indicative of a more glycolytic metabolic phenotype. Therefore, intact mycobactin is critical for regulating a glycolytic metabolic phenotype in CD1 mouse BMDMs, and without this iron chelating siderophore, infected BMDMs have a more oxidative phenotype. These data, in summary, further support the hypothesis that mycobactin drives metabolic changes in infected macrophages through its iron chelating ability.

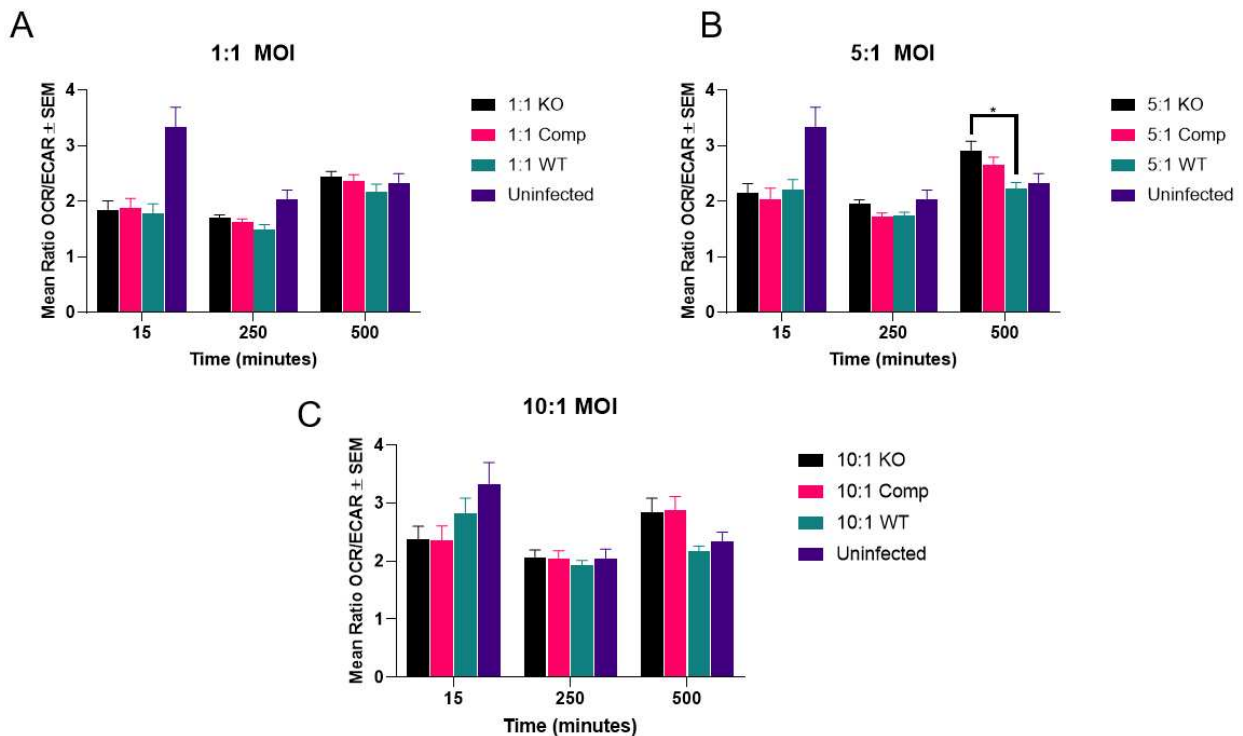


**Figure 2.9: Impact of mycobactin knock-out Mtb on CD1 mouse BMDM metabolic phenotype occurs at late time points post-infection.** CD1 mouse BMDMs infected with either wild-type Mtb H37Rv (WT), mycobactin K knock-out (KO), or complemented (Comp) were assayed on a Seahorse Extracellular Flux Analyzer for eight consecutive hours after a one-hour infection incubation. Mean ratio of OCR/ECAR was plotted for time points of 15, 250, and 500 minutes post-assay, for an MOI of 1:1 (A), 5:1 (B), and 10:1 (C). Uninfected cells have a much higher OCR/ECAR ratio at 15 minutes. Additionally, at late time point of 500 minutes, stratification of metabolic phenotype becomes more pronounced between the different infection conditions,

with WT and Comp Mtb infected cells having a lower OCR/ECAR ratio than the KO infected cells. This further supports the hypothesis that mycobactin is necessary for Mtb to mount a glycolytic shift in macrophage metabolism. Data is presented as mean  $\pm$  SEM. Analysis was conducted via a one-way ANOVA, accounting for unequal variance and non-normal distributions when needed. 3 biological replicates,  $n \geq 12$ . \* =  $p < 0.05$

## 5. Discussion

The research presented herein demonstrates that the Mtb siderophore mycobactin plays a clear role in augmenting macrophage metabolism during early infection, via increased HIF-1 $\alpha$  expression and increased glycolytic metabolism (Figure 2.10). We provide the first line of evidence that a pathogen-driven, hypoxia-independent mechanism of HIF-1 $\alpha$  activation is responsible for early observed metabolic shifts during *in vitro* Mtb infection.

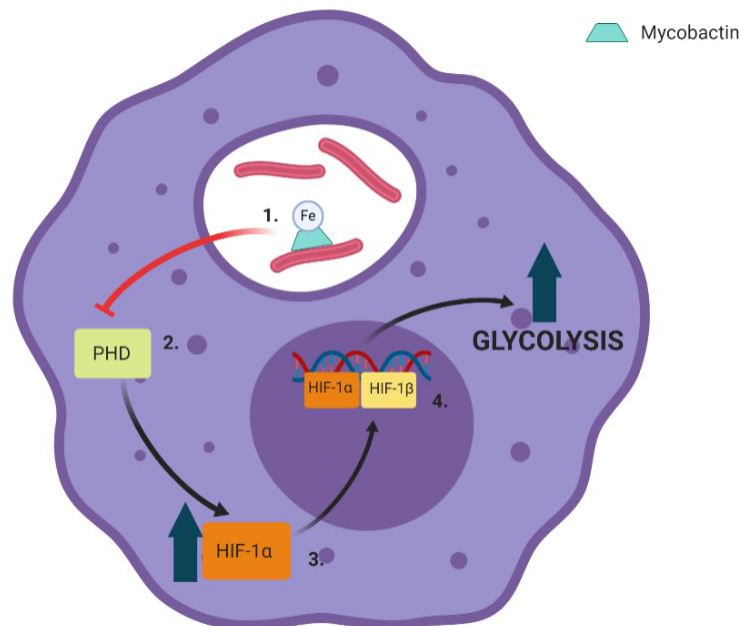


**Figure 2.10: Hypoxia-independent activation of HIF-1 $\alpha$  by mycobactin drives glycolysis during early Mtb infection.** Mycobactin produced by Mtb potently chelates iron (1). Lack of available iron cofactors leads to the inhibition of PHD enzymes (2) and subsequent accumulation of HIF-1 $\alpha$  within the macrophage (3). Accumulated HIF-1 $\alpha$  can translocate to the cell nucleus, where it dimerizes with the HIF-1 $\beta$  subunit, driving the transcription of genes involved in glycolytic metabolism, increasing glycolysis (4).

We demonstrated that MbtJ increased HIF-1 $\alpha$  protein levels via Western Blot in a concentration dependent manner and incited a stronger increase than the control DFO (Figure 2.1). However, some HIF-1 $\alpha$  expression was observed in uninfected macrophages without iron chelation treatment (Figure 2.1). It is possible that cell culture conditions, such as those for the CD1 macrophages which included conditioned media, have pre-existing factors which stabilize HIF-1 $\alpha$ , such as protein kinase A activity,<sup>78,79</sup> specific cytokines such as IL-1<sup>38,39</sup> and metabolites such as lactate and succinate<sup>43-45</sup>. Iron chelation is just one mechanism by which HIF-1 $\alpha$  is activated in a hypoxia-independent manner. While these were not the focus of the project described herein, complex pathogenesis and cell-cell interactions during Mtb infection do not rule out these pathways in the activation and stabilization of HIF-1 $\alpha$  early and throughout the chronic infectious disease process.

Additionally, although unstable HIF-1 $\alpha$  is rapidly degraded within the cytoplasm, active HIF-1 $\alpha$  is localized within nuclear fractions. Due to difficulties in obtaining significant protein yield with nuclear fractionation protocols, whole cell lysates were analyzed instead. Inactive HIF-1 $\alpha$  fragments may have been captured via Western Blot from cytosolic compartments included when cells were lysed. Exploring more fractionation techniques and improving yield would help to reduce this background result. An additional, critical future step includes infecting macrophages with the mbtK knock-out, complement, and parent H37Rv Mtb strains and probing cell lysates for HIF-1 $\alpha$  post-infection. We predict that the macrophages infected with the mycobactin knock-out strain of Mtb would exhibit little to no HIF-1 $\alpha$ , based on results obtained in similar studies.<sup>60</sup> Additionally, mechanism of action could be further elucidated via the use of commercially available antibodies against prolyl-hydroxylated HIF-1 $\alpha$ , as PHD enzymes are inhibited via iron chelation, and as a result there would be a reduction in prolyl-hydroxylated HIF-1 $\alpha$  with iron chelation treatment.

MbtJ was 100 times more potent than DFO with respect to increases in glycolytic metabolism, as a similar magnitude increase in basal ECAR was observed for 1000  $\mu\text{M}$  DFO as it was for 10  $\mu\text{M}$  MbtJ (Figure 2.3A, Figure 2.5A). DFO is derived from the soil bacterium *Streptomyces pilosus*.<sup>61–63</sup> It would follow that a chelator produced by an intracellular bacterial species, like Mtb, which must compete with already limited iron in the host environment, would produce siderophores with much greater iron binding capacity.<sup>64–69</sup> The relative iron binding capability of a ligand is compared via the pM scale, which is defined as  $-\log[\text{Fe}^{3+}]$  at fixed concentrations of metal and ligand and pH 7.4.<sup>72,73</sup> Recent estimates indicate that the pM value of MbtJ is 39.7, compared to a pM of 26.6 for DFO.<sup>72</sup> Although MbtJ is produced by *Mycobacterium avium subspecies paratuberculosis*, it shares structural similarity to mycobactin T produced by Mtb and is commercially available in larger quantities.<sup>80</sup> Further experiments with mycobactin T would be important for validating the hypotheses proposed.

Although both iron chelators, the metabolic response of macrophages exposed to DFO versus MbtJ exhibited some notable differences. MbtJ caused significant increases in mitochondrial spare capacity, proton leak, and maximum respiration at a concentration of 0.1  $\mu\text{M}$ , with these effects plateauing at higher concentrations (Figure 2.6), while these parameters were not modulated with DFO treatment (Figure 2.4). This may be due to the fact that DFO is poorly cell permeable, and must be conjugated to other peptide sequences in order to penetrate the mitochondria and chelate mitochondrial iron stores.<sup>81</sup> MbtJ, in contrast, is lipid soluble and interacts with membranes.<sup>72</sup> Additionally, differences in function may be due to structural differences between DFO and MbtJ. DFO is a hydroxamate-type siderophore, forming five-membered chelate rings, while MbtJ is a mixed-type siderophore containing multiple moiety types, including oxazoline rings.<sup>73</sup> These structural differences may result in functional differences.

It is important to note that basal OCR and ATP production were not impacted for either DFO or MbtJ treatments (Figure 2.4, Figure 2.6). Calculations of ATP production were made using Seahorse instrument data and were not a direct ATP measurement. Additional assays which provide a quantification of ATP would help determine the impact of increasing glycolysis by iron chelation on total cellular ATP production. Further, iron chelation has been demonstrated to impact mitochondrial electron transport chain activity directly, mitochondrial membrane activity, and impact SDH activity.<sup>74-77</sup> Iron is also a key component of mitochondrial health, contributing to structures such as iron-sulfur clusters.<sup>82,83</sup> Therefore, a chelator like MbtJ with very high iron binding capability may have direct mitochondrial metabolic impacts independent of HIF-1 $\alpha$  and glycolytic changes. Additionally, HIF-1 $\alpha$  also plays a role in decreasing mitochondrial metabolism through its upregulation of PDK, which prevents the formation of acetyl-CoA from pyruvate by inhibiting pyruvate dehydrogenase.<sup>84</sup> PDK expression could be analyzed to provide additional mechanistic insight.

Interestingly, while DFO increases the glycolytic reserve of cells exposed, MbtJ decreases this parameter in a concentration dependent manner (Figure 2.3E, Figure 2.5E). Glycolytic reserve is a measure of the capacity of a cell to respond to glycolytic stress, and the ability of the cell to tap into reserve energy stores. It is possible that the higher iron binding capability of MbtJ causes cells to reach their maximum glycolytic capability earlier and thus depletes the reserve and makes it more difficult for cells to respond to stress. Previously mentioned structural differences between DFO and MbtJ may also have contributed to this observed phenomenon. Although no toxic effects were observed microscopically, additional evaluation of the impact of MbtJ on cell survival, glycolytic function, and mitochondrial health are warranted to further investigate this parameter, including cytochrome C and SDH activity.

Mbt K knock-out infected CD1 mouse BMDMs demonstrated minimally reduced glycolysis and increased oxidative metabolism within our *in vitro* experimental study (Figure 2.7, Figure 2.8). While impacts on oxidative metabolism of the knock-out versus wild-type Mtb strains become increasingly severe with increased MOI, the impacts on glycolytic metabolism were less pronounced overall (Figure 2.7, Figure 2.8). The complemented strain was more similar to the KO than the WT with respect to metabolic changes. This could be due to poor complementation, or poor uptake of the complement strain by macrophages. Validation of equivalent bacterial uptake would be warranted in future experiments. It is also possible that the high MOIs of 5:1 and 10:1 cause the cells to reach a maximum level of glycolytic function and there is no room for the cells to become more glycolytically active and glycolytic reserves are depleted. Additionally, this assay did not investigate the potential adverse impacts on mitochondrial metabolism of high MOI. Mtb infection had a much greater impact on oxidative metabolic function than that of purified iron chelators, indicating the important impact of bacterial infection in and of itself on mitochondrial function. Due to the nature of the BSL3 environment in which these experiments were conducted, the ability to observe cell viability post eight-hour time course, such as by Calcein AM, was not possible. Experimental approaches which incorporate cell viability and mitochondrial health parameters post-assay would be ideal in the future to ensure the significant drop in mitochondrial metabolism is not a result of poor cell health at high MOI.

Additionally, limitations of the Seahorse instrument made it risky to conduct measurements past a 500-minute time point, despite that being the time when metabolic phenotype stratifications became most pronounced (Figure 2.9). Pre-incubating with bacteria for longer periods prior to extracellular flux analysis could mitigate this hurdle in future studies. Uninfected CD1 macrophages appear to follow a similar metabolic trajectory to some of the infected cell groups for glycolytic parameters over the course of the eight-hour Seahorse experimental assay (Figure 2.7). It is possible that these macrophages are already primed into an M1-type phenotype due

the use of L929 conditioned media to maintain culture viability and health throughout the assay. Validation of these experiments with another cell type that does not have these culture requirements, such as guinea pig BMDMs, would be an ideal way to increase confidence in these results.

Lastly, our choice to use the CD1 mouse model instead of other commonly used mouse models came from the fact that CD1 mice are outbred, and therefore would more closely represent a heterogeneous population of individuals and be more translatable to human disease. This comes in addition to the ease of obtaining reagents compatible with mouse models. However, it is important to note that many mouse models do not develop hypoxic granuloma lesions.<sup>85</sup> We argue that despite this, early infection models such as ours are prior to the formation of lesion hypoxia in the first place, and thus HIF-1 $\alpha$  would be active via hypoxia-independent mechanisms. Future, important work would take experiments *in vivo* within the CD1 mouse to explore the impact of mycobactin on HIF-1 $\alpha$  expression via IHC as well as the impact on lung macrophage metabolism, via extracellular flux analysis on isolated macrophages. Investigating these parameters at early time points, prior to normal 30-day post infection necropsy time points, would provide novel insight into the early stages of granuloma formation and TB pathogenesis that have not yet been explored. Investigating the role of mycobactin *in vivo* during early Mtb infection will be critical to the translatability of our *in vitro* findings. Additionally, mycobactin K is an acyl transferase, but other mycobactin synthesis gene loci exist.<sup>67-69</sup> Analysis of mutant Mtb strains which knock out multiple steps of the mycobactin biosynthetic pathway would further support our hypotheses and would complement the results presented. In a similar vein, Mtb has a very complex iron acquisition machinery, and it would be interesting to note if other aspects of this pathway including, carboxymycobactin, Mmps, HupB, IrtAB, BrfA, and BrfB play a role in augmenting macrophage metabolism in the same manner.<sup>64</sup>



Ultimately, Mtb has developed complex ways in which it drives changes in the developing granuloma microenvironment, priming host cells to respond to and sustain an infection and preparing cells to be able to survive in environments of hypoxia that will develop during chronic TB. In this way, Mtb promotes its own survival and drives modulations in host immune cell metabolism. A better understanding of the interactions which occur at the host-pathogen interface during Mtb infection will assist in the development of novel therapeutic strategies.

## REFERENCES

1. WHO | Global tuberculosis report 2019. *WHO*  
[http://www.who.int/tb/publications/global\\_report/en/](http://www.who.int/tb/publications/global_report/en/).
2. Tornheim, J. A. & Dooley, K. E. The Global Landscape of Tuberculosis Therapeutics. *Annual Review of Medicine* **70**, 105–120 (2019).
3. Singh, P. *et al.* Breaking the Transmission of TB: A Roadmap to Bridge the Gaps in Controlling TB in Endemic Settings. in *Mycobacterium Tuberculosis: Molecular Infection Biology, Pathogenesis, Diagnostics and New Interventions* (eds. Hasnain, S. E., Ehtesham, N. Z. & Grover, S.) 451–461 (Springer, 2019). doi:10.1007/978-981-32-9413-4\_24.
4. Dooley, K. E., Hanna, D., Mave, V., Eisenach, K. & Savic, R. M. Advancing the development of new tuberculosis treatment regimens: The essential role of translational and clinical pharmacology and microbiology. *PLoS Med* **16**, (2019).
5. Bates, M., Marais, B. J. & Zumla, A. Tuberculosis Comorbidity with Communicable and Noncommunicable Diseases. *Cold Spring Harb Perspect Med* **5**, a017889 (2015).
6. Marais, B. J. *et al.* Tuberculosis comorbidity with communicable and non-communicable diseases: integrating health services and control efforts. *The Lancet Infectious Diseases* **13**, 436–448 (2013).
7. Wallis, R. S. & Hafner, R. Advancing host-directed therapy for tuberculosis. *Nat Rev Immunol* **15**, 255–263 (2015).
8. Kiran, D., Podell, B. K., Chambers, M. & Basaraba, R. J. Host-directed therapy targeting the *Mycobacterium tuberculosis* granuloma: a review. *Semin Immunopathol* **38**, 167–183 (2015).
9. Zumla, A. *et al.* Host-Directed Therapies for Tackling Multi-Drug Resistant Tuberculosis: Learning From the Pasteur-Bechamp Debates. *Clin Infect Dis.* **61**, 1432–1438 (2015).

10. Zumla, A., Rao, M., Dodoo, E. & Maeurer, M. Potential of immunomodulatory agents as adjunct host-directed therapies for multidrug-resistant tuberculosis. *BMC Med* **14**, (2016).
11. Hawn, T. R., Shah, J. A. & Kalman, D. New tricks for old dogs: countering antibiotic resistance in tuberculosis with host-directed therapeutics. *Immunol Rev* **264**, 344–362 (2015).
12. Matty, M. A., Roca, F. J., Cronan, M. R. & Tobin, D. M. Adventures within the speckled band: heterogeneity, angiogenesis, and balanced inflammation in the tuberculous granuloma. *Immunol Rev* **264**, 276–287 (2015).
13. Lenaerts, A., Barry, C. E. & Dartois, V. Heterogeneity in tuberculosis pathology, microenvironments and therapeutic responses. *Immunol Rev* **264**, 288–307 (2015).
14. Orme, I. M. & Basaraba, R. J. The formation of the granuloma in tuberculosis infection. *Seminars in Immunology* **26**, 601–609 (2014).
15. Orme, I. M. A new unifying theory of the pathogenesis of tuberculosis. *Tuberculosis* **94**, 8–14 (2014).
16. Wang, G. L. & Semenza, G. L. Purification and Characterization of Hypoxia-inducible Factor 1. *J. Biol. Chem.* **270**, 1230–1237 (1995).
17. Wang, G. L., Jiang, B. H., Rue, E. A. & Semenza, G. L. Hypoxia-inducible factor 1 is a basic-helix-loop-helix-PAS heterodimer regulated by cellular O<sub>2</sub> tension. *PNAS* **92**, 5510–5514 (1995).
18. Greijer, A. E. *et al.* Up-regulation of gene expression by hypoxia is mediated predominantly by hypoxia-inducible factor 1 (HIF-1). *The Journal of Pathology* **206**, 291–304 (2005).
19. Balamurugan, K. HIF-1 at the crossroads of hypoxia, inflammation, and cancer. *Int. J. Cancer* **138**, 1058–1066 (2016).
20. Jaakkola, P. *et al.* Targeting of HIF- $\alpha$  to the von Hippel-Lindau Ubiquitylation Complex by O<sub>2</sub>-Regulated Prolyl Hydroxylation. *Science* **292**, 468–472 (2001).

21. Kaluz, S., Kaluzová, M. & Stanbridge, E. J. Proteasomal Inhibition Attenuates Transcriptional Activity of Hypoxia-Inducible Factor 1 (HIF-1) via Specific Effect on the HIF-1 $\alpha$  C-Terminal Activation Domain. *Mol. Cell. Biol.* **26**, 5895–5907 (2006).
22. Ivan, M. *et al.* HIF $\alpha$  Targeted for VHL-Mediated Destruction by Proline Hydroxylation: Implications for O<sub>2</sub> Sensing. *Science* **292**, 464–468 (2001).
23. Ullah, M. S., Davies, A. J. & Halestrap, A. P. The Plasma Membrane Lactate Transporter MCT4, but Not MCT1, Is Up-regulated by Hypoxia through a HIF-1 $\alpha$ -dependent Mechanism. *J. Biol. Chem.* **281**, 9030–9037 (2006).
24. Rademakers, S. E., Lok, J., van der Kogel, A. J., Bussink, J. & Kaanders, J. H. Metabolic markers in relation to hypoxia; staining patterns and colocalization of pimonidazole, HIF-1 $\alpha$ , CAIX, LDH-5, GLUT-1, MCT1 and MCT4. *BMC Cancer* **11**, 167 (2011).
25. Firth, J. D., Ebert, B. L. & Ratcliffe, P. J. Hypoxic Regulation of Lactate Dehydrogenase A INTERACTION BETWEEN HYPOXIA-INDUCIBLE FACTOR 1 AND cAMP RESPONSE ELEMENTS. *J. Biol. Chem.* **270**, 21021–21027 (1995).
26. Semenza, G. L. *et al.* Hypoxia Response Elements in the Aldolase A, Enolase 1, and Lactate Dehydrogenase A Gene Promoters Contain Essential Binding Sites for Hypoxia-inducible Factor 1. *J. Biol. Chem.* **271**, 32529–32537 (1996).
27. Semenza, G. L., Roth, P. H., Fang, H. M. & Wang, G. L. Transcriptional regulation of genes encoding glycolytic enzymes by hypoxia-inducible factor 1. *J. Biol. Chem.* **269**, 23757–23763 (1994).
28. Shi, L. *et al.* Infection with *Mycobacterium tuberculosis* induces the Warburg effect in mouse lungs. *Scientific Reports* **5**, 18176 (2015).
29. Shi, L., Jiang, Q., Bushkin, Y., Subbian, S. & Tyagi, S. Biphasic Dynamics of Macrophage Immunometabolism during *Mycobacterium tuberculosis* Infection. *mBio* **10**, e02550-18 (2019).

30. Gleeson, L. E. *et al.* Cutting Edge: Mycobacterium tuberculosis Induces Aerobic Glycolysis in Human Alveolar Macrophages That Is Required for Control of Intracellular Bacillary Replication. *J Immunol* **196**, 2444–2449 (2016).
31. Qualls, J. E. & Murray, P. J. Immunometabolism within the tuberculosis granuloma: amino acids, hypoxia, and cellular respiration. *Semin Immunopathol* **38**, 139–152 (2015).
32. Prosser, G. *et al.* The bacillary and macrophage response to hypoxia in tuberculosis and the consequences for T cell antigen recognition. *Microbes and Infection* **19**, 177–192 (2017).
33. Braverman, J., Sogi, K. M., Benjamin, D., Nomura, D. K. & Stanley, S. A. HIF-1 $\alpha$  Is an Essential Mediator of IFN- $\gamma$ -Dependent Immunity to Mycobacterium tuberculosis. *J Immunol* 1600266 (2016) doi:10.4049/jimmunol.1600266.
34. Werth, N. *et al.* Activation of Hypoxia Inducible Factor 1 Is a General Phenomenon in Infections with Human Pathogens. *PLoS One* **5**, (2010).
35. Baay-Guzman, G. J. *et al.* Dual role of hypoxia-inducible factor 1  $\alpha$  in experimental pulmonary tuberculosis: its implication as a new therapeutic target. *Future Microbiology* (2018) doi:10.2217/fmb-2017-0168.
36. Resende, M. *et al.* Myeloid HIF-1 $\alpha$  regulates pulmonary inflammation during experimental Mycobacterium tuberculosis infection. *Immunology* **159**, 121–129 (2020).
37. Knight, M. & Stanley, S. HIF-1 $\alpha$  as a central mediator of cellular resistance to intracellular pathogens. *Current Opinion in Immunology* **60**, 111–116 (2019).
38. Jung, Y.-J., Isaacs, J. S., Lee, S., Trepel, J. & Neckers, L. IL-1 $\beta$  mediated up-regulation of HIF-1 $\alpha$  via an NF $\kappa$ B/COX-2 pathway identifies HIF-1 as a critical link between inflammation and oncogenesis. *FASEB J* (2003) doi:10.1096/fj.03-0329fje.
39. Feldhoff, L. M. *et al.* IL-1 $\beta$  induced HIF-1 $\alpha$  inhibits the differentiation of human FOXP3 + T cells. *Scientific Reports* **7**, 465 (2017).
40. Al Okail, M. S. Cobalt chloride, a chemical inducer of hypoxia-inducible factor-1 $\alpha$  in U251 human glioblastoma cell line. *Journal of Saudi Chemical Society* **14**, 197–201 (2010).

41. Muñoz-Sánchez, J. & Cháñez-Cárdenas, M. E. The use of cobalt chloride as a chemical hypoxia model. *Journal of Applied Toxicology* **39**, 556–570 (2019).
42. Xia, M. *et al.* Identification of Chemical Compounds that Induce HIF-1 $\alpha$  Activity. *Toxicol Sci* **112**, 153–163 (2009).
43. Tannahill, G. M. *et al.* Succinate is an inflammatory signal that induces IL-1 $\beta$  through HIF-1 $\alpha$ . *Nature* **496**, 238–242 (2013).
44. Lukyanova, L. D., Kirova, Y. I. & Germanova, E. L. The Role of Succinate in Regulation of Immediate HIF-1 $\alpha$  Expression in Hypoxia. *Bull Exp Biol Med* **164**, 298–303 (2018).
45. Bailey, P. S. J. & Nathan, J. A. Metabolic Regulation of Hypoxia-Inducible Transcription Factors: The Role of Small Molecule Metabolites and Iron. *Biomedicines* **6**, (2018).
46. Hirota, K. An intimate crosstalk between iron homeostasis and oxygen metabolism regulated by the hypoxia-inducible factors (HIFs). *Free Radical Biology and Medicine* (2018) doi:10.1016/j.freeradbiomed.2018.07.018.
47. Woo, K. J., Lee, T.-J., Park, J.-W. & Kwon, T. K. Desferrioxamine, an iron chelator, enhances HIF-1 $\alpha$  accumulation via cyclooxygenase-2 signaling pathway. *Biochemical and Biophysical Research Communications* **343**, 8–14 (2006).
48. Nandal, A. *et al.* Activation of the HIF Prolyl Hydroxylase by the Iron Chaperones PCBP1 and PCBP2. *Cell Metabolism* **14**, 647–657 (2011).
49. Cho, E. A. *et al.* Differential in vitro and cellular effects of iron chelators for hypoxia inducible factor hydroxylases. *J. Cell. Biochem.* **114**, 864–873 (2013).
50. Fong, G.-H. & Takeda, K. Role and regulation of prolyl hydroxylase domain proteins. *Cell Death & Differentiation* **15**, 635–641 (2008).
51. Cassat, J. E. & Skaar, E. P. Iron in Infection and Immunity. *Cell Host & Microbe* **13**, 509–519 (2013).

52. Nairz, M., Theurl, I., Swirski, F. K. & Weiss, G. “Pumping iron”—how macrophages handle iron at the systemic, microenvironmental, and cellular levels. *Pflugers Arch - Eur J Physiol* **469**, 397–418 (2017).
53. Ali, M. K. *et al.* Role of iron in the pathogenesis of respiratory disease. *The International Journal of Biochemistry & Cell Biology* **88**, 181–195 (2017).
54. P. Skaar, E. & Raffatellu, M. Metals in infectious diseases and nutritional immunity. *Metallomics* **7**, 926–928 (2015).
55. Marchetti, M. *et al.* Iron Metabolism at the Interface between Host and Pathogen: From Nutritional Immunity to Antibacterial Development. *International Journal of Molecular Sciences* **21**, 2145 (2020).
56. Ellermann, M. & Arthur, J. C. Siderophore-mediated iron acquisition and modulation of host-bacterial interactions. *Free Radical Biology and Medicine* **105**, 68–78 (2017).
57. Saha, M. *et al.* Microbial siderophores and their potential applications: a review. *Environ Sci Pollut Res* **23**, 3984–3999 (2015).
58. Li, K., Chen, W.-H. & Bruner, S. D. Microbial siderophore-based iron assimilation and therapeutic applications. *Biometals* **29**, 377–388 (2016).
59. Golonka, R., Yeoh, B. S. & Vijay-Kumar, M. The Iron Tug-of-War between Bacterial Siderophores and Innate Immunity. *JIN* **11**, 249–262 (2019).
60. Hartmann, H. *et al.* Hypoxia-Independent Activation of HIF-1 by Enterobacteriaceae and Their Siderophores. *Gastroenterology* **134**, 756-767.e6 (2008).
61. Holden, P. & Nair, L. S. Deferoxamine: An Angiogenic and Antioxidant Molecule for Tissue Regeneration. *Tissue Engineering Part B: Reviews* **25**, 461–470 (2019).
62. Mobarra, N. *et al.* A Review on Iron Chelators in Treatment of Iron Overload Syndromes. *Int J Hematol Oncol Stem Cell Res* **10**, 239–247 (2016).

63. Wilson, B. R., Bogdan, A. R., Miyazawa, M., Hashimoto, K. & Tsuji, Y. Siderophores in Iron Metabolism: From Mechanism to Therapy Potential. *Trends in Molecular Medicine* **22**, 1077–1090 (2016).
64. Sritharan, M. Iron Homeostasis in Mycobacterium tuberculosis: Mechanistic Insights into Siderophore-Mediated Iron Uptake. *J. Bacteriol.* **198**, 2399–2409 (2016).
65. Snow, G. A. Isolation and structure of mycobactin T, a growth factor from Mycobacterium tuberculosis. *Biochemical Journal* **97**, 166–175 (1965).
66. Madigan, C. A. *et al.* Lipidomic Analysis Links Mycobactin Synthase K to Iron Uptake and Virulence in M. tuberculosis. *PLoS Pathog* **11**, e1004792 (2015).
67. McMahon, M. D., Rush, J. S. & Thomas, M. G. Analyses of MbtB, MbtE, and MbtF Suggest Revisions to the Mycobactin Biosynthesis Pathway in Mycobacterium tuberculosis. *J Bacteriol* **194**, 2809–2818 (2012).
68. Krithika, R. *et al.* A genetic locus required for iron acquisition in Mycobacterium tuberculosis. *Proc Natl Acad Sci U S A* **103**, 2069–2074 (2006).
69. Quadri, L. E. N., Sello, J., Keating, T. A., Weinreb, P. H. & Walsh, C. T. Identification of a Mycobacterium tuberculosis gene cluster encoding the biosynthetic enzymes for assembly of the virulence-conferring siderophore mycobactin. *Chemistry & Biology* **5**, 631–645 (1998).
70. Phelan, J. J. *et al.* Desferrioxamine Supports Metabolic Function in Primary Human Macrophages Infected With Mycobacterium tuberculosis. *Front. Immunol.* **11**, (2020).
71. Basaraba, R. J. & Bielefeldt-Ohmann, H. Hypoxia inducible factor inducer and methods for using the same. (2012).
72. McQueen, C. F. & Groves, J. T. A reevaluation of iron binding by Mycobactin J. *J Biol Inorg Chem* 1–13 (2018) doi:10.1007/s00775-018-1592-2.
73. Albelda-Berenguer, M., Monachon, M. & Joseph, E. Chapter Five - Siderophores: From natural roles to potential applications. in *Advances in Applied Microbiology* (eds. Gadd, G. M. & Sariaslani, S.) vol. 106 193–225 (Academic Press, 2019).



74. Oexle, H., Gnaiger, E. & Weiss, G. Iron-dependent changes in cellular energy metabolism: influence on citric acid cycle and oxidative phosphorylation. *Biochimica et Biophysica Acta (BBA) - Bioenergetics* **1413**, 99–107 (1999).
75. Yoon, Y.-S., Byun, H.-O., Cho, H., Kim, B.-K. & Yoon, G. Complex II Defect via Down-regulation of Iron-Sulfur Subunit Induces Mitochondrial Dysfunction and Cell Cycle Delay in Iron Chelation-induced Senescence-associated Growth Arrest. *J. Biol. Chem.* **278**, 51577–51586 (2003).
76. Yoon, G. *et al.* Iron chelation-induced senescence-like growth arrest in hepatocyte cell lines: association of transforming growth factor beta1 (TGF-beta1)-mediated p27Kip1 expression. *Biochem J* **366**, 613–621 (2002).
77. Yoon, Y.-S., Cho, H., Lee, J.-H. & Yoon, G. Mitochondrial Dysfunction via Disruption of Complex II Activity during Iron Chelation—Induced Senescence-like Growth Arrest of Chang Cells. *Annals of the New York Academy of Sciences* **1011**, 123–132 (2004).
78. McNamee, E. N., Vohwinkel, C. & Eltzschig, H. K. Hydroxylation-independent HIF-1 $\alpha$  stabilization through PKA: A new paradigm for hypoxia signaling. *Sci. Signal.* **9**, fs11–fs11 (2016).
79. Bullen, J. W. *et al.* Protein kinase A–dependent phosphorylation stimulates the transcriptional activity of hypoxia-inducible factor 1. *Sci. Signal.* **9**, ra56–ra56 (2016).
80. Byers, B. R. *Iron Acquisition by the Genus Mycobacterium: History, Mechanisms, Role of Siderocalin, Anti-Tuberculosis Drug Development.* (Springer Science & Business Media, 2013).
81. Alta, R. Y. P. *et al.* Mitochondria-penetrating peptides conjugated to desferrioxamine as chelators for mitochondrial labile iron. *PLoS One* **12**, (2017).
82. Braymer, J. J. & Lill, R. Iron–sulfur cluster biogenesis and trafficking in mitochondria. *J. Biol. Chem.* **292**, 12754–12763 (2017).

83. Cardenas-Rodriguez, M., Chatzi, A. & Tokatlidis, K. Iron–sulfur clusters: from metals through mitochondria biogenesis to disease. *J Biol Inorg Chem* **23**, 509–520 (2018).
84. Zhao, L., Mao, Y., Zhao, Y., Cao, Y. & Chen, X. Role of multifaceted regulators in cancer glucose metabolism and their clinical significance. *Oncotarget* **7**, 31572–31585 (2016).
85. Via, L. E. *et al.* Tuberculous Granulomas Are Hypoxic in Guinea Pigs, Rabbits, and Nonhuman Primates. *Infect Immun* **76**, 2333–2340 (2008).

## CHAPTER 3: INVESTIGATING THE ROLE OF A LACTATE SHUTTLE WITHIN THE TUBERCULOSIS GRANULOMA MICROENVIRONMENT

### 1. Summary

Lactate, while long considered an inert byproduct of glycolysis, plays a diverse role as a metabolite and as a signaling molecule in many disease processes. Within the tumor microenvironment, a metabolic symbiosis exists between highly glycolytic, hypoxic cells and more oxidative, normoxic cells. Glycolytic cells in this environment uptake glucose, convert it to lactate via lactate dehydrogenase A (LDHA) and export it in large quantities via monocarboxylate transporter 4 (MCT4). Normoxic cells, to preserve glucose for cells which depend on glucose as an energy source, import lactate via monocarboxylate transporter 1 (MCT1) and convert it back to pyruvate through lactate dehydrogenase B (LDHB) activity. These normoxic cells then preferentially use lactate-derived pyruvate to fuel mitochondrial respiration. This lactate shuttle has been demonstrated to be critical in regulating carcinogenesis. However, it has not been explored in the context of similar infectious disease microenvironments, such as those that develop within the tuberculosis (TB) granuloma. Based on this, we explored the role of a lactate shuttle in *Mycobacterium tuberculosis* (Mtb) infection, using both archived guinea pig plasma and granuloma samples and *in vitro* CD1 mouse bone marrow derived macrophage (BMDM) infection models using the LDHA inhibitor sodium oxamate and the MCT1 inhibitor  $\alpha$ -Cyano-4-hydroxycinnamic acid ( $\alpha$ -CHC). We demonstrated that lactate levels increase during Mtb infection both *in vivo* and *in vitro* and that lactate shuttle components are present within primary guinea pig lung lesions. Additionally, inhibition of the lactate shuttle with sodium oxamate significantly blocks glycolytic metabolism in uninfected macrophages and decreases mitochondrial spare capacity. Further, lactate shuttle inhibition reduced the amount of lactate accumulated during *in vitro* Mtb infection; however, inhibitor treatment had minimal impact on bacterial CFUs. Ultimately, the

research herein provides critical proof of concept pointing to a role of a lactate shuttle in modulating Mtb infection and metabolic dynamics within the granuloma microenvironment. A better understanding of the impacts of lactate production, utilization, and signaling within the TB granuloma could lead to novel pathway targets for host-directed therapeutic strategies.

## **2. Introduction**

The metabolic pathway of glycolysis is a complex sequence of reactions that has been well-characterized and studied for decades.<sup>1</sup> Glycolysis can end with the production of pyruvate, which is subsequently converted into intermediates to fuel the citric acid cycle (TCA cycle) and mitochondrial respiration. In addition, via fermentative or aerobic glycolysis, pyruvate can be converted into lactate, which assists the cell in maintaining energetics through regeneration of NAD<sup>+</sup>.<sup>2</sup> For a long time, lactate was considered to be an inert byproduct of anaerobic glycolytic metabolism. However, the field of cancer biology and immunometabolism has shifted this paradigm in recent years.<sup>3,4</sup> Lactate is recognized as a key metabolic intermediate involved in a multitude of processes including angiogenesis, tumor invasion, metastasis, pH homeostasis, immune evasion, maintenance of energetic self-sufficiency, and signaling through G-protein coupled receptor 81 present in diverse organs in the body.<sup>4-10</sup> Recent research aims to determine ways in which lactate signaling and metabolism contributes to disease pathogenesis and progression across different systems.

In the cancer field, lactate has been demonstrated to be directly metabolized and incorporated into the TCA cycle, at times preferred to glucose as a metabolic substrate.<sup>11,12</sup> Additionally, populations of cells within the tumor microenvironment have differential metabolic phenotypes, with varied propensity for glycolysis, lactate transport, or lactate production<sup>13,14</sup> Specifically, highly glycolytic, hypoxic cells in the center of the tumor microenvironment preferentially uptake glucose,

convert it into lactate via lactate dehydrogenase A (LDHA), and export large amounts of lactate via monocarboxylate transporter 4 (MCT4)<sup>13,14</sup> LDHA and MCT4 have been shown to be under transcriptional regulation by hypoxia inducible factor 1-  $\alpha$  (HIF-1 $\alpha$ ), an important transcription factor involved in the host adaptation to hypoxia.<sup>15-18</sup> Normoxic tumor cells closer to the lesion periphery and with access to blood supply preserve glucose for hypoxic cells and instead, import large amounts of lactate via monocarboxylate transporter 1 (MCT1) and convert the lactate back into pyruvate, via lactate dehydrogenase B (LDHB), to use as a metabolic fuel for the TCA cycle.<sup>13,14</sup> These hypoxic and normoxic cells thus work together to preserve energetics during tumor development, contributing to pathogenesis.

These so called lactate shuttles have been described in other tissue systems, such as between fast twitch and slow twitch muscle fibers and between astrocytes, oligodendrocytes, and neurons in the central nervous system.<sup>3,19-28</sup> The important role that lactate shuttles play in both health and disease has led researchers to explore the potential for inhibiting this lactate shuttle as a therapeutic strategy. In the context of cancer, multiple researchers have demonstrated significant tumor volume reduction with MCT1 inhibition using  $\alpha$ -Cyano-4-hydroxycinnamic acid ( $\alpha$ -CHC) and other targeted inhibitors, as well as with LDH inhibition using sodium oxamate and FX-11.<sup>29-37</sup> Use of these inhibitors can create a form of synthetic lethality in cancer cells, and has been demonstrated to selectively kill hypoxic tumor cells.<sup>13,35</sup>

Interestingly, the tuberculosis (TB) granuloma microenvironment and the tumor lesion microenvironment share many similarities. Both have oxygen tension gradients resulting in hypoxic central regions and more oxidative peripheral regions near blood vessels, which creates spatial gradients of cellular metabolism and inflammation.<sup>38-40</sup> Additionally, metabolic changes characteristic of a switch to glycolysis or the Warburg Effect are demonstrated within TB infected macrophages as well as within tumor cells.<sup>41-49</sup> Guinea pig granuloma lesions have also been

demonstrated to accumulate large quantities of lactate, to mM levels seen within tumors.<sup>50,51</sup> Further, *Mycobacterium tuberculosis* (Mtb), the causative agent of TB, has been shown to oxidize lactate as an energy source and requires the ability to metabolize lactate to survive intracellularly.<sup>52</sup> Most recently, inhibition of LDH via the inhibitor FX-11 was demonstrated to limit bacterial growth, decrease the number of necrotic lesions, and potentiate isoniazid treatment in mouse models of Mtb infection.<sup>53</sup>

Based on these similarities, we hypothesized that a lactate shuttle may occur between cells within the hypoxic core of the TB granuloma and normoxic cells present at the lesion periphery or in adjacent, uninvolved lung tissues (Figure 3.1). We investigated the lesion microenvironment by probing for LDHA, LDHB, MCT1, MCT4 and comparing protein localization with HIF-1 $\alpha$  expression to determine if enzymes and transporters involved in the lactate shuttle are present in TB granulomas. In addition, we utilized commercial inhibitors of LDHA and MCT1 to block shuttling of lactate through this pathway to determine the impact this shuttle has on TB disease outcome and bacterial viability. We successfully demonstrate proof of concept that a lactate shuttle is present within the context of the TB granuloma and that the use of lactate as a metabolic substrate is important for TB disease progression.

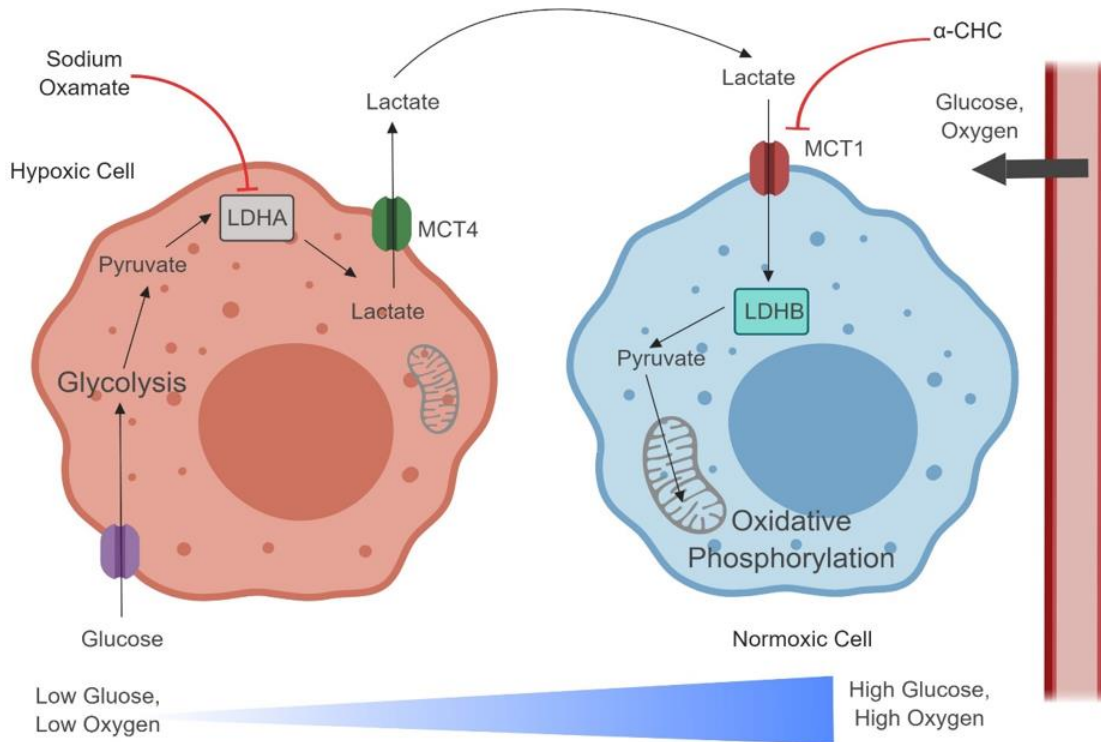


**Figure 3.1: Inhibiting the lactate shuttle within the TB granuloma microenvironment may be an alternative host-directed therapeutic strategy.** Within the context of the TB granuloma, a gradient of glucose and oxygen exists. Central regions of the granuloma, further away from blood vessel nutrient supplies, are hypoxic and have lower glucose. Hypoxic cells rely heavily on glucose uptake and processing through the glycolytic metabolic pathway, turning glucose into lactate via lactate dehydrogenase A (LDHA) enzyme activity. This lactate is exported through monocarboxylate transporter 4 (MCT4). To preserve glucose for hypoxic, highly glycolytic cells, the normoxic cells closer to the periphery of the granuloma import lactate via monocarboxylate transporter 1 (MCT) and enzymatically convert lactate back into pyruvate via lactate dehydrogenase B (LDHB). This lactate-derived pyruvate can then be shuttled into the mitochondria to fuel oxidative respiration. This creates a symbiotic metabolic relationship between hypoxic and normoxic cells within the granuloma microenvironment. Inhibition of this shuttle either through sodium oxamate or  $\alpha$ -Cyano-4-hydroxycinnamic acid ( $\alpha$ -CHC) are viable ways to disrupt the metabolic synergy that maintains cellular survival niches for Mtb. Targeting this shuttle is an unexplored host-directed therapeutic strategy for TB.

### 3. Materials & Methods

#### 3.1. *Bone Marrow Derived Macrophage (BMDM) Cell Culture*

Bone marrow was isolated from the femur of CD1 mice and stock vials were maintained in liquid nitrogen. To differentiate CD1 mouse BMDMs, cells were maintained in media containing 30% L929 cell conditioned media, 20% FBS (Atlas Biologicals), and 1% antibiotic/antimycotic (Thermo Fischer) for seven days, changing media at day four. Post differentiation into BMDMs, cells were maintained in 5% L929 conditioned media, 10% FBS, 1% antibiotic/antimycotic. CD1 mouse cells were confirmed to express macrophage specific markers CD11b and F4/80 by flow cytometry.

#### 3.2. *Extracellular Flux Analysis*

CD1 mouse BMDMs were harvested and plated at 100,000 cells per well in a plate compatible with the XFe24 Seahorse Extracellular Flux Analyzer. Basal readings were obtained, and then treatments were injected via port A. Treatments included 40 mM sodium oxamate (NaOx) (Sigma-Aldrich), 0.125 mM  $\alpha$ -Cyano-4-hydroxycinnamic acid ( $\alpha$ -CHC) (Sigma-Aldrich), 0.1% methanol as a control for  $\alpha$ -CHC, or no treatment. A combined mitochondrial-glycolysis stress test was then performed, with the following injections: oligomycin (Millipore) (port B, 1  $\mu$ M), FCCP (Cayman Chemical) (port C, 1.5  $\mu$ M), rotenone (Sigma-Aldrich)/antimycin A (Sigma-Aldrich)/2DG (Cayman Chemical) (port D, 0.5  $\mu$ M/ 0.5  $\mu$ M/ 50 mM). Glycolytic and mitochondrial metabolic parameters were calculated from the raw instrument data.



### 3.3. *In vitro* infection with H37Rv Mtb

CD1 mouse BMDMs were seeded into 96 well plates at 50,000 cells per well. Cells were exposed to H37Rv Mtb at an MOI of 5:1 for one hour, and then treatments were added. Treatments included 40 mM sodium oxamate (NaOx) (Sigma-Aldrich), 0.125 mM  $\alpha$ -Cyano-4-hydroxycinnamic acid ( $\alpha$ -CHC) (Sigma-Aldrich), 0.1% methanol as a control for  $\alpha$ -CHC, or no treatment. Uninfected cells and bacteria alone were also included as groups and received treatments. Infections were maintained for 48 hours before downstream assays were conducted.

### 3.4. *Bacterial Burden/CFUs*

To determine bacterial CFUs from *in vitro* infection experiments, infected cells were washed with PBS and then lysed with Triton X. Cell lysates were serially diluted in PBS and plated on BD Difco™ 7H11 agar (VWR) agar. Wells with bacteria alone were plated directly. After a 3-6-week incubation at 37°C, colony-forming units were counted and recorded.

### 3.5. *Cell viability*

To detect cell viability, an MTT assay protocol was used per manufacturer instructions (Thermo Fischer). Briefly, supernatants were removed from infected and uninfected wells and fresh media added. Cells were incubated with MTT for four hours at 37C. 50 $\mu$ L of DMSO were added to each well and incubated for 10 minutes at 37C before the plate was read at 540 nm on a Biotek plate reader.

### 3.6. *Guinea pig infection with H37Rv Mtb*

Dunkin Hartley guinea pigs were infected with an aerosol dose of 20-50 CFU of H37Rv Mtb. Mock-treated guinea pigs received OraSweet by mouth at times of treatment for other groups. Metformin (Sigma-Aldrich) treated guinea pigs received metformin dissolved in OraSweet once per day for four weeks prior to infection. BCG vaccination was given intradermally at a dose of  $1 \times 10^5$  CFU six weeks prior to infection. For animals that received both BCG vaccination and metformin, animals were vaccinated 6 weeks prior to infection, and metformin treatment was started 4 weeks prior to infection. Guinea pigs were necropsied at days 30, 60, and 90, and plasma was frozen at -80 C from necropsied animals.

### 3.7. *Detection of lactate*

An L-Lactate Assay Kit (Eton Biosciences) was used per manufacturer's instructions. Briefly, cell supernatant or guinea pig plasma samples were diluted to the limit of detection. Samples were incubated with assay medium for 30 minutes prior to reading the plate at wavelength 490 nm using a Biotek plate reader with colorimetric assay settings.

### 3.8. *Western Blot*

Protein samples previously extracted from isolated guinea pig lung granuloma lesions at day 30 post infection were analyzed for protein quantity via a Pierce BCA assay (Thermo Fischer) and then prepared in sample buffer. 15 µg of protein were loaded per well into a 4-12% Bis-Tris SDS PAGE gel (NuPage, Invitrogen). The gel was run at constant voltage for one hour, and then transferred for two hours onto a 0.45-micron PVDF membrane (GVS) at a constant mAmp. The membrane was blocked with 5% BSA, 0.05% Tween 20 for one hour. Primary antibodies were

incubated overnight in block buffer. TBS supplemented with Tween was used to wash blots for one hour prior to a two-hour incubation with secondary antibody. Blots were washed again for one hour prior to developing using a Pierce ECL chemiluminescence development kit (Thermo Fischer). Blots were imaged using an ImageQuant LAS 4000 and edited via Image J software. Antibodies were used against MCT1 (Santa Cruz Biotech sc-365501), MCT4, (Santa Cruz Biotech sc-376140), and LDHB (Novus H00003945-M01) or beta-actin as control (Invitrogen AM4302).

### 3.9. *Data analysis*

Depending on the data set, one-way or two-way ANOVA was used to determine differences between groups. P less than or equal to 0.05 was considered statistically significant. Tukey's IQR method was used to identify any outliers prior to calculations. Nonparametric tests were used if normality or homoscedasticity were not achieved. Multiple comparison testing was conducted using Tukey, Sidak's or Mann-Whitney multiple comparisons depending on the data analysis procedure. All statistical analysis was performed using GraphPad Prism version 8.3.

## 4. Results

### 4.1. *Plasma lactate is increased in infected guinea pigs and lactate shuttle components are present within lung lesions*

Since lactate levels are known to be elevated within the TB granuloma,<sup>50,51</sup> we wanted to investigate the systemic levels of lactate within infected animals. Using archived samples, we evaluated the concentration of lactate present in the plasma of guinea pigs infected with Mtb at day 30, 60, or 90 post infection (Figure 3.2). Additionally, we evaluated whether interventional strategies, such as BCG vaccination or metformin treatment, or a combination of the two would restore plasma lactate levels to those of uninfected animals. Metformin is a weak mitochondrial

complex I inhibitor that is currently the frontline treatment for individuals with type 2 diabetes mellitus (T2DM), regulating systemic glucose levels.<sup>54</sup> BCG is the current vaccine available against Mtb but is only used widely in highly endemic regions to prevent disseminated forms of TB and is not protective against adult pulmonary infections.<sup>55</sup> Both BCG vaccination and metformin treatment are being investigated in our laboratory with respect to their ability to augment metabolic dynamics on both systemic and cellular levels.

Guinea pig plasma lactate levels are highly elevated above those of uninfected animals during Mtb infection without treatment and remain elevated throughout the progressive disease time course (Figure 3.2A). While not significantly elevated at day 30 of infection, guinea pigs with metformin treatment develop progressively increased levels of plasma lactate over the course of infection, rising to levels that are significantly above those of uninfected animals (Figure 3.2B). BCG vaccination induces a peak plasma lactate level at day 60 post infection, with a significant reduction in lactate levels by day 90, which are no longer significantly elevated from uninfected animals (Figure 3.2C). Interestingly, the combination of BCG vaccination and metformin treatment maintains plasma lactate levels at those that are comparable to uninfected animals for all but the day 60 time point (Figure 3.2D). These data demonstrate that guinea pigs infected with Mtb exhibit high plasma lactate levels and those high levels can be mitigated through interventional strategies such as vaccination or host-directed therapy. Thus, lactate levels may serve as a prognostic marker for disease severity.

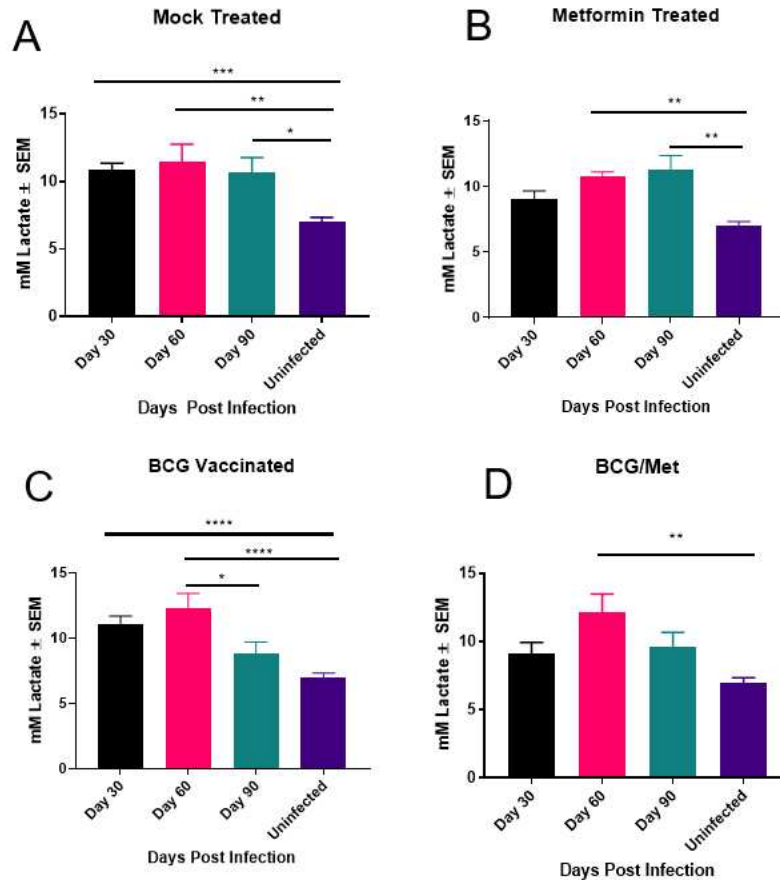


**Figure 3.2: Mtb infected guinea pigs demonstrate increased plasma lactate levels, which can be reduced with specific intervention strategies.** Guinea pig plasma lactate levels were detected via a colorimetric assay kit. Samples were taken across three time points, day 30, day 60, and day 90 post infection and for four treatment groups: mock treated (A), metformin treated (B), BCG vaccinated (C), or a combination treatment of BCG vaccination and metformin treatment (BCG/Met) (D). Uninfected samples were compared as a control. These data demonstrate that interventional strategies such as vaccination and combined vaccination/host-directed therapy can reduce plasma high plasma lactate levels in infected guinea pigs. N = 20 (uninfected), n =6-12 (all other groups). Data is presented as mean  $\pm$  SEM. Analysis was conducted via a one-way ANOVA, accounting for unequal variance and non-normal distributions when needed. \* =  $p < 0.05$ , \*\* =  $p < 0.01$ , \*\*\* =  $p < 0.001$ , \*\*\*\* =  $p < 0.0001$

As the lactate shuttle has never been explored within the context of the TB granuloma, we next aimed to determine if components of the shuttle are present within primary lung lesions. Both guinea pigs had detectable levels of MCT1, MCT4, and LDHB, demonstrating proof of concept that this shuttle could be functional within the lesion microenvironment (Figure 3.3). Varied expression of LDHB between the two individual guinea pigs indicates that there may be

heterogeneous expression of these targets between individuals. Difficulty with antibody reactivity against guinea pig tissue samples prevented us from successfully detecting LDHA or HIF-1 $\alpha$  via Western Blot and prevented detection of any target in IHC applications. In summary, these data provide proof of concept of the role of lactate and lactate shuttles during *in vivo* Mtb infection.

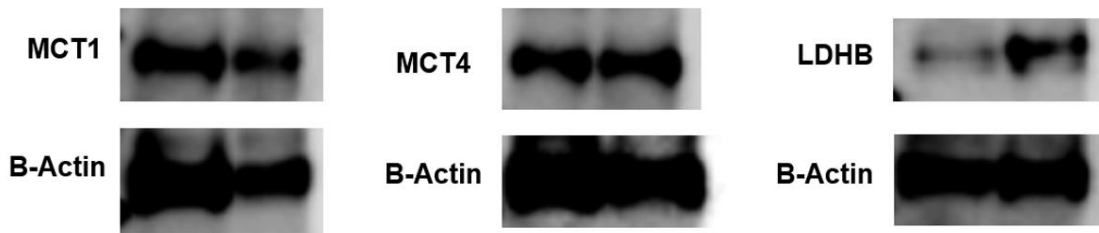


**Figure 3.3: Guinea pig primary lung granuloma lesions contain proteins involved in the lactate shuttle.** Granulomas were isolated from two individual guinea pigs at day 30 post infection and protein extracted. Sample protein levels were normalized before running Western Blots to detect MCT1, MCT4, and LDHB. The left and right columns represent the same two animals. Beta-actin is presented as a loading control. This demonstrates proof of concept and confirms presence of lactate shuttle components within the TB granuloma lesion *in vivo*.

#### 4.2. LDH and MCT inhibition significantly impacts the metabolism of uninfected murine macrophages

To circumvent any additional issues with antibody reactivity or cellular differentiation yield *in vitro*, we chose to conduct all further experiments within the CD1 mouse model. To characterize the impact of inhibiting the lactate shuttle on CD1 mouse BMDM metabolism, we evaluated sodium oxamate (NaOx), an LDHA inhibitor, and  $\alpha$ -Cyano-4-hydroxycinnamic acid ( $\alpha$ -CHC), an MCT1 inhibitor, within uninfected macrophages using Seahorse Extracellular Flux Analyzer experiments. 0.1% methanol was used as a control for  $\alpha$ -CHC, as it had to be dissolved in methanol to achieve appropriate solubility. Untreated macrophages were also used as a control

group. We used the Seahorse instrument's unique ability to customize injection protocols to inject inhibitors after basal readings were measured, and then proceeded with a mitochondrial-glycolysis stress test to determine impact on glycolysis and oxidative metabolism (Figure 3.4). Pre-treatment ECAR readings were not significantly different between groups (Figure 3.5A).

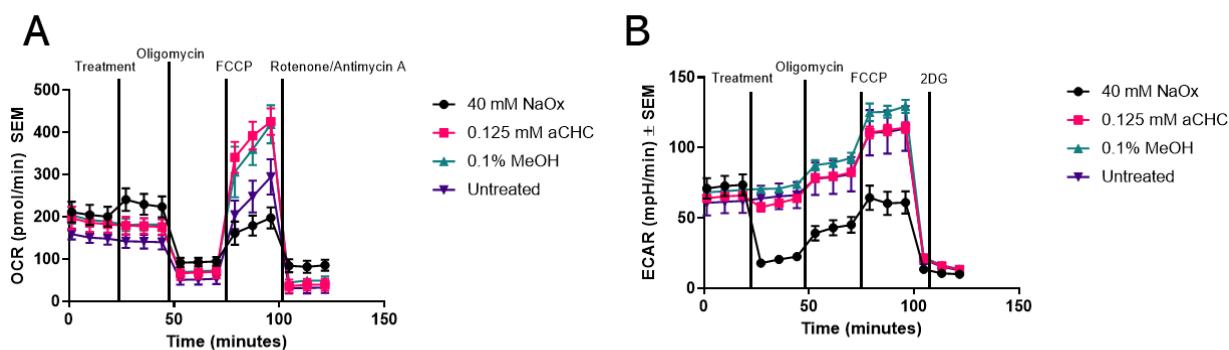


**Figure 3.4: Seahorse Extracellular Flux Analysis injection protocol for LDH and MCT inhibition experiments.** Representative line graphs are presented for oxygen consumption rate (OCR) (A) and extracellular acidification rate (ECAR) (B) to illustrate the order of injected inhibitors. The first instrument port was used to inject the desired treatment: NaOx, aChC, 0.1% methanol, or no treatment.

The basal extracellular acidification rate (ECAR) post-treatment with NaOx was significantly decreased as compared to untreated cells, indicating that LDHA inhibition blocked glycolytic metabolism (Figure 3.5B). MCT1 inhibition via  $\alpha$ -ChC significantly decreased basal ECAR when compared to 0.1% methanol control; however, the decrease in basal ECAR was not statistically significant when compared to the untreated group (Figure 3.5B). Disrupted glycolytic metabolism as a result of NaOx treatment was further exemplified by a decrease in glycolytic capacity, which was significantly less than all other treatment groups (Figure 3.5C). The ratio of oxygen consumption rate (OCR) to ECAR was significantly elevated in NaOx treated cells as compared to all other treatment groups, indicating that LDHA inhibition significantly blocks glycolytic metabolism, shifting cells toward an oxidative metabolic phenotype (Figure 3.5D). Interestingly, mitochondrial spare capacity of cells treated with NaOx was virtually eliminated (Figure 3.5E).

MCT1 inhibition via  $\alpha$ -CHC caused a trending decrease in mitochondrial spare capacity, but this was not statistically significant when compared with the 0.1% methanol control or untreated groups (Figure 3.5E). This indicates that blocking the production of lactate and therefore hindering the cell's capability to maintain glycolytic flux puts a strain on the mitochondria such that it utilizes its spare reserve capacity to compensate. Other oxidative metabolic parameters, including post-treatment OCR, ATP production, and proton leak, were not significantly different between groups (Figure 3.6). Collectively, these data demonstrate the ability for LDH and MCT inhibition to augment macrophage metabolism *in vitro*.

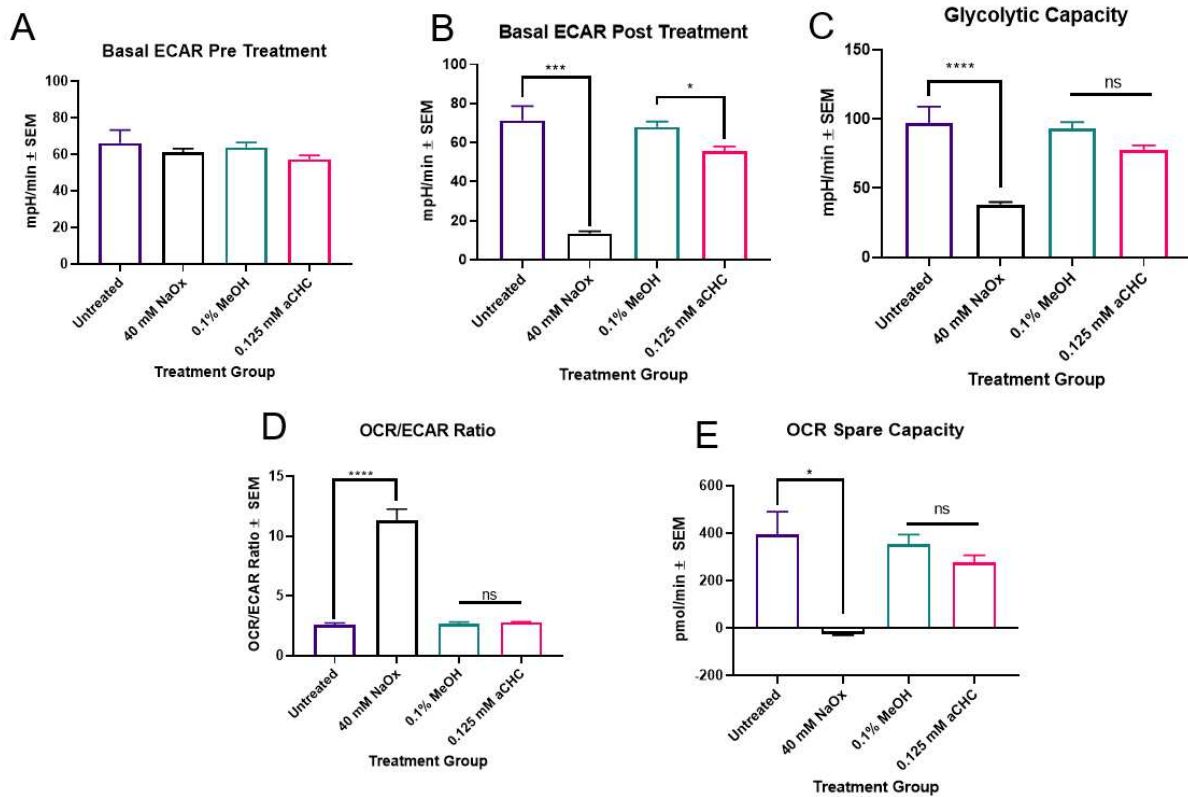


**Figure 3.5: LDH and MCT inhibition significantly blocks glycolysis and eliminates mitochondrial spare capacity in murine macrophages.** Seahorse Extracellular Flux Analyzer assays were utilized to evaluate metabolic parameters for CD1 mouse BMDMs post treatment with either sodium oxamate (NaOx),  $\alpha$ -Cyano-4-hydroxycinnamic acid (aCHC), 0.1% methanol, or no treatment. Methanol was used as a control for aCHC. Treatments were injected into the first plate assay port, and subsequent mitochondrial-glycolytic stress tests were performed. Analyzed parameters included basal extracellular acidification rate (ECAR) pre-treatment (A) and post-treatment (B), as well as glycolytic capacity (C), OCR/ECAR ratio (D), and spare capacity (E).



Overall, these data demonstrate that lactate shuttle inhibition significantly disrupts glycolytic metabolism in uninfected murine macrophages. Data is presented as mean  $\pm$  SEM. Analysis was conducted via a one-way ANOVA, accounting for unequal variance and non-normal distributions when needed. 2 biological replicates, n =9 -10. \* = p < 0.05, \*\* = p < 0.01, \*\*\* = p < 0.001, \*\*\*\* = p < 0.0001, ns = not significant.

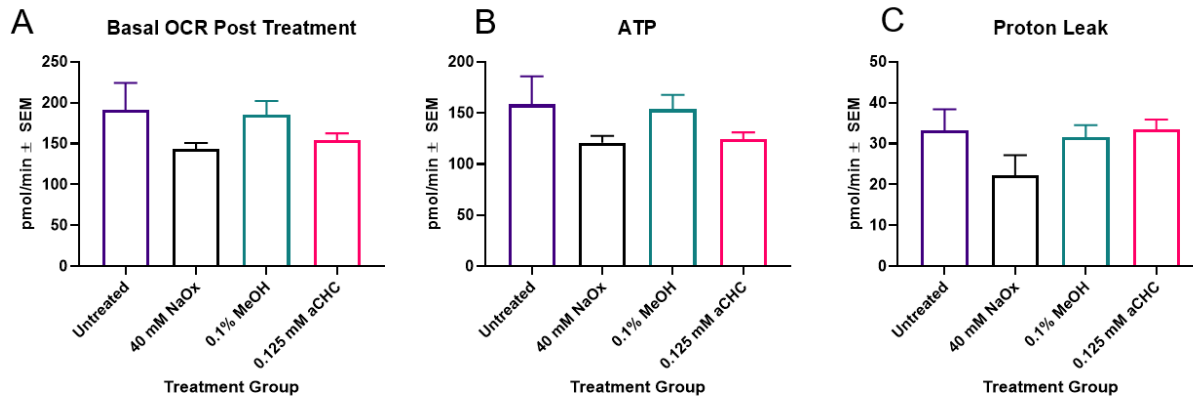


**Figure 3.6: Lactate shuttle inhibition does not impact specific oxidative metabolic parameters.** Seahorse Extracellular Flux Analyzer assays were utilized to evaluate metabolic parameters for CD1 mouse BMDMs post treatment with either sodium oxamate (NaOx),  $\alpha$ -Cyano-4-hydroxycinnamic acid (aCHC), 0.1% methanol, or no treatment. Methanol was used as a control for aCHC. Treatments were injected into the first plate assay port, and subsequent mitochondrial-glycolytic stress tests were performed. No significant differences were observed in basal OCR post-treatment (A), ATP production (B), or proton leak (C). Data is presented as mean  $\pm$  SEM. Analysis was conducted via a one-way ANOVA, accounting for unequal variance and non-normal distributions when needed. 2 biological replicates, n =9 -10.

#### 4.3. *Lactate accumulates in the supernatant of Mtb infected macrophages, and inhibiting the lactate shuttle can reduce lactate levels accumulated in vitro*

After achieving experimental proof that our chosen inhibitors of the lactate shuttle have the desired metabolic impact on CD1 mouse BMDMs, we moved to explore the impact of these inhibitors during Mtb infection *in vitro*. CD1 mouse BMDMs were infected with H37Rv Mtb at an MOI of 5:1 for one hour prior to addition of NaOx,  $\alpha$ -CHC, 0.1% methanol, or no treatment. Uninfected cells and bacteria alone were also included as experimental groups. Infections were maintained for 48 hours prior to the evaluation of lactate present in culture supernatant, cell viability via an MTT assay, and bacterial colony forming units (CFUs).

After 48 hours of Mtb infection, cell viability was significantly reduced across all treatment groups (Figure 3.7). However, there were no significant differences in viability between treatment groups (Figure 3.7). As a result of this finding, all lactate concentration analysis was normalized to cell number to evaluate true impacts of infection on lactate present in cell culture supernatants.

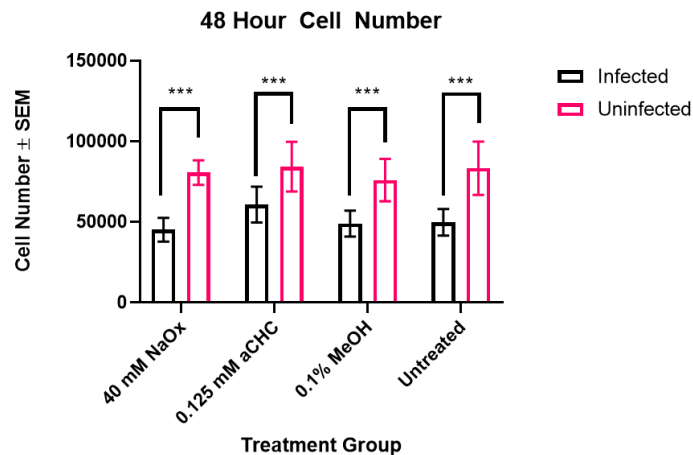


**Figure 3.7: Mtb infection, but not lactate shuttle inhibition, impacts macrophage viability.** CD1 mouse BMDMs were infected with Mtb H37Rv and then treated with sodium oxamate (NaOx),  $\alpha$ -Cyano-4-hydroxycinnamic acid (aCHC), 0.1% methanol, or no treatment for 48 hours. Methanol was used as a control for aCHC. Cell viability was determined via an MTT assay for both uninfected and infected cells. After 48 hours, Mtb infection significantly reduced cell numbers as compared to uninfected cells. However, cell viability was similar across treatment groups. Therefore, lactate shuttle inhibition does not impact cell viability during an *in vitro* infection. Data is presented as mean  $\pm$  SEM. Analysis was conducted via a two-way ANOVA, accounting for unequal variance and non-normal distributions when needed. 2 biological replicates, n = 8. \*\*\* =  $p < 0.001$

In line with our evaluation on the systemic level of plasma lactate in infected guinea pigs, *in vitro* Mtb infection of CD1 mouse BMDMs also significantly increased lactate concentrations within the supernatant (Figure 3.8). This effect was observed across all treatment groups. It is important to note that the colorimetric detection of lactate in the supernatant does not indicate whether this lactate accumulation is due to increased production as a result of infection or reduced import/consumption. Further metabolic substrate analysis, through approaches such as carbon tracing, would help elucidate these mechanisms.

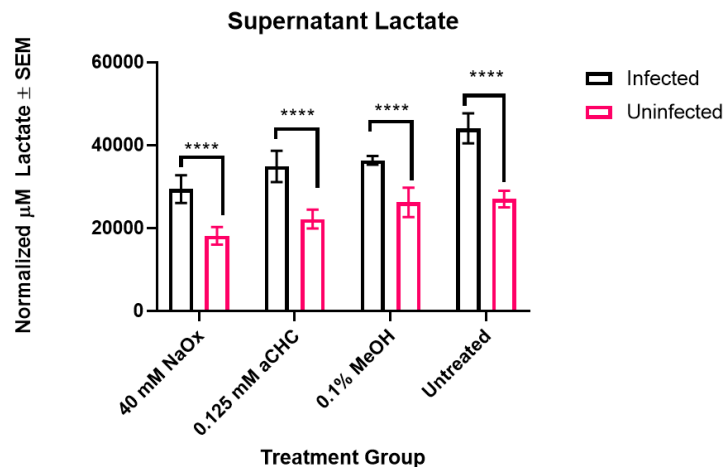


**Figure 3.8: Lactate accumulates within the supernatant of Mtb infected murine macrophages.** CD1 mouse BMDMs were infected with Mtb H37Rv and then treated with sodium oxamate (NaOx),  $\alpha$ -Cyano-4-hydroxycinnamic acid ( $\alpha$ CHC), 0.1% methanol, or no treatment for 48 hours. Methanol was used as a control for  $\alpha$ CHC. Lactate was detected within the supernatant via a colorimetric plate assay and then normalized to cell number. The supernatant of Mtb infected cells accumulated significantly more lactate than that of uninfected cells across all treatment groups. Data is presented as mean  $\pm$  SEM. Analysis was conducted via a two-way ANOVA, accounting for unequal variance and non-normal distributions when needed. 2 biological replicates, n = 8. \*\*\*\* = p < 0.0001

Additional analysis of this data by infection status was warranted to determine the impact of inhibitor treatments on lactate accumulation in culture supernatant. Inhibition of lactate production by NaOx trended to decrease the amount of lactate detected in the supernatant as compared to untreated cells; however, this difference was not statistically significant (Figure 3.9A). MCT1 inhibition by  $\alpha$ -CHC did not differ from the 0.1 % methanol control in its ability to decrease lactate present in the supernatant. These trends remained the same for uninfected cells (Figure 3.9B), and for extracellular bacteria alone (Figure 3.9C). Additional replicates of these experiments would likely increase statistical power and enhance observed trends.

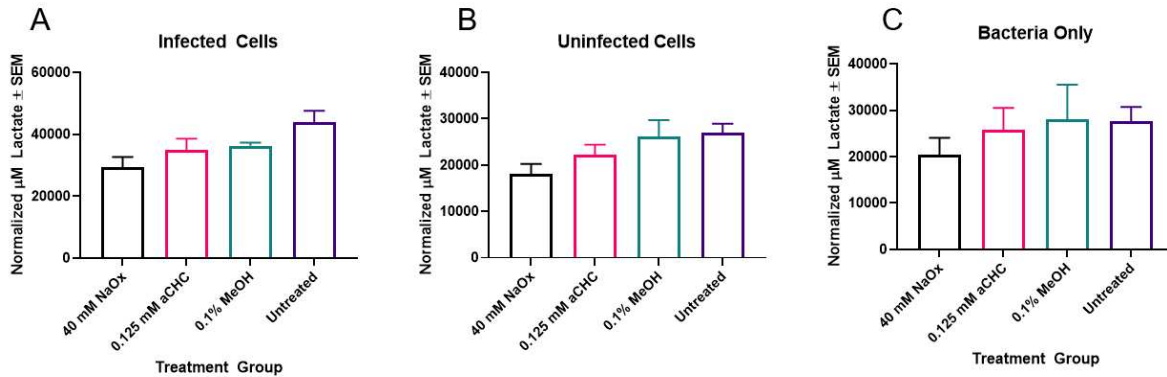


**Figure 3.9: Inhibition of the lactate shuttle reduces supernatant lactate of both Mtb infected macrophages and Mtb alone.** CD1 mouse BMDMs were infected with Mtb H37Rv and then treated with sodium oxamate (NaOx),  $\alpha$ -Cyano-4-hydroxycinnamic acid (aCHC), 0.1% methanol, or no treatment for 48 hours. Bacteria alone were also subjected to the same treatment regimen. Methanol was used as a control for aCHC. Lactate was detected within the supernatant via a colorimetric plate assay and then normalized to cell number or bacterial CFU. Lactate shuttle inhibition by NaOx or aCHC trended to decrease lactate production as compared to untreated groups for infected cells (A), uninfected cells (B), and bacteria alone (C). However, this trend was not statistically significant. Minimal differences between aCHC treated and 0.1% methanol treated groups were observed, particularly within infected cells. Data is presented as mean  $\pm$  SEM. Analysis was conducted via a one-way ANOVA, accounting for unequal variance and non-normal distributions when needed. 2 biological replicates,  $n = 8$ .

Lastly, as LDH inhibition by FX-11 was shown to reduce lung bacterial burden in a mouse model of Mtb infection,<sup>53</sup> we evaluated the impact of lactate shuttle inhibition on bacterial CFUs post 48 hour *in vitro* infection. We observed no statistically significant differences in CFUs between treatment groups (Figure 3.10). Interestingly, inhibition of MCT1 with  $\alpha$ -CHC appeared to increase the number of bacteria recovered from infected cells (Figure 3.10A). Inhibiting lactate transport may sequester lactate intracellularly, providing additional energy substrates for Mtb survival. Methanol appeared to increase bacterial survival when bacteria was present alone (Figure 3.10B), which may represent Mtb's ability to survive on a variety of substrates. Ultimately, these data present promise in the ability of lactate shuttle inhibition to modulate lactate production and utilization during Mtb infection *in vitro*.

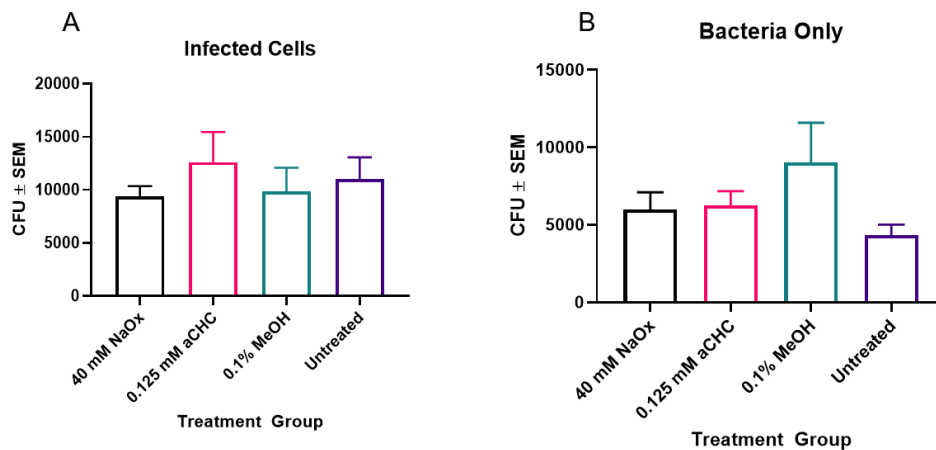


**Figure 3.10: Lactate shuttle inhibition has no significant impact on bacterial CFU.** CD1 mouse BMDMs were infected with Mtb H37Rv and then treated with sodium oxamate (NaOx),  $\alpha$ -Cyano-4-hydroxycinnamic acid (aChC), 0.1% methanol, or no treatment for 48 hours. Methanol was used as a control for aChC. Infected cells were lysed and plated on 7H11 agar quad plates, or bacteria alone wells were plated directly. CFUs were counted three weeks post-plating. Treatment with lactate shuttle inhibitors had no significant impact on bacterial CFU for either infected cells (A) or bacteria alone (B). Fewer bacterial CFU were recovered from extracellular bacteria alone (B) versus bacteria recovered from infected cells (A). MCT inhibition via aChC may increase bacterial CFU recovery from infected cells as compared to other treatment groups, but this increase was not significant. Data is presented as mean  $\pm$  SEM. Analysis was conducted via a one-way ANOVA, accounting for unequal variance and non-normal distributions when needed. 2 biological replicates,  $n = 8$ .

## 5. Discussion

The research described herein investigates the role of lactate shuttle dynamics within the context of Mtb infection and the granuloma microenvironment. Lactate shuttles, while actively studied in other disease systems, have yet to be described for TB. Our work demonstrates that lactate is significantly increased both at a cellular and systemic level during Mtb infection, that components of the lactate shuttle are present within primary granulomas, and that shuttle inhibition has the potential to reduce lactate produced by Mtb infected cells and may impact bacterial CFUs. This work demonstrates the important role metabolites can play during infection and provides novel avenues for pursuit of host-directed therapeutic strategies.

We showed that lactate is systemically increased within the plasma of guinea pigs over a progressive Mtb infection (Figure 3.2). Metformin treatment increased the levels of lactate produced throughout the course of infection (Figure 3.2B). Multiple laboratories, including ours, are investigating the potential of metformin as a host-directed therapy for Mtb infection.<sup>54,56-58</sup> However, metformin has been shown to cause lactic acidosis in subsets of diabetic patients who have other underlying conditions such as renal impairment, cirrhosis, sepsis, or hypoperfusion, and these cases have a mortality rate of 30-50%.<sup>59-62</sup> The induction of lactate production by metformin has been linked to metformin's action against mitochondrial complex I.<sup>63</sup> Cellular metabolic changes occurring within the granuloma microenvironment as well as other inflammatory sequelae of TB progression may predispose individuals to additional systemic increases in plasma lactate when receiving metformin. For guinea pigs that received BCG vaccination, (Figure 3.2C, Figure 3.2D), plasma lactate levels peaked at day 60 post infection. However, by day 90, BCG vaccination and a combination of BCG/metformin brought lactate levels down to those of uninfected guinea pigs (Figure 3.2C, 3.2D). This demonstrates that lactate could be a prognostic indicator for those undergoing TB interventions, and lactate production could be a systemic correlate for disease protection. Investigation of the lactate levels in Mtb infected CD1 mouse models undergoing the same treatment regimens would bring an additional robustness to the current data and would confirm this hypothesis.

Additionally, we showed that the lactate shuttle components MCT1, MCT4, and LDHB are expressed within primary guinea pig lung granulomas (Figure 3.3). Using guinea pig tissue samples proved difficult in Western Blot applications, and the additional shuttle target LDHA as well as HIF-1 $\alpha$  to signify tissue hypoxia were unable to be detected with the antibodies available. We also did not have samples that were from uninvolved lung of the same animals or from uninfected lung that could be used as a direct comparison. Investigating tissue expression of these shuttle components in isolated granulomas from murine infection models would circumvent

issues with antibody reactivity and reagent compatibility. This was a large factor in the decision to pursue *in vitro* infection experiments within the CD1 mouse model, in addition to the outbred nature of these mice providing a more heterogeneous cell population.

Future efforts will focus on determining the spatial distribution of these shuttle components within the granuloma microenvironment. To fully prove the shuttle hypothesis, different phenotypes of cells must be demonstrated to exist in hypoxic versus normoxic regions of the granuloma. Multiplexed IHC approaches would preserve granuloma structure and would allow for comparison of involved versus uninvolved tissue within the same animal.<sup>64-70</sup> Although our intention was to perform these experiments, reagent reactivity, tissue availability, and capacity for multiplexing were limited. It is also important to understand which cell types are contributing to this phenomenon. Within the tumor microenvironment, multiple cell types shuttle lactate to tumor cells including fibroblasts, endothelial cells, and tumor associated macrophages.<sup>14,71-74</sup> It would be interesting to note the relative expression of these shuttle components within the heterogeneous cell populations involved in the TB granuloma lesion and expand our studies outside of only macrophages. Multi-dimensional granuloma culture models could be explored as an *in vitro* application to complement tissue IHC.<sup>75</sup>

We also actively demonstrated that inhibition of LDH and MCT impacted cellular metabolism in uninfected CD1 mouse BMDMs (Figure 3.5). This served as essential proof of concept for future work with *Mtb* infection. Basal ECAR and glycolytic capacity were significantly decreased (Figure 3.5B and 3.5C), while OCR/ECAR ratio was increased (Figure 3.5D), indicating an overall increase in reliance on oxidative metabolic capacity. Interestingly, the mitochondrial spare capacity of cells treated with sodium oxamate was significantly decreased (Figure 3.5E). The spare capacity is a measure of the ability of the cell to respond to mitochondrial stress. Blocking LDHA eliminates the ability for the cell to maintain glycolytic flux through regeneration of NAD<sup>+</sup>,

and this cofactor plays a role in regulating redox homeostasis and therefore mitochondrial respiratory function.<sup>76,77</sup> Eliminating glycolytic function may force the cell to rely heavily on oxidative metabolism through the mitochondria, pushing cells to utilize their reserve and exhausting mitochondrial capacity. Additional assays that determine overall mitochondrial health and bioenergetics under these treatments would be warranted to further explore the impacts of these treatments. It is important to note, however, that despite a drastic reduction in ECAR with sodium oxamate treatment, a compensatory increase in OCR was not observed (Figure 3.6A). A reduction in ECAR does not necessarily indicate a reduction in cellular glucose utilization, as glucose is needed both for the production of ATP and for biosynthetic processes, such as the pentose phosphate pathway and one carbon metabolism.<sup>78</sup> Glucose use also varies considerably between immune cells *in vitro* versus *in vivo* and during different activation states throughout the course of an immune response.<sup>79</sup> Interestingly, cancer cells that are under lactic acidosis demonstrate 5-fold reductions in glycolytic rate without compensatory changes in OCR, indicating that cells within high lactate environments are more economical with their glucose use, and can switch between Warburg-like metabolism and non-glycolytic phenotypes to adapt to changing microenvironments.<sup>80</sup> The duality and flexibility of metabolism within cell populations warrants further metabolic flux analyses to trace the use of glucose and lactate under lactate shuttle inhibition.

It is important to note that sodium oxamate is a structural analogue of pyruvate, competitively inhibiting with enzymatic binding sites on LDH.<sup>36</sup> It is possible that the use of sodium oxamate was not selective of the LDHA versus LDHB reactions, and may have impacted the ability of cells to produce pyruvate from lactate as well as inhibited pyruvate mediated uptake into mitochondria for incorporation into the TCA cycle. Use of other LDH inhibitors with different mechanisms of action, including FX-11, which is a derivative of gossypol inhibiting NADH binding and shows selectivity of LDHA over LDHB, may be warranted.<sup>29</sup> Recently, FX-11 was used as an inhibitor for



an Mtb infection study, leading to reduced bacterial growth, a reduction in necrotic lesion burden, and potentiation of isoniazid.<sup>53</sup> However, due to its mechanism of action, FX-11 has the potential to inhibit other NAD/NADH dependent enzymes important for metabolism, highlighting the need to use complementary assays that evaluate multiple facets of metabolism in the future.

Due to the nature of  $\alpha$ -Cyano-4-hydroxycinnamic acid ( $\alpha$ -CHC), it was necessary to solubilize the compound in methanol. It proved difficult to discern the impacts of the methanol control versus the  $\alpha$ -CHC treatment in multiple instances. Finding an MCT inhibitor that does not require dissolution into methanol would be ideal for future studies. Additionally, MCT1 is capable of transporting more than just lactate across membranes, including pyruvate and ketone bodies<sup>30</sup>, and our experimental approach did not rule out the inhibition of transport of other related small molecules. Lastly,  $\alpha$ -CHC and its derivatives do have some impact on other MCT transporters as well as the mitochondrial pyruvate carrier.<sup>81-83</sup> Finding more specific MCT1 inhibitors, such as those currently in production by Astra Zeneca<sup>84</sup> or using specific knock-out techniques, should be considered in future work.

During *in vitro* Mtb infection, we successfully demonstrated that infected CD1 mouse macrophages have increased lactate present within supernatant samples (Figure 3.8). We normalized lactate concentration to cell number to work to reduce confounding results due to the impact of 48 hours of Mtb infection on cell viability (Figure 3.7). However, LDH is released as a result of mammalian cell death<sup>85-87</sup>, and we did not rule out the possibility that increases in released LDH during infection could contribute to increased lactate levels. It is also important to note that increased lactate within the supernatant of infected cells could be due to increased production and/or reduced import and consumption. Our experimental approach could not discern between these sources for lactate accumulation. Stable isotope tracing<sup>88,89</sup> is a viable alternative method to more accurately trace the metabolism of lactate and better identify its source.

Additionally, analysis of multiple time points to determine the impacts of lactate shuttle inhibition throughout an acute infection time course would add additional robustness to the data presented. Due to laboratory constraints related to the COVID-19 pandemic, the *in vitro* experiments could only be performed at two replicates. Additional replicates would likely make trends that were observed but were not statistically significant more impactful (Figure 3.9, Figure 3.10).

Bacterial CFUs recovered were also lower than anticipated for a 5:1 MOI infection. With 50,000 cells, 5:1 MOI would be 250,000 bacteria. However, we recovered roughly one log less across treatment groups (Figure 3.10). In future experiments, confirmation of the titer of stocks used and potentially longer bacterial incubations to ensure more bacteria are taken up by macrophages will mitigate this issue. One trend observed for MCT inhibitor  $\alpha$ -CHC was that bacterial CFUs increased post-treatment (Figure 3.10A). Blocking lactate transport out of cells may provide additional lactate substrates intracellularly for which Mtb could subsist, as it has been demonstrated that Mtb can oxidize lactate and requires lactate oxidation mechanisms to survive intracellularly.<sup>52</sup> Mtb may rely more heavily on lactate as a substrate while intracellular in glycolytic cells than when extracellular. Discerning the roles of host LDH and bacterial LDH thus warrants further investigation. The reduction of lactate production was not as significant with LDH inhibitor sodium oxamate as might be expected (Figure 3.9). L929 conditioned media used to maintain CD1 mouse macrophage cells may have contained high levels of lactate and this must be investigated to rule out background effects which could have contributed to artificially elevated lactate levels. To mitigate this issue, other cell types that do not require conditioned media to be cultured could be used, such as guinea pig BMDMs, or lactate free media could be used to validate results.

This work raises multiple additional questions. The use of sodium oxamate as an *in vivo* therapy has been investigated for melanoma, and interestingly, sodium oxamate combined with metformin

significantly reduced tumor volume, better than either treatment alone.<sup>35</sup> Our laboratory expertise and knowledge of metformin could make this an interesting host-directed therapeutic approach to explore further *in vivo*, particularly if *in vitro* data is validated. Additionally, lactate is more than just an intermediary of metabolism, but has robust signaling activity. It signals through the receptor GPR81 to induce anti-inflammatory and immunosuppressive activities in a wide variety of cell and tissue types.<sup>90</sup> Analyzing the impact of lactate signaling within the context of the granuloma environment is the subject of future study, and our laboratory has preliminary data to indicate that GPR81 is expressed highly within granuloma microenvironments.

Alterations in lactate production and shuttling during infection would have downstream impacts on many processes relevant to TB disease progression including adaptive immune responses, antigen presentation, and angiogenesis that were outside the scope of this work. Ultimately, proof of concept work presented herein implicates a lactate shuttle within the context of the TB granuloma microenvironment and demonstrates a critical need to explore the dynamic role of lactate as both a metabolite and signaling molecule during *Mtb* infection.

## REFERENCES

1. Bar-Even, A., Flamholz, A., Noor, E. & Milo, R. Rethinking glycolysis: on the biochemical logic of metabolic pathways. *Nature Chemical Biology* **8**, 509–517 (2012).
2. Cassim, S., Vučetić, M., Ždravčić, M. & Pouyssegur, J. Warburg and Beyond: The Power of Mitochondrial Metabolism to Collaborate or Replace Fermentative Glycolysis in Cancer. *Cancers* **12**, 1119 (2020).
3. Sun, S., Li, H., Chen, J. & Qian, Q. Lactic Acid: No Longer an Inert and End-Product of Glycolysis. *Physiology* **32**, 453–463 (2017).
4. San-Millán, I. & Brooks, G. A. Reexamining cancer metabolism: lactate production for carcinogenesis could be the purpose and explanation of the Warburg Effect. *Carcinogenesis* **38**, 119–133 (2017).
5. Porporato, P. E. *et al.* Lactate stimulates angiogenesis and accelerates the healing of superficial and ischemic wounds in mice. *Angiogenesis* **15**, 581–592 (2012).
6. Morais-Santos, F. *et al.* Targeting lactate transport suppresses in vivo breast tumour growth. *Oncotarget* **6**, 19177–19189 (2015).
7. Koukourakis, M. I., Giatromanolaki, A., Simopoulos, C., Polychronidis, A. & Sivridis, E. Lactate dehydrogenase 5 (LDH5) relates to up-regulated hypoxia inducible factor pathway and metastasis in colorectal cancer. *Clin Exp Metastasis* **22**, 25–30 (2005).
8. Pucino, V., Bombardieri, M., Pitzalis, C. & Mauro, C. Lactate at the crossroads of metabolism, inflammation, and autoimmunity. *Eur. J. Immunol.* **47**, 14–21 (2017).
9. Pucino, V. *et al.* Lactate Buildup at the Site of Chronic Inflammation Promotes Disease by Inducing CD4+ T Cell Metabolic Rewiring. *Cell Metabolism* **0**, (2019).

10. Ristic, B., Bhutia, Y. D. & Ganapathy, V. Cell-surface G-protein-coupled receptors for tumor-associated metabolites: A direct link to mitochondrial dysfunction in cancer. *Biochimica et Biophysica Acta (BBA) - Reviews on Cancer* **1868**, 246–257 (2017).
11. Kennedy, K. M. *et al.* Catabolism of Exogenous Lactate Reveals It as a Legitimate Metabolic Substrate in Breast Cancer. *PLoS One* **8**, (2013).
12. Faubert, B. *et al.* Lactate Metabolism in Human Lung Tumors. *Cell* **171**, 358-371.e9 (2017).
13. Sonveaux, P. *et al.* Targeting lactate-fueled respiration selectively kills hypoxic tumor cells in mice. *J Clin Invest* **118**, 3930–3942 (2008).
14. Nakajima, E. C. & Van Houten, B. Metabolic symbiosis in cancer: Refocusing the Warburg lens. *Mol. Carcinog.* **52**, 329–337 (2013).
15. Rademakers, S. E., Lok, J., van der Kogel, A. J., Bussink, J. & Kaanders, J. H. Metabolic markers in relation to hypoxia; staining patterns and colocalization of pimonidazole, HIF-1 $\alpha$ , CAIX, LDH-5, GLUT-1, MCT1 and MCT4. *BMC Cancer* **11**, 167 (2011).
16. Le Floch, R. *et al.* CD147 subunit of lactate/H<sup>+</sup> symporters MCT1 and hypoxia-inducible MCT4 is critical for energetics and growth of glycolytic tumors. *Proc Natl Acad Sci U S A* **108**, 16663–16668 (2011).
17. Firth, J. D., Ebert, B. L. & Ratcliffe, P. J. Hypoxic Regulation of Lactate Dehydrogenase A INTERACTION BETWEEN HYPOXIA-INDUCIBLE FACTOR 1 AND cAMP RESPONSE ELEMENTS. *J. Biol. Chem.* **270**, 21021–21027 (1995).
18. Semenza, G. L. *et al.* Hypoxia Response Elements in the Aldolase A, Enolase 1, and Lactate Dehydrogenase A Gene Promoters Contain Essential Binding Sites for Hypoxia-inducible Factor 1. *J. Biol. Chem.* **271**, 32529–32537 (1996).
19. Gladden, L. B. Lactate metabolism: a new paradigm for the third millennium. *The Journal of Physiology* **558**, 5–30 (2004).
20. Brooks, G. A. Cell–cell and intracellular lactate shuttles. *The Journal of Physiology* **587**, 5591–5600 (2009).

21. Brooks, G. A. The Science and Translation of Lactate Shuttle Theory. *Cell Metabolism* **27**, 757–785 (2018).
22. Ferguson, B. S. *et al.* Lactate metabolism: historical context, prior misinterpretations, and current understanding. *Eur J Appl Physiol* **118**, 691–728 (2018).
23. Brooks, G. A. The tortuous path of lactate shuttle discovery: From cinders and boards to the lab and ICU. *Journal of Sport and Health Science* (2020) doi:10.1016/j.jshs.2020.02.006.
24. Brooks, G. A. The lactate shuttle during exercise and recovery. *Medicine & Science in Sports & Exercise* **18**, 360–368 (1986).
25. Brooks, G. A., Dubouchaud, H., Brown, M., Sicurello, J. P. & Butz, C. E. Role of mitochondrial lactate dehydrogenase and lactate oxidation in the intracellular lactate shuttle. *Proc Natl Acad Sci U S A* **96**, 1129–1134 (1999).
26. Mächler, P. *et al.* In Vivo Evidence for a Lactate Gradient from Astrocytes to Neurons. *Cell Metabolism* **23**, 94–102 (2016).
27. Lee, Y. *et al.* Oligodendroglia metabolically support axons and contribute to neurodegeneration. *Nature* **487**, 443–448 (2012).
28. Magistretti, P. J. & Allaman, I. Lactate in the brain: from metabolic end-product to signalling molecule. *Nature Reviews Neuroscience* **19**, 235–249 (2018).
29. Doherty, J. R. & Cleveland, J. L. Targeting lactate metabolism for cancer therapeutics. *J Clin Invest* **123**, 3685–3692 (2013).
30. Jones, R. & Morris, M. Monocarboxylate Transporters: Therapeutic Targets and Prognostic Factors in Disease. *Clin. Pharmacol. Ther.* **100**, 454–463 (2016).
31. Marchiq, I. & Pouysségur, J. Hypoxia, cancer metabolism and the therapeutic benefit of targeting lactate/H<sup>+</sup> symporters. *J Mol Med* **94**, 155–171 (2016).

32. Mathupala, S. P., Parajuli, P. & Sloan, A. E. Silencing of Monocarboxylate Transporters via Small Interfering Ribonucleic Acid Inhibits Glycolysis and Induces Cell Death in Malignant Glioma: An in Vitro Study. *Neurosurgery* **55**, 1410–1419 (2004).
33. Sonveaux, P. *et al.* Targeting the Lactate Transporter MCT1 in Endothelial Cells Inhibits Lactate-Induced HIF-1 Activation and Tumor Angiogenesis. *PLoS One* **7**, (2012).
34. Miao, P., Sheng, S., Sun, X., Liu, J. & Huang, G. Lactate dehydrogenase a in cancer: A promising target for diagnosis and therapy. *IUBMB Life* **65**, 904–910 (2013).
35. Chaube, B. *et al.* Targeting metabolic flexibility by simultaneously inhibiting respiratory complex I and lactate generation retards melanoma progression. *Oncotarget* **6**, 37281–37299 (2015).
36. Zhao, Z., Han, F., Yang, S., Wu, J. & Zhan, W. Oxamate-mediated inhibition of lactate dehydrogenase induces protective autophagy in gastric cancer cells: Involvement of the Akt–mTOR signaling pathway. *Cancer Letters* **358**, 17–26 (2015).
37. Le, A. *et al.* Inhibition of lactate dehydrogenase A induces oxidative stress and inhibits tumor progression. *Proc Natl Acad Sci U S A* **107**, 2037–2042 (2010).
38. Carmona-Fontaine, C. *et al.* Emergence of spatial structure in the tumor microenvironment due to the Warburg effect. *Proc Natl Acad Sci U S A* **110**, 19402–19407 (2013).
39. Carow, B. *et al.* Spatial and temporal localization of immune transcripts defines hallmarks and diversity in the tuberculosis granuloma. *Nature Communications* **10**, 1823 (2019).
40. Marakalala, M. J. *et al.* Inflammatory signaling in human tuberculosis granulomas is spatially organized. *Nature Medicine* **22**, 531–538 (2016).
41. Singer, K., Cheng, W.-C., Kreutz, M., Ho, P.-C. & Siska, P. J. Immunometabolism in cancer at a glance. *Disease Models & Mechanisms* **11**, dmm034272 (2018).
42. Van den Bossche, J., O'Neill, L. A. & Menon, D. Macrophage Immunometabolism: Where Are We (Going)? *Trends in Immunology* **38**, 395–406 (2017).
43. Warburg, O. On the Origin of Cancer Cells. *Science* **123**, 309–314 (1956).

44. Weinhouse, S., Warburg, O., Burk, D. & Schade, A. L. On Respiratory Impairment in Cancer Cells. *Science* **124**, 267–272 (1956).
45. Wang, S. *et al.* Metabolic reprogramming of macrophages during infections and cancer. *Cancer Letters* **452**, 14–22 (2019).
46. Shi, L. *et al.* Infection with *Mycobacterium tuberculosis* induces the Warburg effect in mouse lungs. *Scientific Reports* **5**, 18176 (2015).
47. Gleeson, L. E. *et al.* Cutting Edge: *Mycobacterium tuberculosis* Induces Aerobic Glycolysis in Human Alveolar Macrophages That Is Required for Control of Intracellular Bacillary Replication. *J Immunol* **196**, 2444–2449 (2016).
48. Shi, L., Jiang, Q., Bushkin, Y., Subbian, S. & Tyagi, S. Biphasic Dynamics of Macrophage Immunometabolism during *Mycobacterium tuberculosis* Infection. *mBio* **10**, e02550-18 (2019).
49. Qualls, J. E. & Murray, P. J. Immunometabolism within the tuberculosis granuloma: amino acids, hypoxia, and cellular respiration. *Semin Immunopathol* **38**, 139–152 (2015).
50. Somashekar, B. S. *et al.* Metabolomic Signatures in Guinea Pigs Infected with Epidemic-Associated W-Beijing Strains of *Mycobacterium tuberculosis*. *J. Proteome Res.* **11**, 4873–4884 (2012).
51. Somashekar, B. S. *et al.* Metabolic Profiling of Lung Granuloma in *Mycobacterium tuberculosis* Infected Guinea Pigs: Ex vivo <sup>1</sup>H Magic Angle Spinning NMR Studies. *J. Proteome Res.* **10**, 4186–4195 (2011).
52. Billig, S. *et al.* Lactate oxidation facilitates growth of *Mycobacterium tuberculosis* in human macrophages. *Scientific Reports* **7**, 6484 (2017).
53. Krishnamoorthy, G. *et al.* FX11 limits *Mycobacterium tuberculosis* growth and potentiates bactericidal activity of isoniazid through host-directed activity. *Disease Models & Mechanisms* **13**, (2020).



54. Oglesby, W., Kara, A. M., Granados, H. & Cervantes, J. L. Metformin in tuberculosis: beyond control of hyperglycemia. *Infection* **47**, 697–702 (2019).
55. Tang, J., Yam, W.-C. & Chen, Z. Mycobacterium tuberculosis infection and vaccine development. *Tuberculosis* **98**, 30–41 (2016).
56. Rodriguez-Carlos, A. *et al.* Metformin promotes Mycobacterium tuberculosis killing and increases the production of human  $\beta$ -defensins in lung epithelial cells and macrophages. *Microbes and Infection* **22**, 111–118 (2020).
57. Lachmandas, E. *et al.* Metformin Alters Human Host Responses to Mycobacterium tuberculosis in Healthy Subjects. *J Infect Dis* **220**, 139–150 (2019).
58. Lin, S.-Y. *et al.* Metformin is associated with a lower risk of active tuberculosis in patients with type 2 diabetes. *Respirology* **23**, 1063–1073 (2018).
59. Boucaud-Maitre, D. *et al.* Lactic acidosis: relationship between metformin levels, lactate concentration and mortality. *Diabet. Med.* **33**, 1536–1543 (2016).
60. DeFronzo, R., Fleming, G. A., Chen, K. & Bicsak, T. A. Metformin-associated lactic acidosis: Current perspectives on causes and risk. *Metabolism* **65**, 20–29 (2016).
61. Doenya-Barak, K., Beberashvili, I., Marcus, R. & Efrati, S. Lactic acidosis and severe septic shock in metformin users: a cohort study. *Crit Care* **20**, (2016).
62. Connelly, P. J. *et al.* Acute kidney injury, plasma lactate concentrations and lactic acidosis in metformin users: A GoDarts study. *Diabetes Obes Metab* **19**, 1579–1586 (2017).
63. Piel, S., Ehinger, J. K., Elmér, E. & Hansson, M. J. Metformin induces lactate production in peripheral blood mononuclear cells and platelets through specific mitochondrial complex I inhibition. *Acta Physiol* **213**, 171–180 (2015).
64. Surace, M. *et al.* Automated Multiplex Immunofluorescence Panel for Immuno-oncology Studies on Formalin-fixed Carcinoma Tissue Specimens. *JoVE (Journal of Visualized Experiments)* e58390 (2019) doi:10.3791/58390.

65. Sorrelle, N. *et al.* Improved Multiplex Immunohistochemistry for Immune Microenvironment Evaluation of Mouse Formalin-Fixed, Paraffin-Embedded Tissues. *The Journal of Immunology* **202**, 292–299 (2019).
66. Hong, G. *et al.* Multiplexed Fluorescent Immunohistochemical Staining, Imaging, and Analysis in Histological Samples of Lymphoma. *JoVE (Journal of Visualized Experiments)* e58711 (2019) doi:10.3791/58711.
67. Bolognesi, M. M. *et al.* Multiplex Staining by Sequential Immunostaining and Antibody Removal on Routine Tissue Sections. *J Histochem Cytochem.* **65**, 431–444 (2017).
68. Tsujikawa, T. *et al.* Quantitative Multiplex Immunohistochemistry Reveals Myeloid-Inflamed Tumor-Immune Complexity Associated with Poor Prognosis. *Cell Reports* **19**, 203–217 (2017).
69. Gorris, M. A. J. *et al.* Eight-Color Multiplex Immunohistochemistry for Simultaneous Detection of Multiple Immune Checkpoint Molecules within the Tumor Microenvironment. *The Journal of Immunology* **200**, 347–354 (2018).
70. Halse, H. *et al.* Multiplex immunohistochemistry accurately defines the immune context of metastatic melanoma. *Scientific Reports* **8**, 11158 (2018).
71. Fiaschi, T. *et al.* Reciprocal Metabolic Reprogramming through Lactate Shuttle Coordinately Influences Tumor-Stroma Interplay. *Cancer Res* **72**, 5130–5140 (2012).
72. Whitaker-Menezes, D. *et al.* Evidence for a stromal-epithelial “lactate shuttle” in human tumors. *Cell Cycle* **10**, 1772–1783 (2011).
73. Rattigan, Y. I. *et al.* Lactate is a mediator of metabolic cooperation between stromal carcinoma associated fibroblasts and glycolytic tumor cells in the tumor microenvironment. *Experimental Cell Research* **318**, 326–335 (2012).
74. Miranda-Gonçalves, V. *et al.* Monocarboxylate transporter 1 is a key player in glioma-endothelial cell crosstalk. *Mol Carcinog* **56**, 2630–2642 (2017).

75. Fitzgerald, L. E., Abendaño, N., Juste, R. A. & Alonso-Hearn, M. Three-Dimensional In Vitro Models of Granuloma to Study Bacteria-Host Interactions, Drug-Susceptibility, and Resuscitation of Dormant Mycobacteria. *Biomed Res Int* **2014**, (2014).
76. Hosios, A. M. & Heiden, M. G. V. The redox requirements of proliferating mammalian cells. *J. Biol. Chem.* **293**, 7490–7498 (2018).
77. Walker, M. A. & Tian, R. NAD(H) in mitochondrial energy transduction: implications for health and disease. *Current Opinion in Physiology* **3**, 101–109 (2018).
78. Obeidat, Y. M. *et al.* Design of a multi-sensor platform for integrating extracellular acidification rate with multi-metabolite flux measurement for small biological samples. *Biosensors and Bioelectronics* **133**, 39–47 (2019).
79. Ma, E. H. *et al.* Metabolic Profiling Using Stable Isotope Tracing Reveals Distinct Patterns of Glucose Utilization by Physiologically Activated CD8+ T Cells. *Immunity* **51**, 856-870.e5 (2019).
80. Xie, J. *et al.* Beyond Warburg effect – dual metabolic nature of cancer cells. *Scientific Reports* **4**, 4927 (2014).
81. Halestrap, A. P. & Denton, R. M. The specificity and metabolic implications of the inhibition of pyruvate transport in isolated mitochondria and intact tissue preparations by alpha-Cyano-4-hydroxycinnamate and related compounds. *Biochem. J.* **148**, 97–106 (1975).
82. Curtis, N. J. *et al.* Pre-clinical pharmacology of AZD3965, a selective inhibitor of MCT1: DLBCL, NHL and Burkitt's lymphoma anti-tumor activity. *Oncotarget* **8**, 69219–69236 (2017).
83. Poole, R. C., Cranmer, S. L., Halestrap, A. P. & Levi, A. J. Substrate and inhibitor specificity of monocarboxylate transport into heart cells and erythrocytes. Further evidence for the existence of two distinct carriers. *Biochem. J.* **269**, 827–829 (1990).

84. Belouèche-Babari, M. *et al.* MCT1 Inhibitor AZD3965 Increases Mitochondrial Metabolism, Facilitating Combination Therapy and Noninvasive Magnetic Resonance Spectroscopy. *Cancer Res* **77**, 5913–5924 (2017).
85. Chan, F. K.-M., Moriwaki, K. & De Rosa, M. J. Detection of Necrosis by Release of Lactate Dehydrogenase Activity. in *Immune Homeostasis: Methods and Protocols* (eds. Snow, A. L. & Lenardo, M. J.) 65–70 (Humana Press, 2013). doi:10.1007/978-1-62703-290-2\_7.
86. Cummings, B. S., Wills, L. P. & Schnellmann, R. G. Measurement of Cell Death in Mammalian Cells. *Current Protocols in Pharmacology* **56**, 12.8.1-12.8.24 (2012).
87. Kabakov, A. E. & Gabai, V. L. Cell Death and Survival Assays. in *Chaperones: Methods and Protocols* (eds. Calderwood, S. K. & Prince, T. L.) 107–127 (Springer, 2018). doi:10.1007/978-1-4939-7477-1\_9.
88. Yuan, M. *et al.* Ex vivo and in vivo stable isotope labelling of central carbon metabolism and related pathways with analysis by LC–MS/MS. *Nature Protocols* **14**, 313 (2019).
89. Balcells, C. *et al.* Tracing metabolic fluxes using mass spectrometry: Stable isotope-resolved metabolomics in health and disease. *TrAC Trends in Analytical Chemistry* (2019) doi:10.1016/j.trac.2018.12.025.
90. Brown, T. P. & Ganapathy, V. Lactate/GPR81 signaling and proton motive force in cancer: Role in angiogenesis, immune escape, nutrition, and Warburg phenomenon. *Pharmacology & Therapeutics* 107451 (2019) doi:10.1016/j.pharmthera.2019.107451.

## CHAPTER 4: CONCLUDING REMARKS AND FUTURE DIRECTIONS

The research described within this thesis sought to investigate pathogen-driven mechanisms by which Mtb augments macrophage metabolism during infection. We investigated the hypothesis that iron chelation by the Mtb siderophore mycobactin results in the activation of HIF-1 $\alpha$  in a hypoxia-independent manner, leading to increased glycolysis, lactate production, and lactate transport. We explored the role of a lactate shuttle within the context of the granuloma microenvironment and hypothesized that the metabolic relationship between hypoxic and normoxic cells within the granuloma contributes to maintaining a niche conducive to Mtb survival and plays a role in disease progression. The mechanistic insights gained will be important for the development of novel host-directed therapeutic strategies to combat TB and will help elucidate the complex interactions which occur at the host-pathogen interface during chronic infectious disease processes.

We successfully demonstrated that mycobactin-mediated iron chelation increases HIF-1 $\alpha$  protein levels and potently increases glycolysis in CD1 mouse bone marrow derived macrophages (BMDMs). We also showcased the impact of infection with a mycobactin synthase knock-out strain of Mtb, further implicating mycobactin as a driver of changes in macrophage metabolism during early infection. Additionally, we demonstrated that lactate levels increase on both a systemic and cellular level during Mtb infection *in vitro* and *in vivo*, and that components of the proposed lactate shuttle are present within guinea pig granulomas. Inhibition of components of the lactate shuttle, including lactate dehydrogenase A (LDHA) and monocarboxylate transporter 1 (MCT1) successfully reduced the concentration of lactate accumulated during infection and may reduce intracellular bacterial survival through augmenting macrophage metabolism.

As was highlighted within the previous chapters, additional work is needed in order to continue answering research questions relevant to the presented projects. First, the impact of Mtb infection and mycobacterial iron chelation on oxidative mitochondrial metabolism was greater than that of glycolytic metabolism. This points to unexplored effects of Mtb infection and mycobacterial iron chelation on mitochondrial health and bioenergetics. The direct impact of mycobactin on mitochondrial electron transport chain activity, mitochondrial membrane potential, mitochondrial fission/fusion, and overall mitochondrial health and integrity is a critical piece of the puzzle that was not experimentally assessed within this thesis project.

Second, technical limitations took multiple forms, including low protein yield from nuclear fractionation protocols, assay length with the Seahorse Extracellular Flux Analyzer, issues with antibody reactivity for Western Blot and IHC applications within the guinea pig model, lactate shuttle inhibitor specificity, and the potential impacts of L929 conditioned media on CD1 mouse BMDM metabolic phenotype. These will all be addressed in future experimental design and approaches. Importantly, a technique of high priority is multi-plexing IHC to probe for components of the lactate shuttle within the structural architecture of the TB granuloma microenvironment. Those experiments will provide critical evidence of differential lactate metabolism and metabolic symbioses between different cell populations within the TB lesion.

Third, time restrictions did not allow for important experimental questions to be probed within *in vivo* infection models, including the impact of infection with mycobactin synthase knock-out strains of Mtb and the impact of lactate shuttle inhibition on infection outcomes. Taking these hypotheses through the translational research pipeline is critical for determining ways in which Mtb drives changes in macrophage metabolism early within the context of infection, such that it primes cells to create a niche conducive for bacterial survival. *In vivo* experiments are thus a top priority for future work and will help validate *in vitro* results presented.

Lastly, the TB research field can continue to look to established hypotheses and methods that have been developed within the context of cancer research, as multiple similarities exist between the tumor and granuloma microenvironments. Particularly, the role of lactate as a signaling molecule is becoming increasingly important for regulating carcinogenesis, promoting tumor invasion and metastasis, and maintaining tumor microenvironments. The dynamic ability of lactate to signal in both autocrine and paracrine manners through GPR81 to regulate anti-inflammatory, immunosuppressive, and angiogenic activities within multiple disease systems points to this receptor as an unexplored target for host-directed therapeutic strategies in the context of TB. This would be a novel direction for study which could have significant rewards. Preliminary IHC results from our laboratory indicate that GPR81 is expressed highly within CD1 mouse granuloma lesions. Additionally, the availability of commercial antagonists and agonists of GPR81, as well as knock-out mouse models, demonstrates clear experimental design pathways for *in vitro* and *in vivo* approaches.

Overall, the heterogeneity of TB disease pathogenesis, the intricacies of macrophage metabolism throughout a chronic disease time course, and the evolutionary capabilities of Mtb to survive intracellularly within macrophages paints a complex picture. However, this complexity is what continues to yield robust lines of research questioning within the TB field. Continual investigation into the interactions that occur at the host-pathogen interface during Mtb infection will advance our understanding of TB pathogenesis, ultimately moving the field closer to effective host-directed therapeutic strategies to combat this global health problem.